AD_____

AWARD NUMBER DAMD17-98-1-8041

TITLE: Tumor-Targeting Peptides For Therapeutic Gene Delivery (97breast)

PRINCIPAL INVESTIGATOR: Renata Pasqualini, Ph.D.

CONTRACTING ORGANIZATION: Burnham Institute
La Jolla, California 92037

REPORT DATE: July 1999

TYPE OF REPORT: Annual

PREPARED FOR: U.S. Army Medical Research and Materiel Command
Fort Detrick, Maryland 21702-5012

REPORT DOCUMENTATION PAGE

Form Approved
OMB No. 0704-0188

1. AGENCY USE ONLY *(Leave blank)*	2. REPORT DATE	3. REPORT TYPE AND DATES COVERED
	July 1999	Annual (1 Jul 98 - 30 Jun 99)

4. TITLE AND SUBTITLE
Tumor-Targeting Peptides For Therapeutic Gene Delivery (97breast)

5. FUNDING NUMBERS
DAMD17-98-1-8041

6. AUTHOR(S)
Renata Pasqualini, Ph.D.

7. PERFORMING ORGANIZATION NAME(S) AND ADDRESS(ES)
Burnham Institute
La Jolla, California 92037

8. PERFORMING ORGANIZATION REPORT NUMBER

9. SPONSORING / MONITORING AGENCY NAME(S) AND ADDRESS(ES)
U.S. Army Medical Research and Materiel Command
Fort Detrick, Maryland 21702-5012

10. SPONSORING / MONITORING AGENCY REPORT NUMBER

11. SUPPLEMENTARY NOTES

12a. DISTRIBUTION / AVAILABILITY STATEMENT
Approved for public release; distribution unlimited

12b. DISTRIBUTION CODE

13. ABSTRACT *(Maximum 200 words)*

Endothelial cells in tumor vessels express angiogenic markers that are not detectable in normal vessels. We have developed an *in vivo* selection system in which phage capable of homing to tumors are recovered from a phage display peptide library following intravenous administration. Using this strategy, we have isolated several tumor-homing peptides that bind to three different receptors that are upregulated in tumor angiogenic vasculature. We plan to use these peptides to generate molecular adaptors for targeted delivery of genes to angiogenic vasculature. These studies may lead to the development of new gene therapy-based tumor treatment strategies that rely on inhibition of angiogenesis. Vector targeting would represent a major advance in breast cancer treatment.

14. SUBJECT TERMS
Breast Cancer
gene therapy, vascular targeting, phage libraries, angiogenesis

15. NUMBER OF PAGES
62

16. PRICE CODE

17. SECURITY CLASSIFICATION OF REPORT	18. SECURITY CLASSIFICATION OF THIS PAGE	19. SECURITY CLASSIFICATION OF ABSTRACT	20. LIMITATION OF ABSTRACT
Unclassified	Unclassified	Unclassified	Unlimited

FOREWORD

Opinions, interpretations, conclusions and recommendations are those of the author and are not necessarily endorsed by the U.S. Army.

N/A Where copyrighted material is quoted, permission has been obtained to use such material.

N/A Where material from documents designated for limited distribution is quoted, permission has been obtained to use the material.

N/A Citations of commercial organizations and trade names in this report do not constitute an official Department of Army endorsement or approval of the products or services of these organizations.

✓ In conducting research using animals, the investigator(s) adhered to the "Guide for the Care and Use of Laboratory Animals," prepared by the Committee on Care and use of Laboratory Animals of the Institute of Laboratory Resources, national Research Council (NIH Publication No. 86-23, Revised 1985).

N/A For the protection of human subjects, the investigator(s) adhered to policies of applicable Federal Law 45 CFR 46.

✓ In conducting research utilizing recombinant DNA technology, the investigator(s) adhered to current guidelines promulgated by the National Institutes of Health.

✓ In the conduct of research utilizing recombinant DNA, the investigator(s) adhered to the NIH Guidelines for Research Involving Recombinant DNA Molecules.

N/A In the conduct of research involving hazardous organisms, the investigator(s) adhered to the CDC-NIH Guide for Biosafety in Microbiological and Biomedical Laboratories.

PI - Signature Date

TABLE OF CONTENTS

TUMOR-TARGETING PEPTIDES FOR THERAPEUTIC GENE DELIVERY

INTRODUCTION

It is well known that angiogenesis, the recruitment of new blood vessels, is an important rate-limiting step in solid tumor growth. New anti-tumor therapies based on the premise that inhibiting angiogenesis suppresses tumor growth are currently being tested in multiple clinical trials (1, 2, 3). Angiogenesis is a multi-stage process that involves the release and activation of angiogenic factors, endothelial cell migration and proliferation, and differentiation into newly formed capillaries (4, 5).

Angiogenic neovasculature expresses markers that are either expressed at much lower levels or not at all in non-proliferating endothelial cells (6-8). The markers of angiogenic endothelium include receptors for vascular growth factors, such as specific subtypes of VEGF and basic FGF receptors (9-12), and the αv integrins (13, 14). Identification of novel molecules characteristic of angiogenic vasculature will improve our understanding of the plasticity of the endothelial phenotype and suggest new therapeutic strategies. Thus far, identification and isolation of such molecules has been slow, mainly because endothelial cells undergo dramatic phenotypical changes when grown in culture (15, 16).

We have developed an *in vivo* system using peptides expressed on the surface of bacteriophage to study organ- and tumor-specific vascular homing (17, 18, 19, 20). Random oligonucleotides are individually fused to cDNAs encoding a phage surface protein, generating collections of phage particles displaying unique peptides in as many as 10^9 permutations (21, 22); in the *in vivo* procedure, phage capable of homing to certain organs or tumors following an intravenous injection are recovered from such phage display peptide libraries. The ability of individual peptides to target a tissue can also be analyzed by this method (17, 18). Furthermore, this system provides an innovative way of identifying endothelial cell surface markers expressed *in vivo* (17, 19, 20).

Unlike earlier antibody work in which tumor specific antigens were selected *in vitro*, our method directly selects molecules capable of homing to tumor vasculature *in vivo*. Thus, in addition to providing novel tools for selective vascular targeting of therapies, this new technology will further our understanding of tumor endothelium specificity and define the role these markers play in angiogenesis. One of the unique and highly attractive features of this method is that it detects the availability of the target receptors in the tissue based not only on expression level, but also on accessibility to a circulating probe.

With the knowledge that solid tumors cannot progress without the generation of new blood vessels, the development of strategies to inhibit this process has been the focus of intense research. There are a variety of approaches not involving gene therapy that are under evaluation for their ability to suppress tumor neovascularization (4, 5, 23-27). They include treatments

using recombinant proteins, monoclonal antibodies and small molecules such as TNP-470, a potent angiogenesis inhibitor (28, 29). Current clinical trials with TNP-470 include patients with cervical cancer, pediatric solid tumors, lymphomas, acute leukemias and AIDS-related Kaposi's sarcoma (3, 30). Preliminary results suggest that the use of therapies that destroy angiogenic vasculature could be a viable approach to avoid drug resistance in cancer therapy (31-33). To date, most tumor treatment strategies utilize systemic administration of the therapeutic agent. Recently though, gene transfer of a cDNA coding for mouse angiostatin into murine fibrosarcoma cells has been shown to suppress primary and metastatic tumor growth *in vivo*. Implantation of stable clones expressing mouse angiostatin in mice dramatically inhibits primary tumor growth and pulmonary micrometastases. The tumor cells in the dormant micrometastases exhibit a high rate of apoptosis balanced by a high proliferation rate. These studies also provide support for a novel approach for cancer treatment by antiangiogenic gene therapy with specific angiogenesis inhibitors (34).

The antitumoral effects that follow the local delivery of angiostatin have been studied in xenograft murine models. Angiostatin delivery was achieved by a defective adenovirus expressing a secretable angiostatin K3 molecule from the cytomegalovirus promoter (AdK3). In *in vitro* studies, AdK3 selectively inhibited endothelial cell proliferation; AdK3-infected endothelial cells also showed a marked mitosis arrest. A single intratumoral injection of AdK3 into pre-established rat C6 glioma or human MDA-MB-231 breast carcinoma grown in athymic mice was followed by arrest of tumor growth, which was associated with angiogenesis inhibition. AdK3 therapy also induced a 10-fold increase in apoptotic tumor cells as compared with a control adenovirus (35). Similar results were obtained using a related approach on an RT2 glioma model (36). These data support the feasibility of targeted antiangiogenesis using adenovirus-mediated gene transfer and indicate that gene therapy can potentially expand the horizons of tumor antiangiogenesis therapy: First, because of the possibility of achieving high concentrations of the therapeutic agent in a given area; Second, because the agent can be produced endogenously, and for a sustained period (24, 37).

In addition, gene therapy can also be designed to deliver the therapeutic gene upon systemic administration. However, for those advantages to be fully explored, one major requirement needs to be made feasible: the targeted delivery of genes to angiogenic vasculature.

In an effort to achieve vector targeting, a few groups have reported on gene therapy-based adenovirus retargeting strategies that redirect the adenovirus to receptors endogenously present on the cell surface of tumor cells (reviewed in ref. 37). By using a bifunctional conjugates consisting of a blocking antiadenoviral knob Fab linked to basic fibroblast growth factor, gene transduction of target cells in vitro was improved; recombinant adenoviruses encoding either the firefly luciferase reporter gene, or the herpes simplex thymidine kinase gene, demonstrated quantitative enhancement of expression. Moreover, tumor cell lines that were previously refractory to native adenovirus transduction could be successfully transduced by the addition of the conjugate (38). Other bispecific antibodies have been used successfully to target entry of an adenovirus vector into endothelial cells expressing a receptor up-regulated during angiogenesis,

such as the construction of Ad vectors which contain modifications to the Ad fiber coat protein that redirect virus binding. Retargeting has been demonstrated using αv integrin [AdZ.F(RGD)] or heparan sulfate [AdZ.F(pK7)] cellular receptors. These vectors were constructed by a novel method involving E4 rescue of an E4-deficient Ad with a transfer vector containing both the E4 region and the modified fiber gene. AdZ.F(RGD) increased gene delivery *in vitro* to endothelial and smooth muscle cells expressing αv integrins. Likewise, AdZ.F(pK7) increased transduction 5- to 500-fold in multiple cell types lacking high levels of Ad fiber receptor, including macrophage, endothelial, smooth muscle, fibroblast, and T cells. In addition, AdZ.F(pK7) significantly increased gene transfer *in vivo* to vascular smooth muscle cells of the porcine iliac artery following balloon angioplasty. Although binding to the fiber receptor still occurs with these vectors, they demonstrate the feasibility of tissue-specific receptor targeting in cells which express low levels of Ad fiber receptor (39, 40). Heterologous ligands have also been incorporated into the HI loop of the fiber knob, and preliminary results using artificial systems *in vitro* suggested that this locale possesses properties consistent with its employment in adenovirus retargeting strategies (41).

These studies address the utility of adenoviral retargeting and indicate that practical use of gene therapy approaches can be developed based on our vascular targeting technology. Here we have been exploring the homing ability of angiogenic vasculature-homing peptides by incorporating them as targeting devices for gene delivery systems. Of all the vector systems currently being explored, adenoviruses have the greatest potential to test the principles of cancer gene therapy (37, 42-46). Here we plan to develop a new approach for vector targeting. We will first obtain virus-binding antibodies that can ablate the endogenous tropism of the adenovirus vectors. These antibodies will then be utilized to form molecular conjugates with the homing peptides in order to redirect adenovirus gene transfer upon systemic delivery.

The studies undertaken in this proposal specifically focused on the use of peptide sequences with selective angiogenic vasculature targeting properties. We are now seeking to validate these probes as delivery vehicles in targeting approaches.

Phage capable of homing to tumor angiogenic vasculature were recovered from a phage display peptide library following intravenous administration. Using this strategy, we have isolated several tumor-homing phage. Among those were phage displaying the tripeptide asparagine-glycine-arginine (NGR), glycine-serine-arginine (GSL), and a double cyclic RGD (RGD-4C). We have shown that each of those peptides bind to three different receptors in tumor angiogenic vasculature. Based on our *in vivo* studies targeting tumors with NGR-, GSL- and RGD-4C-phage, our idea is that such peptides are suitable for the generation of molecular adaptors for the targeted delivery of therapies to angiogenic vasculature.

PROPOSAL BODY

The tasks originally approved for this proposal are listed below.

1. **To perform in vivo screenings to select phage-displayed peptides that home into human breast cancer xenografts.** We will use various phage peptide library configurations and a series of human breast carcinoma cell lines injected in the mammary fat pad of immuno-deficient mice.

2. **To test the tumor-homing phage selected in the screenings for their tumor vasculature and tumor stroma binding specificities.** Each tumor homing phage displayed peptides will be tested individually for their ability to home into tumors in vivo. Immuno-staining experiments will be performed to ascertain the location of the target molecules.

3. **To generate a panel of monoclonal antibodies against adenovirus.** RBF superimmune mice will be immunized with adenovirus. Hybridomas will be screened using a number of strategies and clones producing antibodies to surface viral antigens will be characterized.

4. **To use the reagents described above to produce Fab conjugates that can be used for maximizing the delivery of Adenovirus-based gene vectors to tumors in vivo.**

In the following pages we report on significant progress on each specific aim during the past year.

We have isolated phage that home into tumors. The distinct phage display 3 classes of peptides (NGR, GSL and RGD-4C). We have shown that phage displaying such peptides bind selectively to angiogenic tumor vessels when injected into tumor-bearing mice (20). The RGD-4C peptide binds to αv integrins in angiogenic vessels (18, 20). The receptor for NGR-containing peptides in the tumor vasculature is CD13 (47, 48). We have evidence that the receptor for the GSL-containing peptides is the proteoglycan NG2 (49, 50).

The phage methodology that we have developed is appropriate for the search of homing sequences, and it can serve as a model for the selective targeting of angiogenic vasculature. Our published results show that when cytotoxic drugs are coupled to peptide motifs that target tumor vasculature, they appear to be more effective and to cause fewer untoward effects than when the drugs are administered alone. To demonstrate the feasibility of therapeutic tumor targeting, we coupled a tumor-targeting peptide to doxorubicin to see if the peptides could improve the efficacy and/or toxicity profile of a drug. We have shown that this could be accomplished in an impressive manner. Doxorubicin, when coupled to a tumor-targeting peptide, is both less toxic and more effective than free doxorubicin or doxorubicin coupled to an unrelated peptide (see below) (20).

Many existing therapies could be made more effective if site-specific delivery could be achieved, particularly vectors for cancer gene therapy (42-46). The utility of adenovirus vectors for gene therapy is being intensely investigated, and there are a number of genetic approaches that are being explored for the treatment of cancer. These include the transfer of "suicide" genes that convert inactive pro-drugs into cytotoxic compounds, transcomplementation of defective tumor-suppressor genes and the use of oncolytic viruses (37, 51, 52).

As discussed above, vectors that drive the expression of antiangiogenic agents such as endostatin and angiostatin, as well as suicide or pro-apoptotic genes have also shown promise as antitumor agents. In an independent but related line of work, our group has recently reported on novel homing-proapoptotic peptides for cancer treatment (53).

We found that some cell death receptors require embedded pro-apoptotic peptide sequences (54). These sequences and structurally similar pro-apoptotic antibiotic peptides disrupt negatively charged membranes and thus induce mitochondrial swelling and mitochondria-dependent cell-free apoptosis (55). We integrated this concept with our vasculature targeting technology by introducing homing pro-apoptotic peptides (HPPs) composed of 2 functional domains. The homing domain is designed to guide the HPP to targeted cells and allow its internalization. The pro-apoptotic domain is non-toxic outside of cells but promotes disruption of mitochondrial membranes and subsequent cell death when internalized by target cells. Our prototype peptide is only 21 amino acids long, is selectively toxic to endothelial cells undergoing angiogenesis *in vitro*, and has strong anti-tumor activities in mice. For the homing domain, we used either the cyclic (disulfide bond between cysteines) CNGRC peptide or the double cyclic ACDCRGDCFC peptide, both of which have tumor-homing properties (18, 20) and for which there is evidence of internalization (20, 56, 57). We synthesized this domain from all L-amino acids because of the presumed chiral nature of its receptor interaction. Homing pro-apoptotic peptides represent a new class of anti-cancer agents that can be optimized for maximum therapeutic effect by adjusting properties such as residue placement, domain length, peptide hydrophobicity and hydrophobic moment (58). Beyond this, future HPPs might be designed to disrupt membranes using a completely different type of pro-apoptotic domain such as β-strand/sheet-forming peptides (59). Our results provide a glimpse at the potential of a novel cancer therapy combining two principles of specificity — homing to targeted cells and selective apoptosis of targeted cells (53).

Here we proposed to extend our findings with drug conjugates and targeted pro-apoptotic peptides, by developing molecular adaptors that can be used to target gene therapy vectors to tumor vasculature *in vivo* following intravenous administration. Our hypothesis is that the homing peptides we have isolated can be incorporated into targeted gene transfer methodologies that will increase the efficiency and decrease the harmful effects of delivering genes into normal cells. Specifically we will compare the properties of various tumor-targeting peptides for their ability to target adenovirus vectors when combined as molecular adaptors to peptides that bind to the viral gene therapy vectors.

Our results suggest that it may be possible to use αv-, CD13-, and NG2-directed peptides (RGD-4C, CNGRC, and GSL) to target genes to angiogenic vasculature and from there, into the target tissue. Peptides may have advantages in this regard, especially when compared to antibody-based approaches, because they are smaller, more likely to diffuse efficiently within the tumor, and less likely to be immunogenic. Targeted delivery of gene therapy vectors, especially adenoviral ones, may also lead to reduced immunogenicity against the virus, one of the major complicating factors that hamper the success and efficiency of gene therapy-based approaches to date.

Targeting of tumor vasculature with phage

We reasoned that *in vivo* selection could be used to target endothelial markers on angiogenic tumor vessels. We have tested this hypothesis and have successfully targeted the blood vessels in several human tumor types. Injection of phage libraries into the circulation of mice bearing human breast carcinoma xenografts followed by recovery of phage from the tumors led to the identification of a number of peptide motifs that selectively directed the phage into the tumors. Different libraries yielded different peptides, but three main motifs emerged. One of the motifs contained the sequence RGD (arginine-glycine-aspartic acid; (60). The RGD sequence was embedded in a peptide structure that, as we have previously shown, binds selectively to αv integrins (61, 18). As the αvβ3 and αvβ5 integrins are known markers of angiogenic vessels (12, 62, 63), we had previously tested phage carrying this motif, CDCRGDCFC (termed RGD-4C), for tumor targeting. This phage homes into tumors in a highly selective manner and its homing is specifically inhibited by the cognate peptide (18, 20). One of the two new peptides that accumulated in tumors, was derived from a library with the structure $CX_3CX_3CX_3C$ (20). This peptide, CNGRCVSGCAGRC, contained the NGR (asparagine-glycine-arginine) motif, which has been identified previously as a cell adhesion motif (64, 65). We tested two other peptides that contain the NGR motif, but are otherwise entirely different from the CNGRCVSGCAGRC peptide. One of them is a linear peptide, NGRAHA (64), and the other a cyclic one, CVLNGRMEC. The CNGRCVSGCAGRC-phage and both of the other NGR-displaying phage homed into the tumors. The tumor homing was not dependent on the tumor type or on species; the phage accumulated selectively in the human breast carcinoma used in the selection, as well as in a human Kaposi's sarcoma and a mouse melanoma (data not shown). We synthesized the minimal cyclic NGR peptide from the CNGRCVSGCAGRC-phage and found that this peptide (CNGRC), when co-injected with the phage, inhibited the accumulation of CNGRCVSGCAGRC-phage and of the two other NGR-displaying phage in breast carcinoma xenografts.

The RGD-4C homes selectively to the breast cancer tumor and its homing is readily inhibited by the free RGD-4C peptide (18). The tumor homing of RGD-4C phage was not inhibited by the CNGRC peptide, even when the peptide was used in amounts 10-fold greater than those that inhibited the homing of the NGR phage. The tumor homing of the NGR phage was also partially inhibited by the RGD-4C peptide, but this peptide was 5-10 times less potent than the CNGRC

peptide. Thus, the two peptides displaying RGD and NGR appear to bind to different, albeit perhaps somehow related, receptor sites in tumor vasculature. An unrelated cyclic peptide, GACVFSIAHECGA had no effect in the tumor homing ability of either phage.

Immunostaining of tissues for phage also showed that the NGR phage homing selectively homes into tumors. In one set of experiments, phage were allowed to circulate for 3-5 minutes, followed by perfusion. In the second set of experiments, tissues were analyzed 24 hours after phage injection. At this time point, there is almost no phage left in the circulation, and perfusion is no longer needed (18, 20). Strong phage staining was seen in tumor vasculature but not in normal endothelia. Testing of the CNGRCVSGCAGRC-phage homing to MDA-MB-435 cell-derived breast carcinoma xenografts and KS1767 cell-derived Kaposi's sarcoma xenografts gave a similar result. The two other NGR phage, NGRAHA and CVLNGRMEC, also showed strong tumor staining (data not shown). In both tumor types, phage was clearly detected in the tumor vessels in the 3-5 minute time frame. The phage appeared to have accumulated and the staining was spread outside the blood vessels and into the tumors at 24 hours.

Increased permeability of tumor blood vessels (23, 65) may account for the spreading of phage proteins into the parenchyma of tumors. Receptor-mediated internalization by angiogenic endothelial cells (20, 56, 57), and subsequent transfer to tumor tissue may also play a role.

The CNGRCVSGCAGRC-phage yielded the largest difference between phage staining in tumor tissues compared to normal tissues among all of the tumor-homing peptides analyzed. Several control organs were also studied and gave very low or no immunostaining, confirming the specificity of the NGR motifs for tumor vessels (20). Spleen and liver contained detectable phage; the uptake by the reticuloendothelial system is a general property of the phage particle and independent of the peptide it displays (17, 18). These immunostaining results with the NGR phage are similar to observations made with the RGD-4C phage (18). The time frame for the phage staining experiments presented was based on our previous experiments on kinetic of phage clearance after intravenous administration (18, 220, 66). We have more recently also examined the intermediate time points (1, 3, 8, 12h), and observed similar results.

Control phage were injected in tumor-bearing mice and showed no homing to tumors. Those controls include (i) phage without insert, (ii) unselected phage library mixtures, (iii) phage selected and shown to home to other normal vascular beds, and (iv) phage displaying peptides that are unrelated to NGR. In addition, an insertless phage with a different selective marker - ampicillin instead of tetracyclin (66) - was co-injected with the NGR phage at the same input to assess specificity within the same tumor-bearing animal. Plating the phage recovered from the tissues on tetracyclin and ampicillin plates showed that over 10-fold more NGR phage than ampicillin phage accumulated in the tumor. In contrast, slightly more ampicillin phage than the NGR phage were recovered from other control organs tested. Moreover, co-injection of CNGRC-phage with a 10-fold excess of phage particles engineered to be non-infective did not affect tumor homing, whereas this procedure decreased the accumulation of phage in trapping organs that are members of the reticuloendothelial system, such as the spleen and the liver (18).

The accumulation of the NGR phage into tumors is not a result of increased tumor vascularization in comparison to normal tissues. There is an extensive body of literature to the effect that tumors do not contain more blood vessels than normal organs (23). In fact, quite the opposite is observed; it is well established that solid tumors are less vascularized than many normal tissues. In a tumor, approximately 100 tumor cells can be supported by one endothelial cell. In contrast, every cell within normal tissues lives adjacent to an endothelial cell in a capillary blood vessel, or in certain cases, lies between two capillary blood vessels (23). Therefore, the accumulation of the NGR phage in tumor vasculature is specific and reflects NGR-phage binding to tumor vasculature, and not simply phage trapping.

These experiments make an important point because they demonstrate that it is possible to develop probes that target angiogenic vasculature, a common feature in all solid tumors. Moreover, targeting tumor vasculature, unlike conventional tumor targeting, possesses an intrinsic amplification mechanism; it has been estimated that 100 tumor cells should die for each destroyed endothelial cell in tumor blood vessels. Finally, because tumor endothelial cells are diploid and nonmalignant, they are unlikely to lose a cell surface target receptor or acquire resistance to therapy through mutation and clonal evolution (31-33).

Receptors for NGR, RGD-4C and GSL tumor vasculature-homing phage

The fact that the receptors for our tumor-homing phage are known represent a major advantage because one is able to evaluate the presence of the receptors in human tumors using antibodies in addition to phage. This information is obviously crucial in terms of the development of realistic therapy targeting strategies that can be applicable to cancer patients.

Several lines of evidence have implicated the integrins αvß3 and αvß5, the receptors for the RGD-4C tumor-homing phage, in the angiogenic process. It has been shown that αv integrins are selectively expressed in angiogenic vasculature in human tumors but not selectively expressed in normal vasculature (18, 20, 62). Moreover, αv integrin antagonists have been shown to block the growth of neovessels (13, 14, 67); in these experiments, endothelial cell apoptosis was identified as the explanation for the inhibition of angiogenesis (13, 14). Concordant with these findings, it appears that two distinct cytokine-induced pathways that lead to angiogenesis depend on specific αv integrins. Angiogenesis initiated by bFGF can be inhibited by an anti-αvß3 blocking antibody, whereas VEGF-mediated angiogenesis can be prevented by a blocking antibody against αvß5. The integrins αvß3 and αvß5 have been reported to be preferentially displayed in different types of ocular neovascular disease in humans (62, 63).

As for the characterization of the NGR receptor - CD13 - we have evidence that NGR-containing phage co-localizes with CD13/APN in human tumors where it binds to tumor blood vessels but not to resting vessels in normal tissues. We also have immunohistochemical evidence also that CNGRC-phage binds to human tumor vessels in tissue sections but not to normal vessels. A negative control phage with no insert (fd phage) did not bind to normal or tumor tissue sections.

These findings prompted us to evaluate expression of CD13/APN in cell lines, in normal vasculature and in the vasculature of tumors and other angiogenic tissues.

Flow cytometry and immunohistochemistry showed that CD13/APN is expressed in a number of tumor cells and HUVECs. CD13/APN was not detected in the vasculature of normal organs of mouse and human tissues. Immunohistochemistry also enabled us to analyze the distribution of CD13/APN in tumor cells, tumor vasculature, and normal vasculature. Our studies clearly demonstrate that CD13/APN, the NGR receptor in tumor vessels, is specifically expressed in angiogenic endothelial cells and pericytes of both human and mouse tissue **(Table 1, Figure 1)**.

Confocal microscopy showed that CD13/APN expression is confined to the endothelial cells and pericytes in breast carcinoma human tissue sections **(Figure 2)**. Similar staining patterns were obtained with the NGR phage and the anti-CD13 antibodies. In each case, reactivity could be detected in the vasculature of the tumors but not in that of normal tissues. Unquestionable direct evidence for the identity of the NGR receptor as CD13 derived from recent experiments involving studies using CNGRC phage and anti-CD13 antibodies. We have shown that the staining with anti-CD13 antibodies in human tumor tissue sections can be abrogated by pre-incubation of the tumor section with NGR-phage but not a control phage (48). We have also demonstrated that the homing of the CNGRC phage into tumors *in vivo* is inhibited by co-injection with anti-CD13 antibodies, but not control antibodies **(Figure 3)**. In some of the experiments, the tumors were generated by injecting MDA-MD-435 breast carcinoma, a cell line that does not express CD13. Conversely, Hodgkin's lymphoma, C8161 melanoma, and Kaposi's sarcoma cell lines express high levels of CD13. The targeting of the CNGRC-phage or the CNGRC-dox conjugate *in vivo* is equally efficient, whether or not the tumor cells express CD13/NGR receptor.

During the past decade, 2 independent lines of research have lead to compelling evidence that the proteoglycan NG2 is upregulated in angiogenic vasculature. Elegant immunohistochemical studies have shown that NG2 is highly expressed in pericytes (49, 50). In collaboration with Dr. William Stallcup at the Burnham Institute, we have shown that NG2 not only is overexpressed, but that it plays an important role in tumor and retinal neovascularization. An interesting connection between NG2 and our GSL tumor homing peptide came to light because we found that *in vitro* panning on immobilized NG2 yielded GSL-containing phage. GSL-phage, as well as other novel NG2-binding peptides isolated *in vitro*, mediate selective phage homing to retinal neovasculature. Experiments using wild-type and NG2-null mice bearing tumors further demonstrated that NG2 serves as a target for tumor-vasculature homing phage (49). We have *in vitro* and *in vivo* data strongly indicating that GSL-phage specifically binds to NG2.

Proteoglycans have been shown to function in the binding and entry of many viruses into cells (68). Proteoglycans have also been shown to mediate gene transfer into cultured cells by methods relying on polylysine or carionic liposomes (68). These observations suggest that NG2 might be a suitable receptor for the uptake of targeted gene therapy vectors *in vivo*. We plan to explore this possibility using GSL-containing molecular adaptors.

Molecular adaptors for targeted delivery of genes to angiogenic vasculature

Selection of adenovirus-binding antibodies

In order to establish molecular adaptors with dual specificities (containing a tumor vasculature-homing moiety and an adenovirus binding moiety), we have generated monoclonal antibodies against adenovirus. We were successful in isolating distinct monoclonal antibodies that interact with adenovirus **(Table 2)**. We have determined the affinity and specificity for each of the antibodies by performing ELISA assays **(Figure 4)** and Biacore studies. Clones 3B2 and 1C5 bind to adenovirus fiber knob, as determined by ELISA, using a recombinant fiber knob fusion protein **(Figure 5)**.

We have further characterized the anti-adenovirus antibodies by investigating whether the antibodies can block adenovirus infectivity **(Figure 6)**. The antibody 1C5 was the most effective in this type of assay. We have also tested the reactiviy of multiple clones for their ability to recognize adenoviral proteins by Western Blot analysis and immunofluorescence of infected cells. Both clones 1C5 and 3B2 reacted strongly with adenovirus-infected cells **(Figure 7)**.

The next step is to conjugate the best antibodies to our tumor-homing peptides and evaluate their potential as gene therapy targeting. In vitro, we were able to show - using tow different kinds of antibody conjugates - that impressive targeting effects can be achieved. As a prototype, we have used a peptide that recognizes membrane dipeptidase. This peptide contains the motif GFE. MDP is a protease that is highly expressed on the surface of certain tumor cell lines. Increased gene expression using a promoter gene was observed when 436 breast carcinoma monolayers were incubated with adenovirus in the presence of the conjugate. Using chemical conjugates, we could also detect an Fc-dependent targeting effect using antibody conjugate made with the 1C5 monoclonal antibody **(Figure 8)**.

KEY RESEARCH ACCOMPLISHMENTS:

- **We have performed in vivo screenings and have selected phage-displayed peptides that home into human breast cancer xenografts.**
- **We have characterized the tumor-homing phage selected in the screenings for their selectivity in homing to tumor vasculature.**
- **We have characterized the receptors for tumor homing peptides in angiogenic vasculature.**
- **We have generated and characterized a panel of monoclonal antibodies against adenovirus.**

REPORTABLE OUTCOMES

None at this time

CONCLUSION

The ability to target genes to malignant tumors has been a long standing goal in medical oncology. Unfortunately, to date, there are only a few selected situations in which targeted delivery is actually feasible. Tumor targeting approaches tend to be either highly invasive or suffer from a lack of specificity and incomplete tissue penetration. Several lines of research have recently converged to explore vascular targeting by taking advantage of the differences between the newly formed vessels in tumors and the mature vessels in normal tissues.

Our approach is particularly novel because it directly selects *in vivo* for circulating probes capable of preferential homing into tumors. We have now uncovered new markers in the vasculature of tumor vasculature, providing a new means for selective targeting of therapies and new insights into endothelial tissue specificities. During the remaining of the grant duration, we plan to use the reagents described above to produce Fab conjugates that can be used for maximizing the delivery of Adenovirus-based gene vectors to tumors *in vivo*.

REFERENCES

1. Folkman J. Angiogenesis in cancer, vascular, rheumatoid and other disease. Nature Med. **1**:27-31, 1995.

2. Folkman J. Addressing tumor blood vessels. Nature Biotechnol. **15**: 510, 1997.

3. Twardowski P. and Gradishar WJ. Clinical trials of antiangiogenic agents. Curr. Opin. Oncol. **9**:584-589, 1997.

4. Rak JW, St. Croix BD, and Kerbel RS. Consequences of angiogenesis for tumor progression, metastasis and cancer. Anticancer Drugs **6**:3-18, 1995.

5. Zetter, BR. Angiogenesis and tumor metastasis. Ann. Rev. Med. **49**: 407-424, 1998.

6. Arap W, Pasqualini R, and Ruoslahti E. Chemotherapy targeted to tumor vasculature. Curr. Opin. Oncol. **10**:560-565, 1998.

7. Burrows FJ, and Thorpe PE. Vascular targeting - a new approach to the therapy of solid tumors. Pharmacol. Ther. **64**:155-174, 1994.

8. Buckle R. Vascular targeting and the inhibition of angiogenesis. Ann. Oncol. (Suppl.) **4**:45-50, 1994.

9. Mustonen T, and Alitalo K. Endothelial receptor tyrosine kinases involved in angiogenesis. J. Cell Biol. **129**:895-898, 1995.

10. Lappi D A. Tumor targeting through fibroblast growth factor receptors. Sem. Cancer Biol. **6**: 279-288, 1995.

11. Martiny-Baron G, and Marme D. VEGF-mediated tumor angiogenesis: a new target for cancer therapy. Curr. Opin. Biotechnol. **6**:675-680, 1995.

12. Rettig WJ, Garin-Chesa P, Healey JH, Su SL, Jaffe EA, and Old LJ. Identification of endosialin, a cell surface glycoprotein of vascular endothelial cells in human cancer. Proc. Natl. Acad. Sci. USA **89**:10832-10836, 1992.

13. Brooks PC, Clark RA, and Cheresh DA. Requirement of vascular integrin _ vß3 for angiogenesis. Science **264**:569-571, 1994.

14. Brooks PC, Montgomery AM, Rosenfeld M, Reinsfeld RA, Hu T, Klier G, and Cheresh DA. Integrin _ vß3 antagonists promote tumor regression by inducing apoptosis of angiogenic blood vessels. Cell **79**:1157-1164, 1994.

15. Sage EH. Angiogenesis inhibition in the context of endothelial cell biology. Adv. Oncol. **12**:17-29, 1996.

16. Watson CA, Camera-Benson L, Palmer-Croker R, and Pober JS. Variability among human umbilical vein endothelial cell cultures. Science **268**:447-448, 1995.

17. Pasqualini R and Ruoslahti E. Organ targeting *in vivo* using phage display peptide libraries. Nature **380**:364-366, 1996.

18. Pasqualini R, Koivunen E, and Ruoslahti E. _v integrins as receptors for tumor targeting by circulating ligands. Nature Biotechnol. **15**:542-546, 1997.

19. Rajotte D, Arap W, Hagedorn M, Koivunen E, Pasqualini R, and Ruoslahti E. Molecular heterogeneity of the vascular endothelium revealed by *in vivo* phage display. J. Clin. Invest. **102**:430-437, 1998.

20. Arap W, Pasqualini R, and Ruoslahti E. Cancer treatment by targeted drug delivery to tumor vasculature. Science **279**:377-380, 1998.

21. Smith GP, and Scott JK. Searching for peptide ligands with an epitope library. Science **228**:1315-1317, 1985.

22. Smith GP, and Scott JK. Libraries of peptides and proteins displayed in filamentous phage. Meth. Enzymol. **21**:228-257, 1993.

23. Folkman, J. *In* Cancer: Principles and practice of oncology. (eds. DeVita, V.T., Hellman, S. & Rosenberg, S. A.) pp. 3075-3087 (Lippincott-Raven Publishers, Philadelphia-New York), 1997.

24. Bicknell, R. *In* Tumour angiogenesis. (eds. Bicknell, R., Lewis, C.E., and Ferrara, N.) pp. 19-28 (Oxford University Press Inc., Oxford), 1997.

25. O'Reilly MS, Boehm T, Shing Y, Fukai N, Vasios G, Lane WS, Flynn E, Birkhead JR, Olsen BR, and Folkman J. Endostatin: an endogenous inhibitor of angiogenesis and tumor growth. Cell **88**:277-285, 1997.

26. O'Reilly MS, Holmgren L, Shing Y, Chen C, Rosenthal RA, Moses M, Lane WS, Cao Y, Sage EH, and Folkman J. Angiostatin: a novel angiogenesis inhibitor that mediates the suppression of metastases by a Lewis lung carcinoma. Cell **79**:315-328, 1994.

27. Folkman J. Angiogenesis inhibitors generated by tumors. Mol. Med. **1**:120-122, 1995.

28. Lowther, WT, McMillen, DA, Orville, AM, and Matthews, BW. The anti-angiogenic agent fumagillin covalently modifies a conserved active-site histidine in the *E. coli* methionine aminopeptidase. Proc. Natl. Acad. Sci. USA **95**:12153-12157, 1998.

29. Ingber D, Fujita T, Kishimoto S, Sudo K, Kanamaru T, Brem H, and Folkman J. Synthetic analogues of fumagillin that inhibit angiogenesis and suppress tumour growth. Nature **348**:555-557, 1990.
30. Folkman J. Antiangiogenic gene therapy. Proc Nat. Acad.of Sci. USA. **95**:9064-9066, 1998.

31. Kerbel RS. Inhibition of tumor angiogenesis as a strategy to circumvent acquired resistance to anti-cancer therapeutic agents. Bioessays. **13**:31-36, 1991.

32. Kerbel RS. A cancer therapy resistant to resistance. Nature **390**:335-336, 1997.

33. Boehm T, Folkman J, Browder T, and O'Reilly MS. Antiangiogenic therapy of experimental cancer does not induce acquired drug resistance. Nature **390**:404-407, 1997.

34. Cao Y, O'Reilly MS, Marshall B, Flynn E, Ji RW, and Folkman J. Expression of angiostatin cDNA in a murine fibrosarcoma suppresses primary tumor growth and produces long-term dormancy of metastases. J. Clin. Invest. **101**:1055-1063, 1998.

35. Griscelli F, Li H, Bennaceur-Griscelli A, Soria J, Opolon P, Soria C, Perricaudet M, Yeh P, and Lu H. Angiostatin gene transfer: inhibition of tumor growth in vivo by blockage of endothelial cell proliferation associated with a mitosis arrest. Proc. Natl. Acad. Sci. USA **95**:6367-72, 1998.

36. Tanaka T, Cao Y, Folkman J, and Fine HA. Viral vector-targeted antiangiogenic gene therapy utilizing an angiostatin complementary DNA. Cancer Res. **58**:3362-3369, 1998.

37. Kong H. and Crystal RG. Gene therapy strategies for tumor antiangiogenesis. J. Natl. Cancer Inst. **90**:273-286, 1998.

38. Goldman CK, Rogers BE, Douglas JT, Sosnowski BA, Ying W, Siegal GP, Baird A, Campain JA, and Curiel DT. Targeted gene delivery to Kaposi's sarcoma cells via the fibroblast growth factor receptor. Cancer Res. **57**:1447-1451, 1997.

39. Wickham TJ, Haskard D, Segal D, and Kovesdi I. Targeting endothelium for gene therapy via receptors up-regulated during angiogenesis and inflammation. Cancer Immunol. Immunother. **45**:149-151, 1997.

40. Wickham TJ, Segal DM, Roelvink PW, Carrion ME, Lizonova A, Lee GM, and Kovesdi I. Targeted adenovirus gene transfer to endothelial and smooth muscle cells by using bispedific antibodies. J. Virol. **70**:6831-6838, 1996.

41. Krasnykh V, Dmitriev I, Mikheeva G, Miller CR, Belousova N, and Curiel DT. Characterization of an adenovirus vector containing a heterologous peptide epitope in the HI loop of the fiber knob. J. Virol.**72**:1844-1852, 1998.

42. Muzyczka N. Adeno-associated virus (AAV) vectors: will they work? J. Clin. Invest. **94**:1351, 1994.

43. Vile RG. Gene therapy for cancer, the course ahead. Cancer Met. Rev. **3**:403-410, 1996.

44. Weichselbaum RR and Kufe D. Gene therapy of cancer. Lancet **349**:Suppl 2:SII10-2, 1997.

45. Weitzman MD, Wilson JM, and Eck SL. Adenovirus vectors in cancer gene therapy. Gene Therapy and Vector Systems **2**:17-25, 1997.

46. Zhang J, and Russell S. Vectors for cancer gene therapy. Cancer Met. Rev. **3**:385-401, 1996.

47. Look AT, Ashmun RA, Shapiro LH, Peiper SC. Human myeloid plasma membrane glycoprotein CD13 (gp150) is identical to aminopeptidase N. J. Clin. Invest. **83**:1299-1307, 1989.

44. Mechtersheimer G, and Moller P. Expression of aminopeptidase N (CD13) in mesenchymal tumors. Am. J. Pathol. **137**:1215-1222, 1990.

48. Pasqualini R, Arap W, Koivunen E, Kain R, Lahdenranta J, Shapiro L, Sakamoto M, Stryn A, and Ruoslahti E. CD13 is a receptor for tumor vasculature-homing peptides and plays a role in angiogenesis. Submitted.

49. Burg M, Pasqualini R, Arap W, Stallcup W, and Ruoslahti E. Identification of NG2 proteoglycan-binding peptides that home to tumor neovasculature. Cancer Res. 59:2869-2874, 1999.

50. Schlingemann RO, Rietveld FJ, de Waal RM, Ferrone S, and Ruiter DJ. Expression of the high molecular weight melanoma-associated antigen by pericytes during angiogenesis in tumors and in healing wounds. Am. J. Pathol. **136**:1393-1405, 1990.

51. Martin LA.and Lemoine N.R. Direct cell killing by suicide genes. Cancer Met. Rev. **3**:301-316, 1996.

52. Mullen CA. Metabolic suicide genes in gene therapy. Pharmac. Ther. **63**:199-207, 1994.

53. Ellerby M, Arap W, Andrusiak R, Del Rio G, Kain R, Ruoslahti E, Bredesen D, and Pasqualini R. Targeted proapoptotic peptides for cancer therapy. Nature Med. **9**:1032-1039, 1999.

54. Bredesen DE. *et al.* P75(NTR) and the concept of cellular dependence – seeing how the other half die. Cell Death Differ. **5**:365-371, 1998.

55. Ellerby HM *et al.* Establishment of a cell-free system of neuronal apoptosis: comparison of premitochondrial, mitochondrial, and postmitochondrial phases. J. Neurosci. **17:**6165-6178, 1997.

56. Hart SL *et al.* Cell binding and internalization by filamentous phage displaying a cyclic Arg-Gly-Asp-containing peptide. J. Biol. Chem. **269**:12468-12474, 1994.

57. Bretscher MS. Endocytosis and recycling of the fibronectin receptor in CHO cells. EMBO J. **8**:1341-1348, 1989.

58. Dathe M *et al.* Hydrophobicity, hydrophobic moment, and angle subtended by charged residues modulate antibacterial and haemolytic activity of amphipathic helical peptides. FEBS Lett. **403**:208-212, 1997.

59. Mancheno JM, Martinez del Pozo A, Albar JP, Onaderra M, and Gavilanes JG. A peptide of nine amino acid residues from *a*-sarcin cytotoxin is a membrane-perturbing structure. J. Peptide Res. **51**:142-148, 1998.

60. Ruoslahti E. RGD and other recognition sequences for integrins. Ann. Rev. Cell Dev. Biol. **12**:697-715, 1996.

61. Koivunen E, Wang B, and Ruoslahti E. Phage libraries displaying cyclic peptides with different ring sizes: ligand specificities of the RGD-directed integrins. BioTechnol. **13**:265-270, 1995.

62. Friedlander M, Brooks PC, Sharffer RW, Kincaid CM, Varner JA, and Cheresh DA Definition of two angiogenic pathways by distinct _ v integrins. Science **270**:1500-1502, 1995.

63. Friedlander M, Theesfeld CL, Sugita M, Fruttiger M, Thomas MA, Chang S, and Cheresh DA. Involvement of integrins avb3 and avb5 in ocular neovascular diseases. Proc. Natl. Acad. Sci. USA **93**:9764-9769, 1996.

64. Koivunen E, Gay DA, and Ruoslahti E. Selection of peptides binding to the a5b1 integrin from phage display library. J. Biol. Chem. **268**:20205-20210, 1993.

65. Healy JM, Murayama O, Maeda T, Yoshino K, Sekiguchi K, and Kikuchi M. Peptide ligands for integrin avb3 selected from random phage display libraries. Biochemistry **34**:3948-3955, 1995.

66. Pasqualini R, Arap W, Rajotte D, and Ruoslahti E. In *Phage Display of Proteins and Peptides*. (eds. Barbas, C., Burton, D., Silverman, G. & Scott J.) Cold Spring Harbor Press, New York, in press.

67. Hammes H-P, Brownlee M, Joonczyk A, Sutter A, and Preissner KT. Subcutaneous injection of a cyclic peptide antagonist of vitronectin receptor-type integrins inhibits retinal neovascularization. Nature. Med. **5**:529-533, 1996.

68. Mounkes LC, Zong W, Cipres-Palacin G, Heath TD, and Debs RJ. Proteoglycans mediate cationic liposome-DNA complex-based gene delivery in vitro and in vivo. J. Biol. Chem. **273**:26164-26170, 1998.

APPENDICES

Pasqualini, R., Koivunen, E., and Ruoslahti, E. (1997) αv Integrins as receptors for tumor targeting by circulating ligands. **Nature Biotechnol.** *15*:542-546.

Pasqualini, R., Arap, W., and Ruoslahti, E. (1998) Cancer treatment by targeted drug delivery to tumor vasculature. **Science** *279*:377-380.

Arap, W., **Pasqualini, R**. and Ruoslahti, E. (1998) Chemotherapy targeted to tumor vasculature. **Curr. Opin.Oncol.** *10*: 560-565.

Burg, M., **Pasqualini, R.**, Arap, W., Ruoslahti, E., and Stallcup, W. (1999) Identification of NG2 proteoglycan-binding peptides that home to tumor neovasculature. **Cancer Res.** 59:2869-2874.

Ellerby, M., Arap, W., Ellerby, L.M., Kain, R., Andrusiak, R., Del Rio, G., Krajewski, S., Lombardo, C.R., Rao, R., Ruoslahti, E., Bredesen, D. and **Pasqualini, R.** (1999) Anti-cancer activity of targeted pro-apoptotic. **Nature Med**. 5:1032-1038.

FIGURE LEGENDS:

Figure 1 Immunoperoxidase staining for APN in tumor and normal tissues in mice. (a), a xenograft tumor grown from MDA-MB-435 human breast carcinoma cells in a nude mouse. Anti-mouse APN shows positive staining in the tumor blood vessels. (b), the tumor cells and blood vessels in this xenograft are negative with anti-human APN which does not react with mouse APN . Mouse liver (c) and spleen (d) show no significant staining with the anti-mouse APN antibody.

Figure 2 APN expression in human angiogenesis. Upper-right panel: confocal immunofluorescence image showing anti-APN staining of a medium-size vessel in a human breast carcinoma. APN staining is present both at the endothelial surface and in a subendothelial layer. Lower-right panel: staining with an antibody anti-APA, a pericyte marker. Left panels, phase contrast of the corresponding images. Magnification 400X.

Figure 3 Phage expressing the NGR peptide motif bind to APN. Inhibition of NGR phage tumor homing by anti-APN. Tumor-bearing mice with size-matched MDA-MB-435 tumors were coinjected with 10^9 TU/mouse of the indicated phage together with anti-APN IgG or normal rat IgG. The number of phage TU recovered from the tumors is shown (mean±SEM; n=3).

Figure 4 ELISA using anti-adenovirus monoclonal antibodies. Microtiter wells were coated with adenovirus intact particles and incubated with the indicated antibodies in serial dilutions. The mean of triplicates in one representative experiment is shown. There was no reactivity above background with the blocking protein used as a control (BSA).

Figure 5 ELISA using anti-adenovirus monoclonal antibodies and recombinant fiber knob. Microtiter wells were coated with recombinant fiber knob at 2 μg/ml and incubated with the indicated antibodies. The mean of triplicates in one representative experiment is shown. There was no reactivity above background with the blocking protein used as a control (BSA).

Figure 6 Neutralization of Ad5 infection by anti-adenovirus monoclonal antibodies. Shown are the % of lacZ-positive cells (100% corresponds to the number of positive cells observed with an irrelevant antibody. The data presented are the means of two duplicate wells in two independent experiments.

Figure 7 Immunofluorescence images showing adenovirus staining of infected cell monolayers using anti-adenovirus monoclonal antibodies. DAPI was used for nuclear staining.

Figure 8 (a) MDP receptor-targeted sensitization of MDA-MB-435 breast cancer cells to adenovirus mediated gene transfer. MDA-MB-435 breast cancer cells were seeded, grown for 24h and then incubated adenovirus carrying a lacZ reporter gene. The vector was incubated with the cells in the presence of various concentrations of either Fab, Fab-CARAC or Fab-GFE conjugates for 90 minutes. ß-galactosidase expressing cells were visualized with Xgal 24h following the onset of Ad-infection. ß-gal positive cells were counted microscopically. **(b) Fc receptor-targeted sensitization of MDA-MB-435 breast cancer cells to adenovirus mediated gene transfer.** MDA-MB-435 breast cancer cells were seeded, grown for 24h and then incubated adenovirus carrying a lacZ reporter gene. The vector was incubated with the cells in the presence of various concentrations of either the 1C5IIE11 antibody or its Fab fragment for 90 minutes. ß-galactosidase expressing cells were visualized with Xgal 24h following the onset of Ad-infection. ß-gal positive cells were counted microscopically.

Table 1. Expression of CD13/APN in normal and tumor vasculature

anti-CD13 monoclonals:	WM15 ab	1H4 ab
blood vessels in normal organs		
brain	-	-/+
kidney	-	-
skin	-	-
liver	-	-
lung	-	-
spleen	-	-
intestine	-	-
heart	-	-
retina	-	-
spinal cord	+/-	+/-
tumor vasculature*		
endothelial cells	++++	++++
pericytes	++++	+++

*Human tumors tested: breast, colon, gastric, and esophageal carcinomas. Analysis of normal mouse tissues and tumors (MDA-MB-435 and Kaposi's sarcoma) with anti-mouse anti-CD13 antibodies (R3-63 and 2M7) showed similar results.

Table 2
DAMD17-98-1-8041

Clone	Isotype	Fiber knob binding	Neutralization	ELISA	IF	Western Blot	IP	Over all rating of affinity
3B2ID10	IgG2b	+++	++	++	++	−	+++	++
1C5IIE11	IgG2b	++	+++	+++	++	−	+++	+++
5C7IB3	IgG1	−	(+)	+	−	−	+	+
10C3E11	IgG2b	(+)	(+)	++	−	−	+	+
9D12H2	IgG1	(+)	(+)	+	−	-	+	+
10G6A1	IgG2b	−	−	+	−	−	+	+

Figure 1
DAMD17-98-1-8041

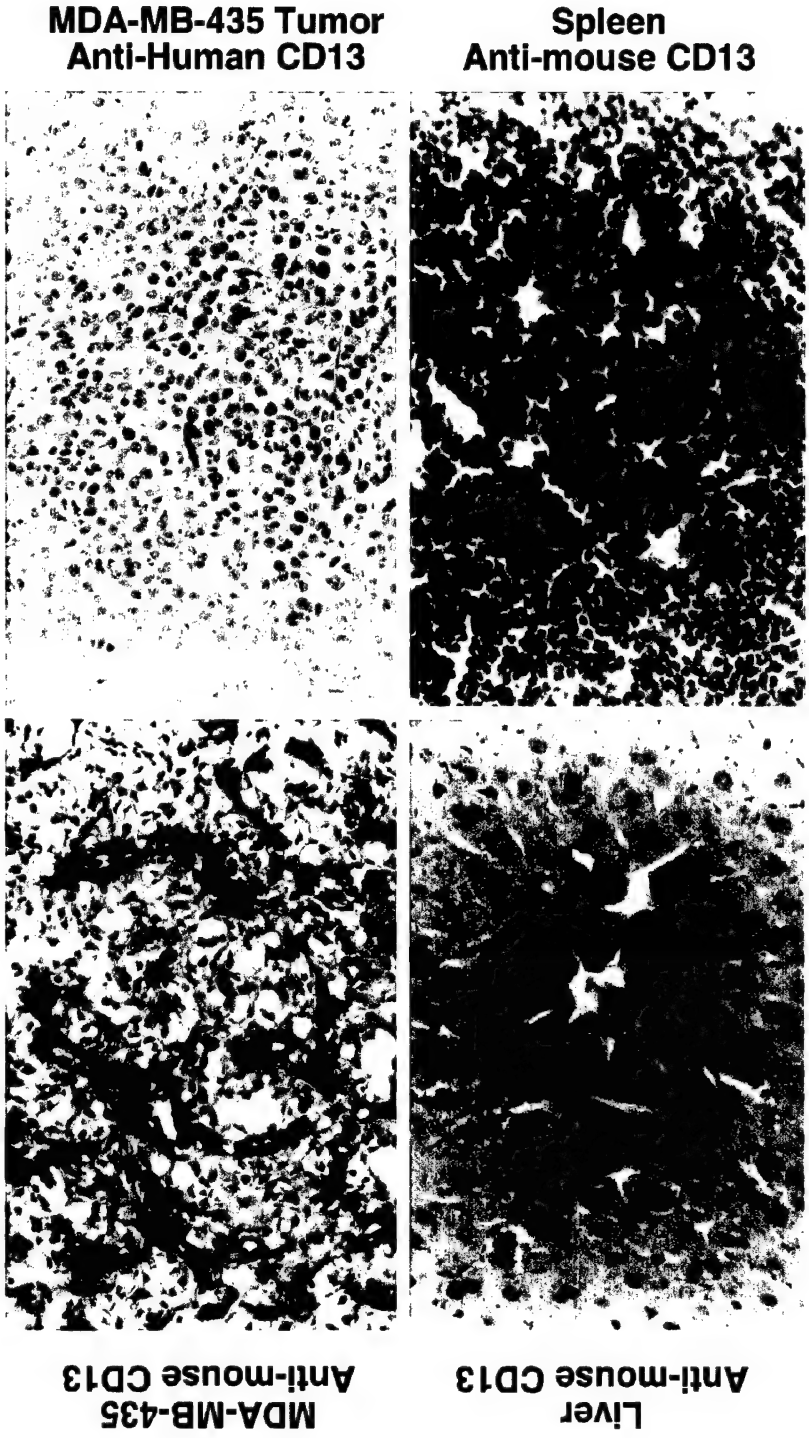

Figure 2
DAMD17-98-1-8041

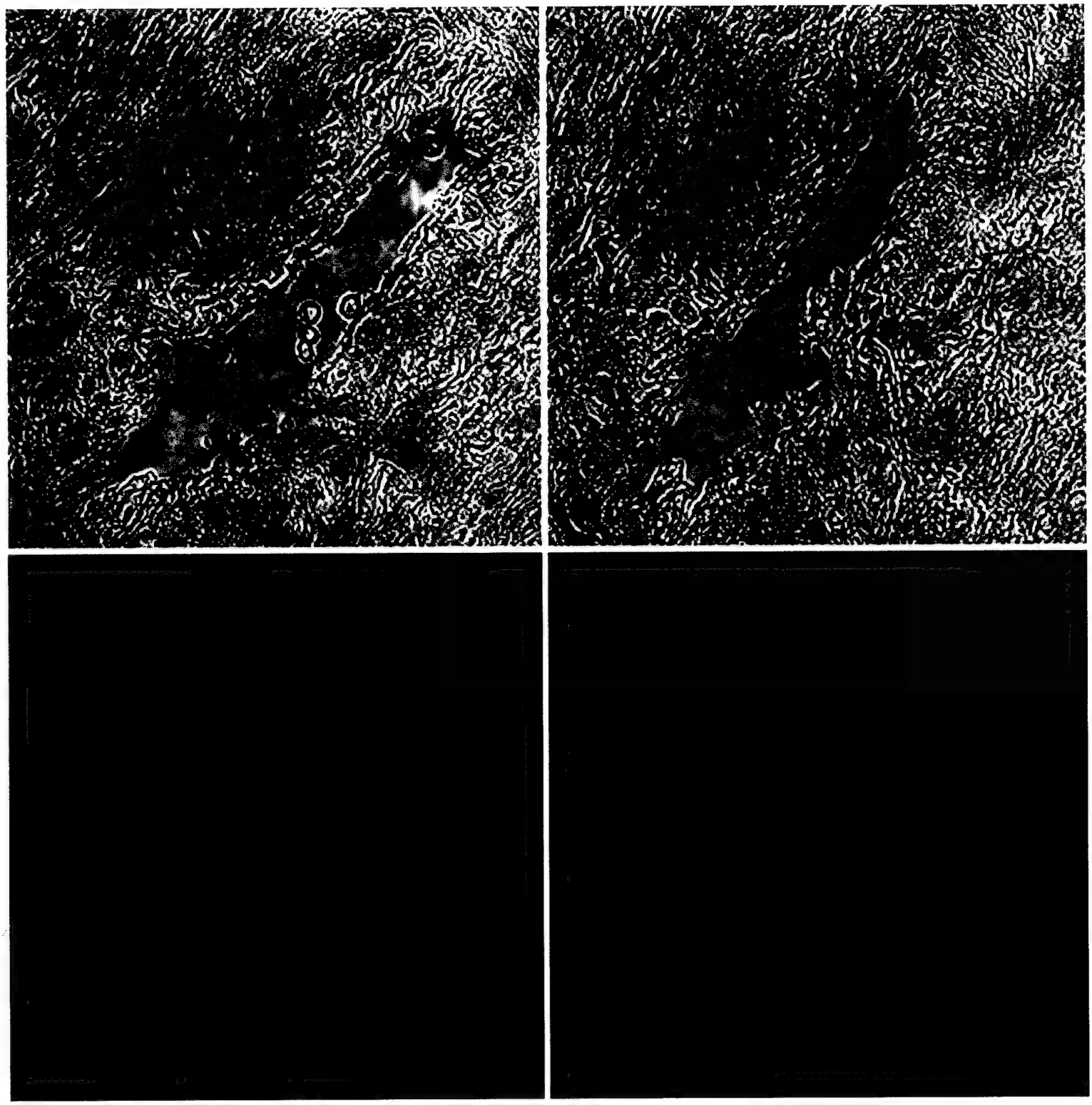

Figure 3
DAMD17-98-1-8041

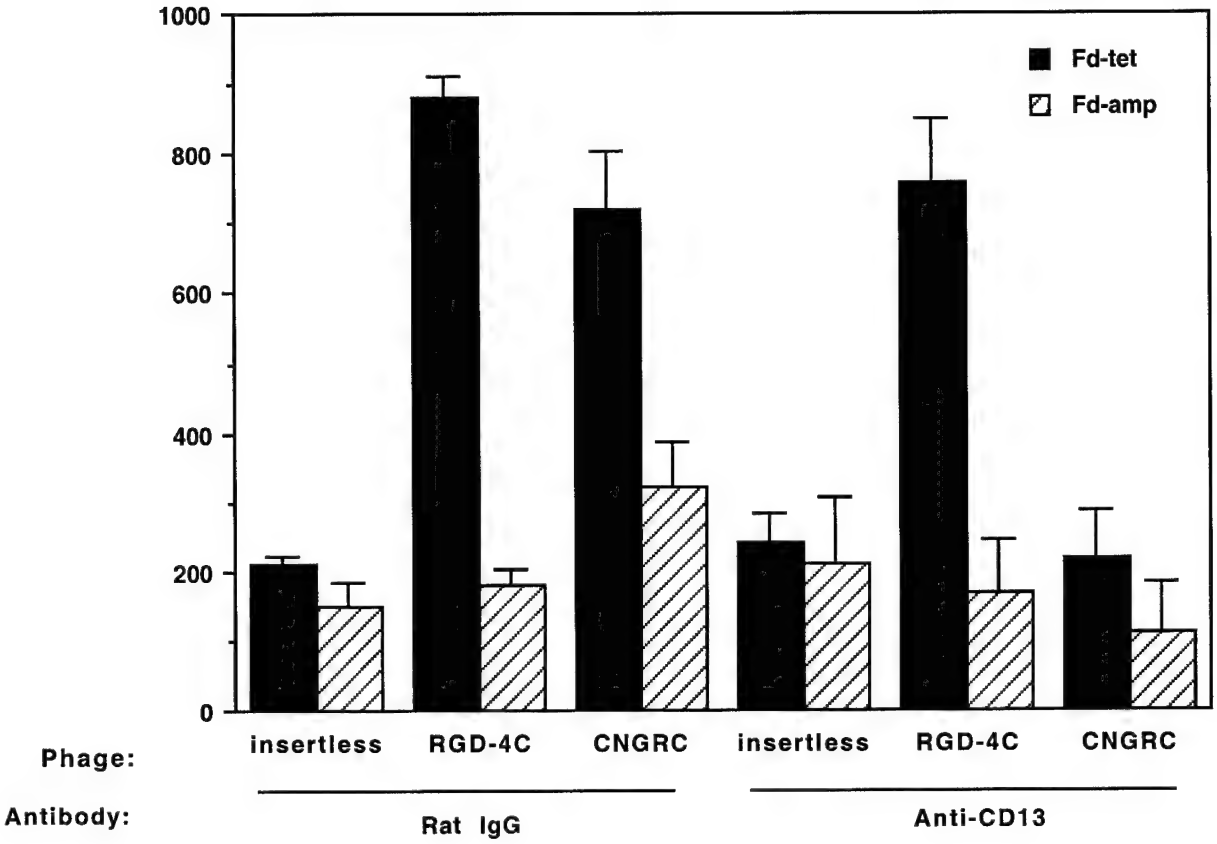

Figure 4
DAMD17-98-1-8041

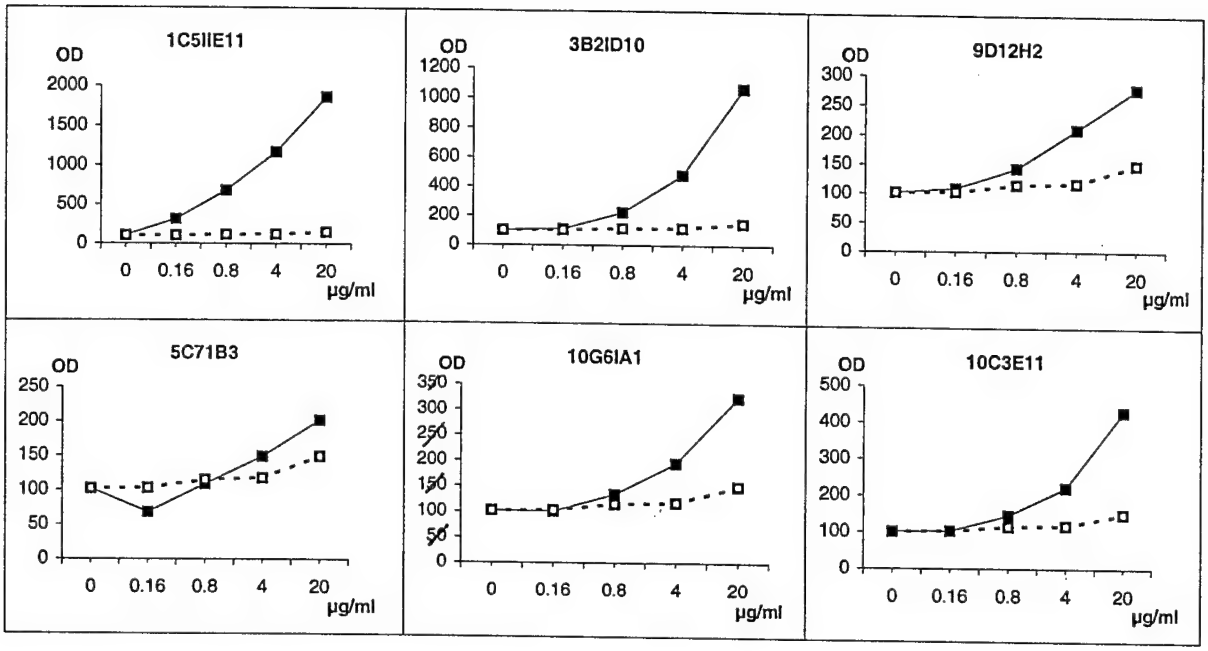

Figure 5
DAMD17-98-1-8041

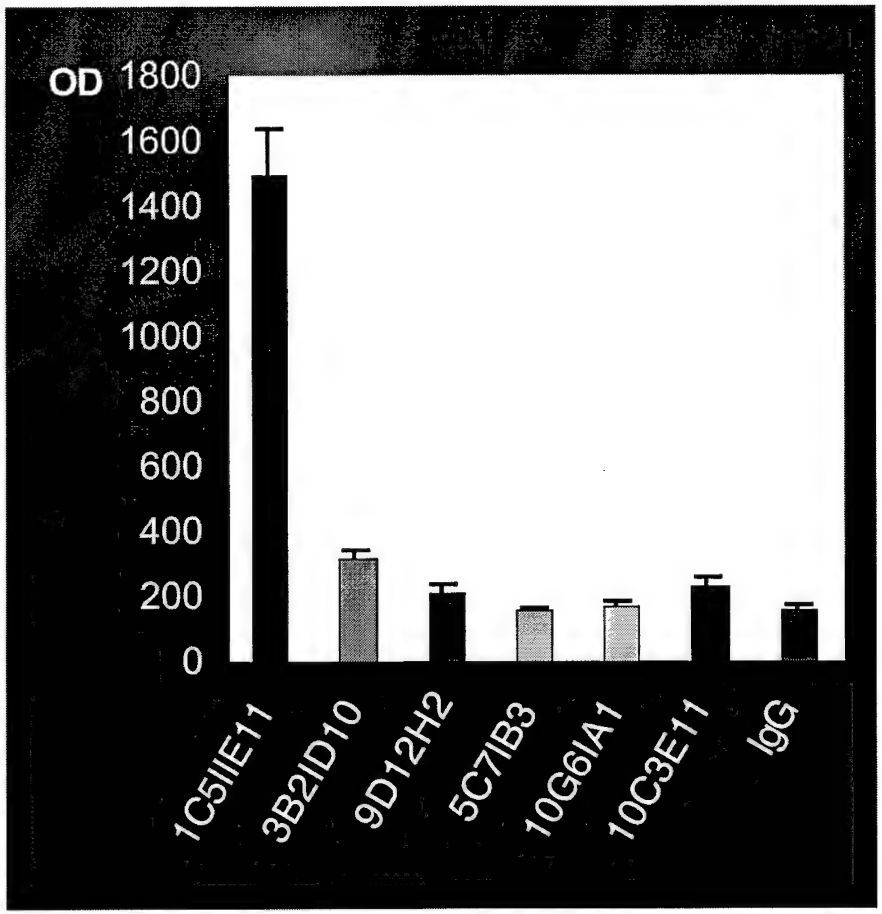

Figure 6
DAMD17-98-1-8041

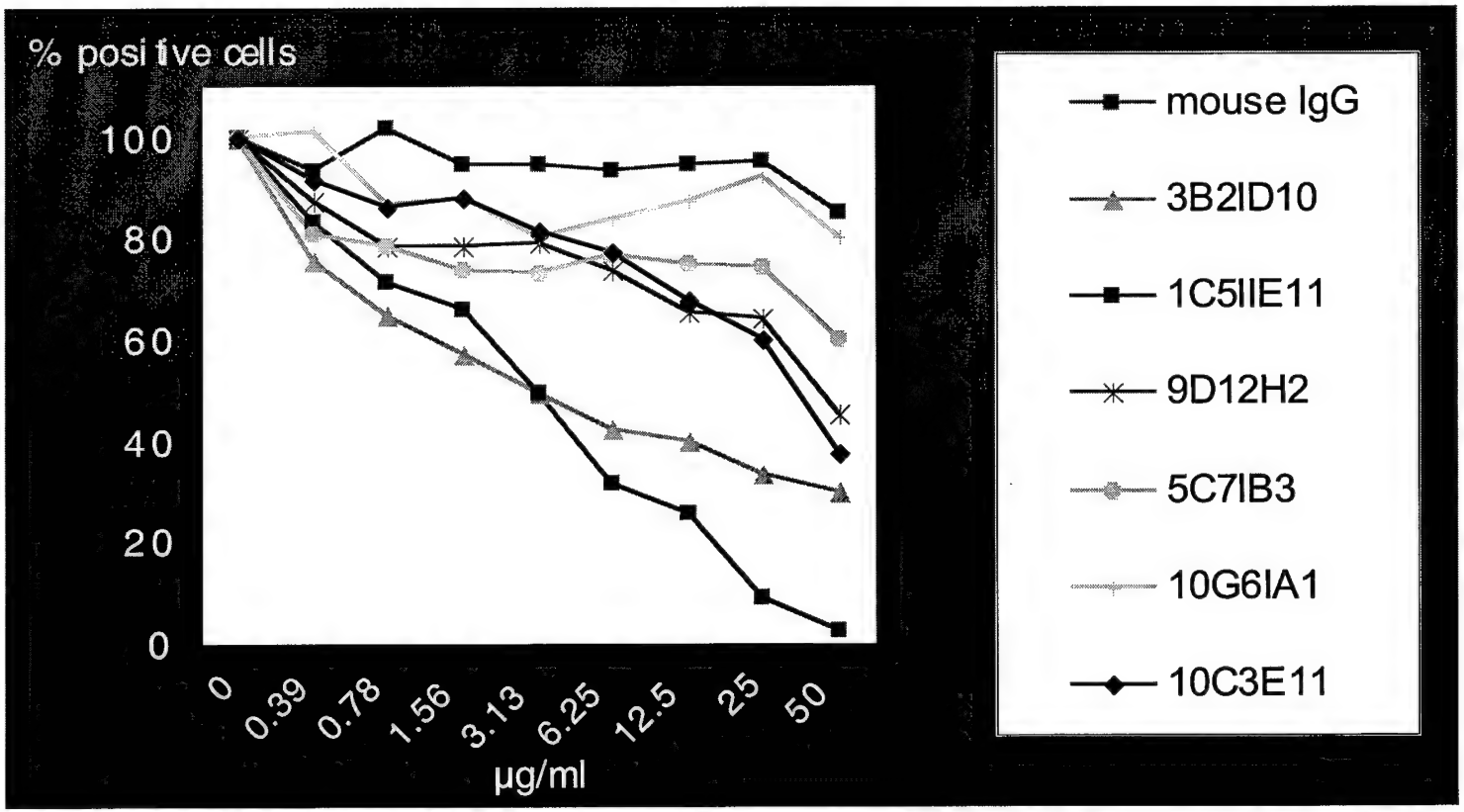

Figure 7
DAMD17-98-1-8041

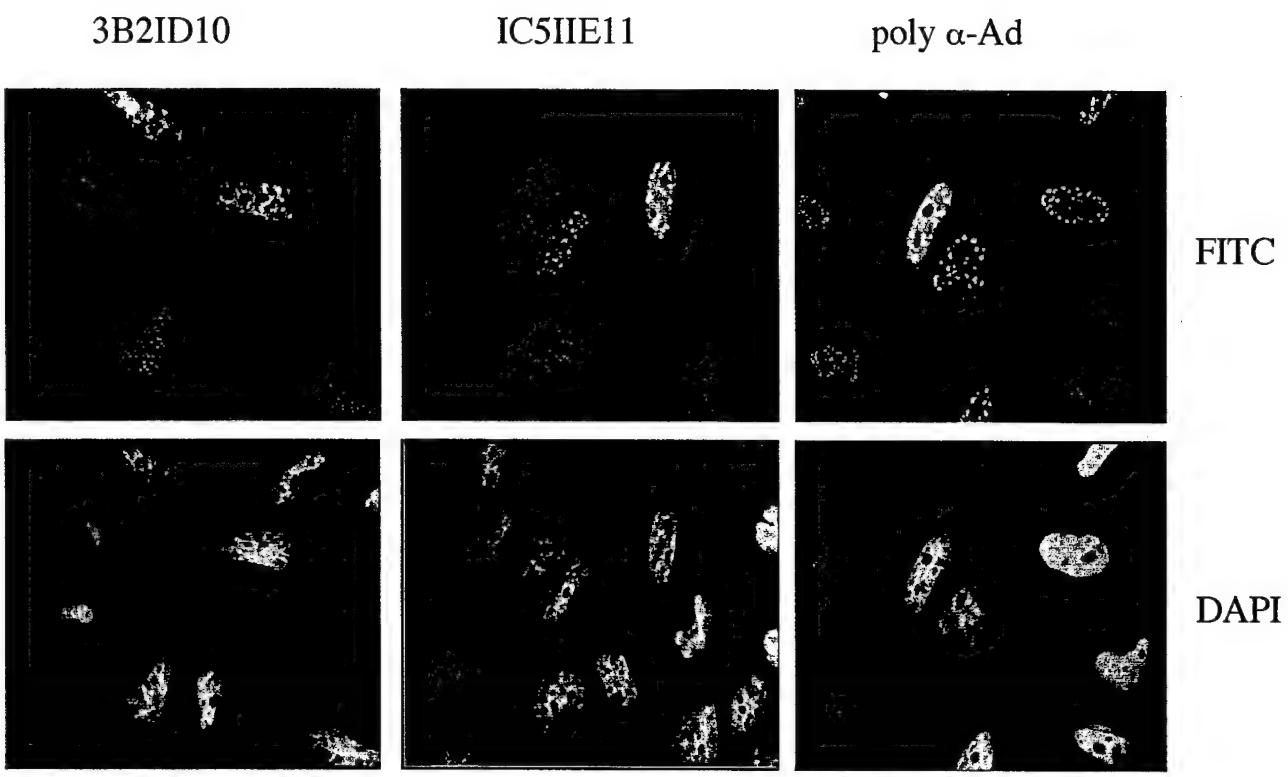

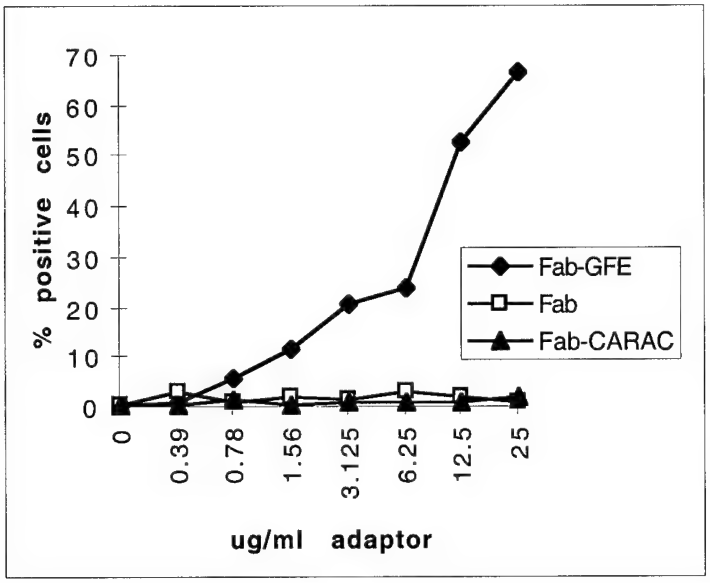

Figure 8a
DAMD17-98-1-8041

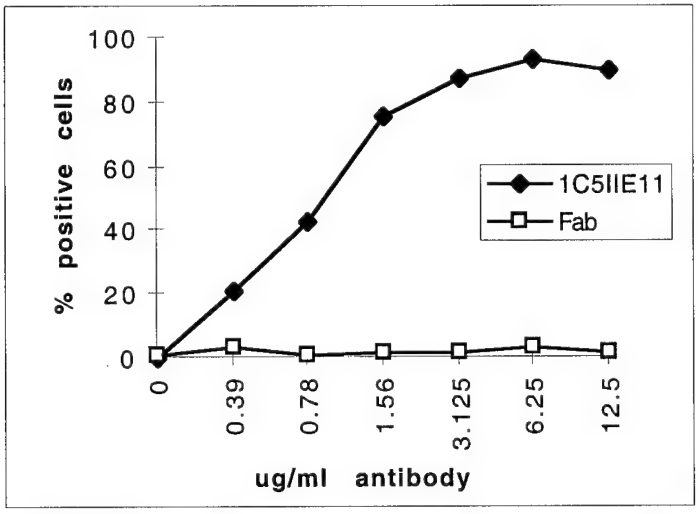

Figure 8b
DAMD17-98-1-8041

αv Integrins as receptors for tumor targeting by circulating ligands

Renata Pasqualini*, Erkki Koivunen[1], and Erkki Ruoslahti*

La Jolla Cancer Research Center, The Burnham Institute, La Jolla, CA, and [1]Department of Biosciences, Division of Biochemistry, University of Helsinki, Finland.
**Corresponding authors: (e-mail: rarap@ljcrf.edu [RP]; ruoslahti@ljcrf.edu [ER]).*

Received 14 January 1997; accepted 3 April 1997

Phage displaying an Arg-Gly-Asp (RGD)-containing peptide with a high affinity for αv integrins homed to tumors when injected intravenously into tumor-bearing mice. A substantially higher amount of αv-directed RGD phage than control phage was recovered from malignant melanomas and breast carcinoma. Antibodies detected the αv-directed RGD phage in tumor blood vessels, but not in several normal tissues. These results show that the αv integrins present in tumor blood vessels can bind circulating ligands and that RGD peptides selective for these integrins may be suitable tools in tumor targeting for diagnostic and therapeutic purposes.

Keywords: phage display, tumor targeting, RGD, angiogenesis, integrins

Endothelial cells in different parts of the vasculature are not alike; various organs and tissues express specific endothelial surface markers, while a separate set of surface molecules marks the endothelium at sites of inflammation[1–6].

Tumor vasculature undergoes continuous angiogenesis and expresses molecular markers that characterize these vessels. The markers in angiogenic endothelium include certain receptors for vascular growth factors, such as various VEGF receptors[7–13], and the αvβ3 integrin[14]. Preventing the αvβ3 integrin, and in some cases αvβ5, from binding to their ligands causes apoptosis in the endothelial cells of newly formed blood vessels[15,16]. Peptides that mimic ligands of these integrins and anti-integrin antibodies capable of inhibiting their ligand-binding have antitumor effects[16,17]. Blockers of αv integrins also show promise as inhibitors of pathological angiogenesis in other situations, such as in retinopathy[18].

An immunohistochemical study indicates that various integrins, including αvβ3, can be expressed on the apical surface of blood vessels[19]. We asked whether αvβ3 integrins are active and available for binding of circulating ligands and whether the expression levels of this integrin in tumor and normal vasculature are sufficiently different to permit tumor targeting.

We recently developed an in vivo targeting system that uses peptides expressed on the surface of bacteriophage to study organ-specific targeting[6]. Peptides in as many as 10^9 permutations are expressed on the surface of phage where the peptide is fused to one of the phage surface proteins[20]; in the in vivo procedure, phage capable of homing into certain organs or tissues following an intravenous injection are selected from such a peptide library. The ability of individual peptides to target a tissue can also be analyzed by this method[6].

We use phage-displayed peptides to target tumors, focusing on targeting of αv integrins in tumor blood vessels with a selected peptide. Many integrins, the αv integrins in particular, recognize an Arg-Gly-Asp (RGD) sequence as the critical determinant in their ligands. Peptides containing the RGD sequence are commonly employed as specific probes for the various integrins[21]. We used a nine-amino acid peptide that contains an RGD sequence in a cyclic conformation with two disulfide bonds, which is highly selective for the αv integrins[22]. We have found that phage bearing this cyclic nonapeptide, CDCRGDCFC, become selectively concentrated in tumors, suggesting that αv-directed peptides can be useful in diagnostic and therapeutic tumor targeting.

Results

Targeting of CDCRGDCFC-phage into tumors. We studied the distribution of phage carrying the CDCRGDCFC peptide (RGD-4C phage) and various control phage after intravenous injection into tumor-bearing nude mice. MD-MBA-435 human breast cancer tumor (diameter 1–1.5 cm) grown in the mammary fat pad was used as the initial target. The phage was rescued from the tissues 4 min after the injection, and the number of phage per gram of tissue was quantitated. The control phage mixture shows no appreciable enrichment in any organ without multiple rounds of selection, allowing comparison of the RGD-4C phage distribution with that of unselected control phage. The control phage mixture (and several individual phage used as additional controls, see below) were found in about 20-fold higher levels in the two normal tissues studied, the brain and the kidney, than in the tumors (Fig. 1A); the difference probably reflects greater blood flow into these normal organs than into tumor tissue. In contrast, twofold to threefold more of the RGD-4C phage was rescued from the tumors than from the control tissues, and less of this phage was found in the control tissues than of the control phage.

We have also quantitated the RGD-4C phage in tumor and brain tissues obtained after the mice were perfused through the heart, and have found that 20-fold more RGD-4C phage can be recovered from the tumor (not shown). This observation is in agreement with the immunostaining data detailed below (performed under the same conditions), which also show that the majority of phage in the normal tissues is not bound to the tissues, and it is likely to represent background.

The difference in the amount of the RGD-4C phage relative to the control unselected phage mixture was, on average, tenfold

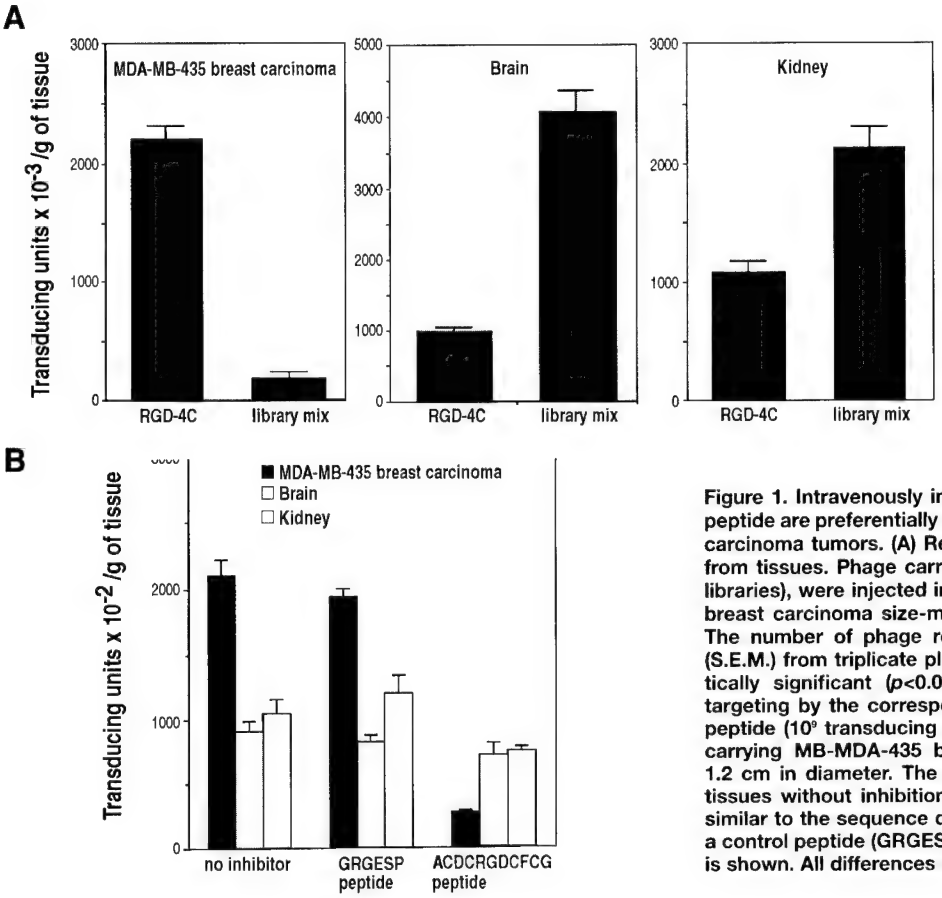

Figure 1. Intravenously injected phage carrying an αv-directed RGD peptide are preferentially recovered from MDA-MB-435 derived breast carcinoma tumors. (A) Recovery of αv-directed CDCRGDCFC-phage from tissues. Phage carrying the peptide, or pooled phage (CX5-7C libraries), were injected in the tail vein of mice bearing MDA-MB-435 breast carcinoma size-matched tumors (about 1.2 cm in diameter). The number of phage recovered and standard error of the mean (S.E.M.) from triplicate platings are shown. All differences are statistically significant ($p<0.001$). (B) Inhibition of CDCRGDCFC-phage targeting by the corresponding soluble peptide. Phage carrying the peptide (10^9 transducing units) were injected in the tail vein of mice carrying MB-MDA-435 breast carcinoma tumors that were about 1.2 cm in diameter. The amounts of phage recovered from various tissues without inhibition and in the presence of a soluble peptide similar to the sequence displayed by the phage (ACDCRGDCFCG) or a control peptide (GRGESP) are shown. S.E.M. from triplicate platings is shown. All differences are statistically significant ($p<0.001$).

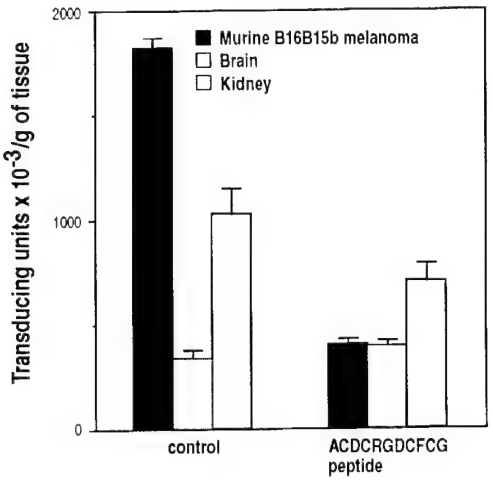

Figure 2. Targeting of the CDCRGDCFC-phage into B16B15b murine melanoma tumors. Phage carrying the peptide (10^9 transducing units) were injected in the tail vein of mice bearing tumors that were about 1 cm in diameter. The phage was coinjected with 500 μg of either the corresponding soluble peptide, ACDCRGDCFCG, or a control peptide (GRGESP). The number of phage recovered is shown. S.E.M. from triplicate platings is shown; all differences are statistically significant ($p<0.001$).

(10 independent experiments). Taking into account this difference and also the lower background of the RGD-4C phage in the control organs, the overall tumor selectivity of the RGD-4C phage is estimated to be in the range of 40-fold to 80-fold. In addition, the specificity of the RGD-4C localization into the tumors was further demonstrated by a substantial reduction in the tumor accumulation upon coinjection of the cognate RGD peptide, ACDCRGDCFCG, (Fig. 1B). Coinjection of a control peptide, which has no appreciable affinity for integrins (GRGESP), had no effect; similar results were obtained in six experiments. In contrast to what was seen in the tumors, the RGD-4C peptide reduced only slightly, or did not affect at all, the amount of RGD-4C phage recovered from brain and kidneys, supporting the conclusion that the phage was nonspecifically trapped in these organs. Another RGD phage, which carries a peptide selective for the α5β1 integrin, CRGDGWC (ref. 22), was also tested. It was found to be similar to the control phage mixture, showing no preferential accumulation into the MDA-MB-435–derived tumors (data not shown).

The RGD-4C phage also accumulated preferentially into subcutaneous murine B16B15b melanoma (Fig. 2) and human C8161 melanoma tumors (data not shown). The tumor homing was, in each case, greatly reduced by coinjection of the cognate peptide, but not by the GRGESP control peptide (Fig. 2). We also observed that when the C8161-derived and MDA-MB-435–derived tumors were smaller than 0.5 cm, less specific targeting was seen than with

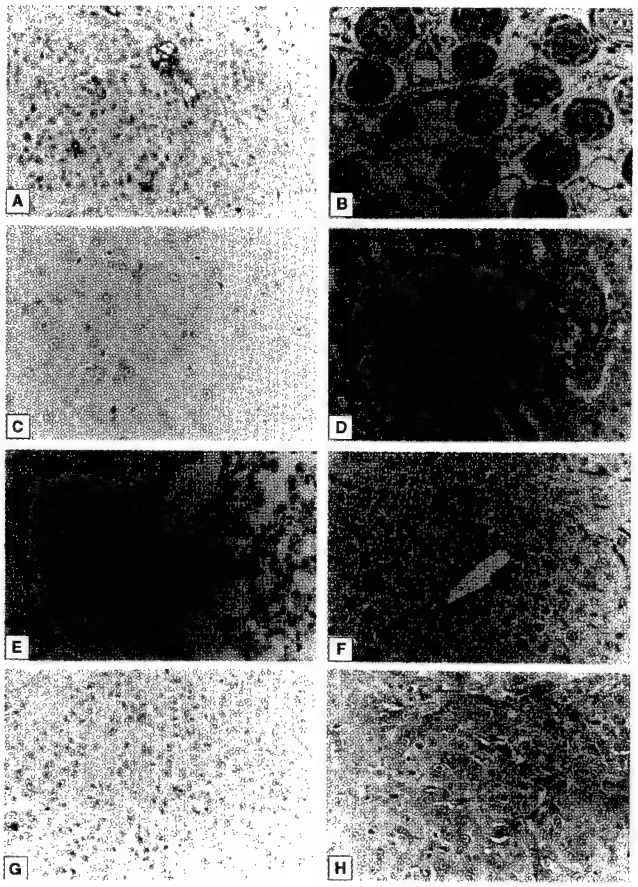

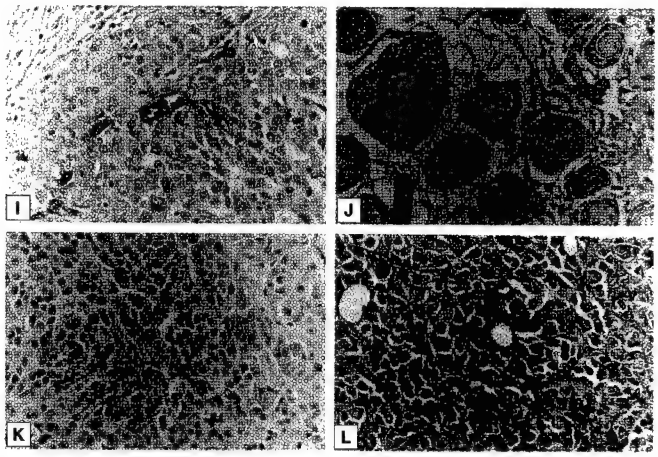

Figure 3. Immunohistochemical staining of phage in tumors and tissues of tumor-bearing mice. Phage carrying the αv-directed peptide CDCRGDCFC or insertless control phage were injected intravenously into mice. An antibody against M13 phage and a polyclonal anti-αvβ3 were used for staining. (A through F) Mice that received the phage carrying the αv-directed peptide CDCRGDCFC. (A) MDA-MB-435 breast carcinoma tumor tissue. (B) Skin adjacent to the tumor. (C) Brain. (D). Kidney. (E) Lung. (F) Liver. (G) Phage staining of MDA-MB-435 tumor tissue from a mouse that received insertless phage. (H) MDA-MB-435 tumor tissue stained with anti-αvβ3 antiserum. (I through L) Mice bearing B16B15b-derived melanoma. (I and J) Mice injected with the phage carrying the αv-directed peptide CDCRGDCFC. (I) Tumor. (J) Skin adjacent to the tumor. (K) Phage in tumor tissue from mice that received the insertless phage. (L) Tumor tissue stained with the anti-αvβ3 antiserum. Magnification = 400x.

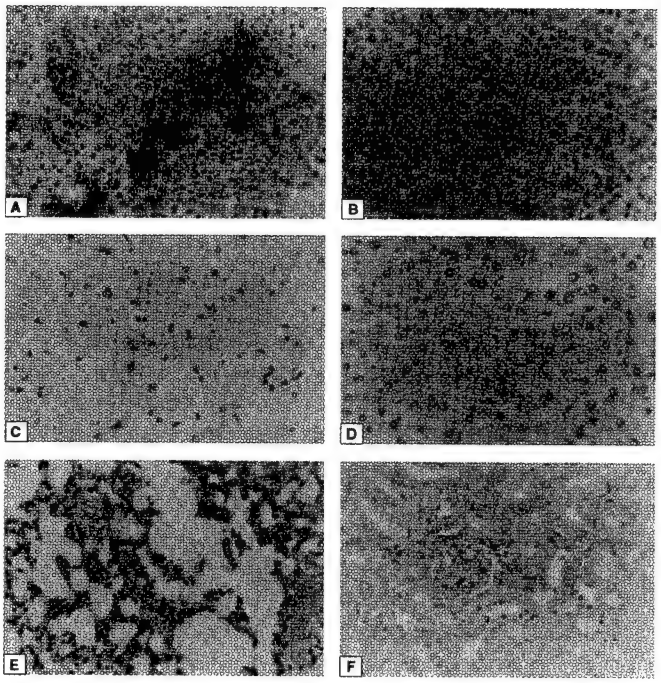

Figure 4. Detection of phage antigens in tissues 24 h after intravenous injection. Phage carrying the αv-directed peptide CDCRGDCFC or insertless control phage were injected intravenously into mice. (A, C, E, F) Mice that received the phage carrying the αv-directed peptide CDCRGDCFC. (A) MDA-MB-435 breast carcinoma tumor tissue. (C) Brain. (E) Lung. (F) Kidney. (B) Phage staining of MDA-MB-435 tumor tissue from a mouse that received insertless phage. (D) Brain tissue from an animal injected with a brain-selective phage (CSSRLDAC-phage[6]). Magnification = 100x.

larger tumors. This is likely due to the lower degree of vascularization in the smaller tumors, which we observed by staining for von Willebrand factor as a marker of blood vessels.

Immunohistochemical staining of phage in tumors and tissues of tumor-bearing mice. The phage experiments described above were performed by quantitating the phage in tissue extracts after a short circulation time. This experimental arrangement was chosen to avoid having the specifically bound phage be taken up by the cells and inactivated. However, we did note that perfusion of the mice through the heart reduced the background phage counts in the nontumor tissues. As any phage inactivation was not likely to be critical in immunostaining experiments, the mice were perfused prior to processing the tissues for staining. Marked staining for the phage was seen in an MDA-MB-435–derived breast carcinoma tumor from an animal injected with the RGD-4C phage (Fig. 3A), whereas injection of the control phage mixture or an insertless control phage (Fig. 3G) gave no staining in size-matched tumors. The staining observed in the tumors followed the small blood vessels and appeared to localize to the endothelial lining. Control tissues (skin adjacent to the tumor, brain, kidney, and lung) from animals injected with the RGD-4C phage showed no staining (Figs. 3B to E).

In keeping with the previously observed capture of circulating phage into tissues containing a reticuloendothelial system (RES) component[6], both the RGD-4C and control phage caused staining in the liver (Fig. 3F). Phage quantitation experiments have shown that the liver uptake of the phage can be prevented by coinjecting the mice with an excess of noninfective fuse 5 phage (not shown). This and the fact that the liver localization was independent of the peptide carried by the phage clearly indicate that the liver uptake is a property of the phage, not of the peptide.

Immunostaining also localized the RGD-4C phage to blood

vessels within the melanoma tumors (Fig. 3I). The skin adjacent to the tumor was not stained (Fig. 3J) and control phage gave no staining in the tumor (Fig. 3K).

The MDA-MB-435 carcinoma and the B16B15b melanoma cells express the αvβ3 integrin, as determined by FACS analysis (data not shown). Immunostaining of tumor sections with a polyclonal anti-αvβ3 antibody revealed staining of both the tumor tissue and the blood vessels in it (Figs. 3H and L).

To mimic more closely a clinically relevant tumor-targeting situation, we have also conducted a series of experiments in which the αvβ3-directed RGD phage was allowed to circulate for 24 h prior to harvesting of the tissues for immunostaining. At the 24 h time point, about 90% of the phage had been eliminated from the circulation. Immunostaining revealed phage proteins in and around the small blood vessels within the tumor (Fig. 4A), but all other organs studied (with the exception of the liver and the spleen) were negative (Fig. 4B, C, E, and F). A phage carrying a brain-homing peptide stays inside the blood vessels, even after 24 h (Fig. 4D).

Discussion

We have shown that an RGD peptide selective for αv integrins can direct phage displaying such a peptide to home into tumors. Blood vessels appear to be the structural component targeted by the phage displaying the αv-directed peptide.

We used peptides displayed on phage as a probe in our tumor targeting experiments. While phage as a carrier has some limitations, such as being taken up by the RES[6,23], it can serve to illustrate the potential of peptides to target materials into selected tissues. In this regard, the phage mimics the targeting of particles, such as liposomes, as well as the viruses used in gene therapy. The phage can readily be detected in tissues both by counting infectious phage particles and by employing immunohistochemistry. Moreover, the specificity of the RGD-4C phage can be assessed by inhibiting the localization with free peptide and by using control phage that carry another peptide or no peptide at all.

Several observations attested to the specificity of the tumor targeting by the αv-directed RGD-4C phage and the peptide displayed by it. First, only the phage carrying the RGD-4C peptide accumulated in tumors, whereas phage carrying another RGD peptide with a different integrin specificity or phage with unrelated inserts did not (except those we have specifically selected for tumor homing after multiple rounds, data not shown). Secondly, the difference between the tumor accumulation of the RGD-4C phage and various control phage was substantial, an average of tenfold. Taking into account the lower background of the RGD-4C phage in nontumor tissues, the estimated tumor selectivity of this phage is even more impressive. Thirdly, the cognate peptide inhibited the tumor homing of the RGD-4C phage. This latter result shows that the phage homing is dependent on the peptide displayed by the phage, and is not caused by some other coincidental property of the phage. Another control, lack of any effect by a control peptide on the tumor homing of the RGD-4C phage, further substantiates the specificity.

The large difference in the tumor homing of the RGD-4C phage relative to control phage reflects the potential of the system in tumor targeting. We did recover significant quantities of the RGD-4C phage from various control organs in the experiments that used phage counting as the read-out. However, at least a majority, if not all, of this phage recovery represents nonspecific background, because it was not reduced upon coinjection of the cognate peptide. Moreover, perfusion of the mice greatly improved the tumor tissue/normal tissue ratio. Examination of histological sections of the tumors revealed fewer blood vessels in the tumors than, for example, in the brain (Fig. 3), suggesting that the background phage level in a given tissue may reflect the number of blood vessels in that tissue.

The liver and spleen, unlike the other normal tissues we analyzed, contained phage detectable by immunostaining even after perfusion, which tends to minimize or eliminate background in other organs. The RES is known to capture circulating particles, including phage[23], and this appears to be the reason for the presence of phage in liver and spleen. Administration of noninfective phage prevents the capture by the RES of phage from a coinjected peptide library (data not shown), making it possible to reduce or eliminate this limitation of the phage targeting system. As the liver uptake is property of the phage, and not related to the peptide carried by the phage, it is not likely to limit the tumor-targeting potential of the RGD-4C peptide. This potential is illustrated by the high overall tumor selectivity; the expectation is that other materials coupled to the same peptide would display similar preference for tumors.

Even though both the endothelia and the tumors themselves expressed the αv integrin(s) targeted by the RGD-4C peptide, our observations indicate that the RGD-4C phage binds to the blood vessels within the tumors. Endothelial binding of the phage was strongly suggested by the staining results, which showed that the phage is confined to the tumor blood vessels. Our earlier results with phage targeting into the brain and kidney also showed exclusive blood vessel localization of the phage[6]. The endothelium is a likely—and the tumor cells an unlikely—target for the RGD-4C phage (and targeting using phage-displayed peptides in general). The large size of the phage (900 nm in length) makes it unlikely that the phage would exit the circulation and penetrate into tissues[24], particularly within the few minutes we allowed the phage to circulate. Moreover, the vasculature is a likely common denominator for the three tumors we targeted with the RGD-4C phage, because the tumors came from two different species (murine and human) and represented two distinct tumor types (melanoma and carcinoma). As blood vessels in tumors are known to be "leaky"[24–28], it may be that in vivo screening will also yield phage capable of binding to receptor molecules in the parenchyma of tumors.

RGD peptides are generally accepted as probes for integrin functions in vitro and in vivo. Moreover, drugs are being developed based on peptides and their mimetics that specifically block individual integrins[21]. Blocking ligand binding by the αvβ3 (or αvβ5) integrin with RGD peptides or antibodies shows promise as an antiangiogenic therapy. Such treatment causes apoptosis in those endothelial cells that are in the process of forming new blood vessels, while not harming established blood vessels[14–18]. These results imply that αv integrin(s), while accessible to soluble peptides and antibodies in neovasculature, are engaged in endothelial cell interactions with the underlying extracellular matrix. However, in agreement with immunohistochemical studies showing αvβ3 on the apical surface of blood vessels[19], our results show that sufficient amounts of these integrins are accessible to a particulate ligand from the circulation, and that the available integrin is concentrated in tumor vasculature.

The experimental paradigm in which RGD-C–phage was allowed to circulate for 24 h parallels an actual drug targeting into a tumor in a clinical setting. Under these conditions the tumor contained substantial phage staining, whereas less than 10% of the injected phage was left in the circulation, and all normal tissues examined, except the RES, were devoid of phage staining. The breast carcinoma cells used in these experiments express the αvβ3 integrin as do many human tumors[14], and binding of the phage to the tumor cells may have contributed to the staining outside the blood vessels in the 24-h experiments. These results suggest that it may be possible to use αv-directed reagents, either peptides or antibodies, to carry drugs, radionuclides, genes, and other thera-

peutic substances and devices into tumor vasculature, and from there, into tumor parenchyma. Peptides may have advantages in this regard, because they are smaller, more likely to diffuse efficiently within the tumor, and less likely to be immunogenic.

Experimental protocol

Animals. Female 2-month old nude mice (Harlan Sprague Dawley, San Diego, CA) were used in this study. The animals were cared for according to the Institute's animal facility guidelines. Avertin (0.015 ml/g) was used as anesthetic.

Cell lines and tumors. The human tumor cells used in this study were: human MDA-MB-435 breast carcinoma[29], murine B16B15b melanoma[30], and C8161 human melanoma[31]. Cells were cultured in DMEM, 10% FCS (Irvine Scientific, Irvine, CA) with sodium pyruvate, L-glutamine, and penicillin/streptomycin (Gibco BRL, Bethesda, MD). Culture medium was changed 12 h before the cells were injected into mice. Cells were detached from monolayers at 80% confluence with PBS containing 2.5 mM EDTA, washed three times with DMEM, counted, and resuspended in DMEM. Tumor cells were injected in the mammary fat pad (10^5 per site); tumor growth was monitored daily. Between 20 to 40 days postinjection, when the tumors were 0.4 to 1.5 cm in diameter, animals bearing tumors of similar sizes were selected and used for targeting experiments and histological analysis.

Tumor targeting. Phage (10^9 transducing units) were injected intravenously into mice carrying tumors, and the phage that had accumulated in the tumor and in various tissues were quantitated as described[6], with minor modifications. In brief, 2 to 4 min after the injection, the mice were snap frozen in liquid nitrogen while under deep anesthesia. To recover the bound phage, the carcasses were partially thawed at room temperature, and organs and tumors were removed, weighed, and ground in 1 ml of DMEM-PI (DMEM containing the protease inhibitors phenyl methyl sulphonyl fluoride (1 mM), aprotinin (20 μg/ml), and leupeptin (1 μg/ml). Tissue and tumor samples were washed three times with ice-cold DMEM-PI containing 1% BSA and incubated with 1 ml of competent K91-kan bacteria for 20 min at room temperature. Ten milliliters of NZY medium containing 0.2 μg/ml tetracycline were added, the mixture was incubated at room temperature for 20 min, and 5 to 50 μl aliquots diluted in 100 μl of TBS/1% gelatin were plated in agar plates in the presence of 40 μg/ml of tetracycline. After 12 h, the colonies were counted. In peptide inhibition experiments, phage were coinjected with 500 μg of ACDCRGDCFCG or GRGESP. The peptides, ACDCRGDCFCG and GRGESP, were synthesized by Immunodynamics Inc. (San Diego, CA) and purified to homogeneity by HPLC. The ACDCRGDCFCG peptide (RGD-4C) is a cyclic peptide that reproduces the sequence of the insert in a phage isolated from a peptide-display library and includes two amino acids from the phage sequence as flanking exocyclic residues at each end[22]. As the present experiments were carried out in mice, we confirmed that the RGD-4C peptide binds specifically to αv integrins in mouse endothelial cells (Bend 3)[32] by showing that the attachment of these cells to vitronectin (an αv integrin function) could be inhibited without affecting their attachment to fibronectin or laminin, which are β1 integrin functions (results not shown). Control experiments also showed that none of the peptides used in this work affected the ability of the phage to infect bacteria. The selectivity of the RGD-4C towards tumors was calculated based on multiple parameters; (1) the overall number of RGD-4C phage recovered from the tumors, brain, and kidney; (2) the background counts found in tumors, brain, and kidney for unselected phage mixtures (which is high in brain and kidney); and (3) the lower background of the RGD-4C phage in the control organs. A mixture of phage was used as a control in most of the experiments to eliminate the bias that the use of a single control phage might introduce in an experiment. We have, however, also used individual phage as controls.

Immunohistochemical staining of phage in tumor blood vessels. Tissue sections were prepared from mice injected with phage as described above; the anesthetized mice were then perfused through the heart with DMEM. In some experiments, the phage were allowed to circulate for 24 h. The organs and tumors were fixed in Bouin's solution; an antibody against M13 (Pharmacia, Piscataway, NJ) was used for the staining, followed by a peroxidase-conjugated secondary antibody (Sigma, St. Louis, MO), as described[6]. Tumor sections were also stained with a rabbit polyclonal antibody against αvβ3[32].

Acknowledgments

We thank Wadih Arap, Eva Engvall, and Kathryn Ely for comments on the manuscript, the Institute's Animal Facility staff for their assistance, and Garth Nicolson (University of Texas, M.D. Anderson Cancer Center) for the B16B15b melanoma cell line. This work was supported by grants CA 28896 and Cancer Center Support Grant CA 30199 from the National Cancer Institute. EK is supported by the Academy of Finland; RP was supported by the Arthritis Foundation and the Susan G. Komen Breast Cancer Foundation.

1. Pauli, B.U., Augustin-Voss, H.G., El-Sabban, M.E., Johnson, R.C., and Hammer, D.A. 1990. Organ-preference of metastasis. The role of endothelial cell adhesion molecules. *Cancer Metastasis Rev.* **9:**175–189.
2. Zetter, B.R. 1990. The cellular basis of site-specific tumor metastasis. *N. Engl. J. Med.* **322:**605–612.
3. Springer, T.A. 1994. Traffic signals for lymphocyte recirculation and leukocyte emigration: the multistep paradigm. *Cell* **76:**301–314.
4. Butcher, E.C. and Picker, L.J. 1996. Lymphocyte homing and homeostasis. *Science* **272:**60–66.
5. Goetz, D.J., El-Sabban, M.E., Hammer, D.A., and Pauli, B.U. 1996. Lu-ECAM-1-mediated adhesion of melanoma cells to endothelium under conditions of flow. *Int. J. Cancer* **65:**192–199.
6. Pasqualini, R. and Ruoslahti, E. 1996. Organ targeting in vivo using phage display peptide libraries. *Nature* **380:**364–366.
7. Baillie, C.T., Winslet, M.C., and Bradley, N.J. 1995. Tumour vasculature—a potential therapeutic target. *Br. J. Cancer* **72:**257–267.
8. Burrows, F.J. and Thorpe, P.E. 1994. Vascular targeting—a new approach to the therapy of solid tumors. *Pharmacol. Ther.* **64:**155–174.
9. Buckle, R. 1994. Vascular targeting and the inhibition of angiogenesis. *Ann. Oncol.* **4(suppl.):**45–50.
10. Mustonen, T. and Alitalo, K. 1995. Endothelial receptor tyrosine kinases involved in angiogenesis. *J. Cell Biol.* **129:**895–898.
11. Lappi, D.A. 1995. Tumor targeting through fibroblast growth factor receptors. *Semin. Cancer Biol.* **6:**279–288.
12. Martiny-Baron, G. and Marme, D. 1995. VEGF-mediated tumor angiogenesis: a new target for cancer therapy. *Curr. Opin. Biotechnol.* **6:**675–680.
13. Rettig, W.J., Garin-Chesa, P., Healey, J.H., Su, S.L., Jaffe, E.A., and Old, L.J. 1992. Identification of endosialin, a cell surface glycoprotein of vascular endothelial cells in human cancer. *Proc. Natl. Acad. Sci. USA* **89:**10832–10836.
14. Brooks, P.C., Clark R.A., and Cheresh, D.A. 1994. Requirement of vascular integrin αvβ3 for angiogenesis. *Science* **264:**569–571.
15. Friedlander, M., Brooks, P.C., Sharffer, R.W., Kincaid, C.M., Varner, J.A., and Cheresh, D.A. 1995. Definition of two angiogenic pathways by distinct αv integrins. *Science* **270:**1500–1502.
16. Brooks, P.C., Montgomery, A.M., Rosenfeld, M., Reisfeld, R.A., Hu, T., Klier, G., et al. 1994. Integrin αvβ3 antagonists promote tumor regression by inducing apoptosis of angiogenic blood vessels. *Cell* **79:**1157–1164.
17. Brooks, P.C., Stromblad S., Klemle R., Visscher D., Sarkar F.H., and Cheresh, D.A. 1995. Anti-integrin αvβ3 blocks human breast cancer growth and angiogenesis in human skin. *J. Clin. Invest.* **96:**1815–1822.
18. Hammes, H.-P., Brownlee, M., Joonczyk, A., Sutter, A., and Preissner, K.T. 1996. Subcutaneous injection of a cyclic peptide antagonist of vitronectin receptor-type integrins inhibits retinal neovascularization. *Nature. Med.* **5:**529–533.
19. Conforti, G., Dominguew-Jimenez, C., Zanetti, A., Gimbrone, M.A., Cremona, O., Marchisio, P.C., et al. 1992. Human endothelial cells express integrin receptors on the luminal aspect of their membrane. *Blood* **80:**437–446.
20. Smith, G.P. and Scott, J.K. 1993. Libraries of peptides and proteins displayed in filamentous phage. *Methods Enzymol.* **21:**228–257.
21. Ruoslahti, E. 1996. RGD and other recognition sequences for integrins. *Annu. Rev. Cell Dev. Biol.* **12:**697–715.
22. Koivunen, E., Wang, B., and Ruoslahti, E. 1995. Phage libraries displaying cyclic peptides with different ring sizes: ligand specificities of the RGD-directed integrins. *Bio/Technology* **13:**265–270.
23. Geter, M.R., Trigg, M.E., and Merril, C.R. 1973. Fate of bacteriophage lambda in non-immune germ-free mice. *Nature* **246:**221–223.
24. Shockley, T.R., Lin, K., Nagy, J.A., Tompkins, R.G., Dvorak, H.F., and Yarmush, M.L. 1991. Penetration of tumor tissue by antibodies and other immunoproteins. *Ann. N.Y. Acad. Sci.* **618:**367–382.
25. Dvorak, H.F., Nagy, J.A., and Dvorak, A.M. 1991. Structure of solid tumors and their vasculature: implications for therapy with monoclonal antibodies. *Cancer Cells* **3:**77–85.
26. Folkman, J. 1995. Angiogenesis in cancer, vascular, rheumatoid and other disease. *Nature Med.* **1:**27–31.
27. Hanahan, D. and Folkman, J. 1996. Patterns and emerging mechanisms of the angiogenic switch during tumorigenesis. *Cell* **86:**353–364.
28. Rak, J.W., St. Croix, B.D., and Kerbel, R.S. 1995. Consequences of angiogenesis for tumor progression, metastasis and cancer. *Anticancer Drugs* **6:**3–18.
29. Price, J.E., Polyzos, A., Zhang, R.D., and Daniels, L.M. 1990. Tumorigenicity and metastasis of human breast carcinoma cell lines in nude mice. *Cancer Res.* **50:**717–721.
30. Nicolson, G.L., Inoue, T., Van Pelt, C.S., and Cavanaugh, P.G. 1990. Differential expression of a Mr. approximately 90,000 cell surface transferrin receptor-related glycoprotein on murine B16 metastatic melanoma sublines selected for enhanced brain or ovary colonization. *Cancer Res.* **50:**515–520.
31. Welch, D.R., Bisi, J.E., Miller, B.E., Conaway, D., Seftor, E.A., Yohem, K.H., et al. 1991. Characterization of a highly invasive and spontaneously metastatic human malignant melanoma cell line. *Int. J. Cancer* **47:**227–237.
32. Montesano, R., Pepper, M.S., Möhle-Steinlein, U., Risau, W., Wagner, E.F., and Orci, L. 1990. Increased proteolytic activity is responsible for the aberrant morphogenetic behavior of endothelial cells expressing the middle T oncogene. *Cell* **62:**435–445.

Cancer Treatment by Targeted Drug Delivery to Tumor Vasculature in a Mouse Model

Wadih Arap,* Renata Pasqualini,* Erkki Ruoslahti†

In vivo selection of phage display libraries was used to isolate peptides that home specifically to tumor blood vessels. When coupled to the anticancer drug doxorubicin, two of these peptides—one containing an α_v integrin–binding Arg-Gly-Asp motif and the other an Asn-Gly-Arg motif—enhanced the efficacy of the drug against human breast cancer xenografts in nude mice and also reduced its toxicity. These results indicate that it may be possible to develop targeted chemotherapy strategies that are based on selective expression of receptors in tumor vasculature.

Endothelial cells in the angiogenic vessels within solid tumors express several proteins that are absent or barely detectable in established blood vessels (*1*), including α_v integrins (*2*) and receptors for certain angiogenic growth factors (*3*). We have applied in vivo selection of phage peptide libraries to identify peptides that home selectively to the vasculature of specific organs (*4*, *5*). The results of our studies imply that many tissues have vascular "addresses." To determine whether in vivo selection could be used to target tumor blood vessels, we injected phage peptide libraries into the circulation of nude mice bearing human breast carcinoma xenografts.

Recovery of phage from the tumors led to the identification of three main peptide motifs that targeted the phage into the tumors (*6*). One motif contained the sequence Arg-Gly-Asp (RGD) (*7*, *8*), embedded in a peptide structure that we have shown to bind selectively to $\alpha_v\beta_3$ and $\alpha_v\beta_5$ integrins (*9*). Phage carrying this motif, CDCRGDCFC (termed RGD-4C), homes to several tumor types (including carcinoma, sarcoma, and melanoma) in a highly selective manner, and homing is specifically inhibited by the cognate peptide (*10*).

A second peptide motif that accumulated in tumors was derived from a library with the general structure $CX_3CX_3CX_3C$ (X = variable residue, C = cysteine) (*6*). This peptide, CNGRCVSGCAGRC, contained the sequence Asn-Gly-Arg (NGR), which has been identified as a cell adhesion motif (*11*). We tested two other peptides that contain the NGR motif but are otherwise different from CNGRCVSGCAGRC: a linear peptide, NGRAHA (*11*), and a cyclic peptide, CVLNGRMEC. Tumor homing for all three peptides was independent of the tumor type and species; the phage homed to a human breast carcinoma (Fig. 1A), a human Kaposi's sarcoma, and a mouse melanoma (*12*). We synthesized the minimal cyclic NGR peptide from the CNGRCVSGCAGRC phage and found that this peptide (CNGRC), when coinjected with the phage, inhibited the accumulation of the CNGRCVSGCAGRC phage (Fig. 1A) and of the two other NGR-displaying phages in breast carcinoma xenografts (*12*).

The third motif—Gly-Ser-Leu (GSL) and its permutations—was frequently recovered from screenings using breast carcinoma (*6*), Kaposi's sarcoma, and malignant melanoma, and homing of the phage was inhibited by the cognate peptide (Fig. 1B). This motif was not studied further here.

The RGD-4C phage homes selectively to breast cancer xenografts (Fig. 1C). This homing can be inhibited by the free RGD-4C peptide (*10*), but not by the CNGRC peptide, even when this peptide was used in amounts 10 times those that inhibited the homing of the NGR phage (Fig. 1D). Tumor homing of the NGR phage was also partially inhibited by the RGD-4C peptide (Fig. 1E), but this peptide was only 10 to 20% as potent as CNGRC. An unrelated cyclic peptide, GACVFSIAHECGA, had no effect on the tumor-homing ability of either phage (*12*). Thus, our in vivo screenings yielded two peptide motifs, RGD-4C and NGR, both of which had previously been reported

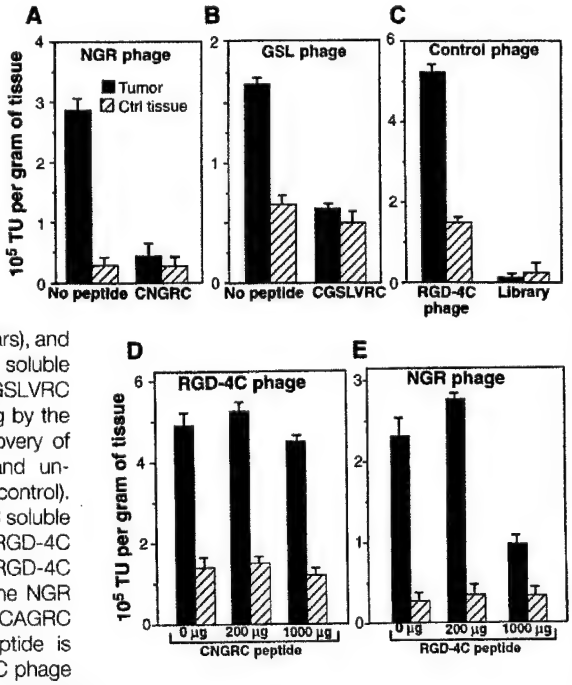

Fig. 1. Recovery of phage displaying tumor-homing peptides from breast carcinoma xenografts. Phage [10^9 transducing units (TU)] was injected into the tail vein of mice bearing size-matched MDA-MB-435–derived tumors (~1 cm^3) and recovered after perfusion. Mean values for phage recovered from the tumor or control tissue (brain) and the SEM from triplicate platings are shown. (**A**) Recovery of CNGRCVSGCAGRC phage from tumor (solid bars) and brain (striped bars), and inhibition of the tumor homing by the soluble peptide CNGRC. (**B**) Recovery of CGSLVRC phage and inhibition of tumor homing by the soluble peptide CGSLVRC. (**C**) Recovery of RGD-4C phage (positive control) and unselected phage library mix (negative control). (**D**) Increasing amounts of the CNGRC soluble peptide were injected with the RGD-4C phage. (**E**) Increasing amounts of the RGD-4C soluble peptide were injected with the NGR phage. Inhibition of the CNGRCVSGCAGRC phage homing by the CNGRC peptide is shown in (A); inhibition of the RGD-4C phage by the RGD-4C peptide has been reported (*10*).

Cancer Research Center, The Burnham Institute, 10901 North Torrey Pines Road, La Jolla, CA 92037, USA.

*These authors contributed equally to this report.
†To whom correspondence should be addressed. E-mail: ruoslahti@burnham-inst.org

to bind to integrins (*9*, *11*). The affinity of NGR for integrins is about three orders of magnitude less than that of RGD peptides (*7*, *11*). Nevertheless, the homing ratio (tumor/control organ) of the phage displaying the NGR motif was three times that of the RGD-4C phage (*12*). This discrepancy in activities, and the cross-inhibition results described above, strongly suggest that the NGR and RGD-4C peptides bind to different receptors in the tumors.

We next studied phage homing to tumors by immunostaining (Fig. 2). In one set of experiments (*13*), phage was allowed to circulate for 3 to 5 min, followed by perfusion (*10*) and immediate tissue recovery. In the second set, tissues were analyzed 24 hours after phage injection, when there is almost no phage left in the circulation (*10*). Strong phage staining in tumor vasculature, but not in normal endothelia, was seen in the short-term experiments with CNGRCVSGCAGRC phage in MDA-MB-435 cell–derived human breast carcinoma xenografts (Fig. 2A) and SLK cell–derived human Kaposi's sarcoma xenografts (Fig. 2B). The two other NGR phages, NGRAHA and CVLNGRMEC, also showed strong tumor staining (*12*), whereas a control phage showed no staining (Fig. 2, E and F). At 24 hours, the staining pattern indicated that the NGR phage had spread outside the blood vessels and into the tumors (Fig. 2, C and D). This spreading may be attributable to increased permeability of tumor blood vessels (*14*) or uptake of the phage by angiogenic endothelial cells (*15*) and subsequent transfer to tumor tissue.

The CNGRCVSGCAGRC phage showed the greatest tumor selectivity among all the peptides analyzed. Several control organs showed very low or no immunostaining, confirming the specificity of the NGR motif for tumor vessels; heart (Fig. 2G) and mammary gland (Fig. 2H) are shown (*16*). Spleen and liver, which are part of the reticuloendothelial system (RES), contained phage; uptake by the RES is a general property of the phage particle and is independent of the peptide it displays (*10*, *17*). These immunostaining results with the NGR phage are similar to observations made with the RGD-4C phage (*10*).

To determine whether the tumor-homing peptides RGD-4C and CNGRC could be used to improve the therapeutic index of cancer chemotherapeutics, we coupled them to doxorubicin (dox) (*18*). Dox is one of the most frequently used anticancer drugs and one of a few chemotherapeutic agents known to have antiangiogenic activity (*19*). The dox-peptide conjugates were used to treat mice bearing tumors derived from human MDA-MB-435 breast carcinoma cells.

The commonly used dose of dox in nude mice with human tumor xenografts is 50 to 200 μg/week (*20*). Because we expected the dox conjugates to be more effective than the free drug, we initially used the conjugates at a dose of dox-equivalent of only 5 μg/week (*13*, *21*). Tumor-bearing mice treated with RGD-4C conjugate outlived the control mice, all of which died from widespread disease (Log-Rank test, $P < 0.0001$; Wilcoxon test, $P = 0.0007$) (Fig. 3A). In a dose-escalation experiment, tumor-bearing mice were treated with the dox-RGD-4C conjugate at 30 μg of dox-equivalent every 21 days for 84 days and were then observed, without further treatment, for an extended period of time. All of these mice outlived the dox-treated mice by more than 6 months, suggesting that both primary tumor growth and metastasis were inhibited by the conjugate. Many of the tumors in the mice that received the dox-RGD-4C conjugate (30 μg of dox-equivalent every 21 days) showed marked skin ulcer-

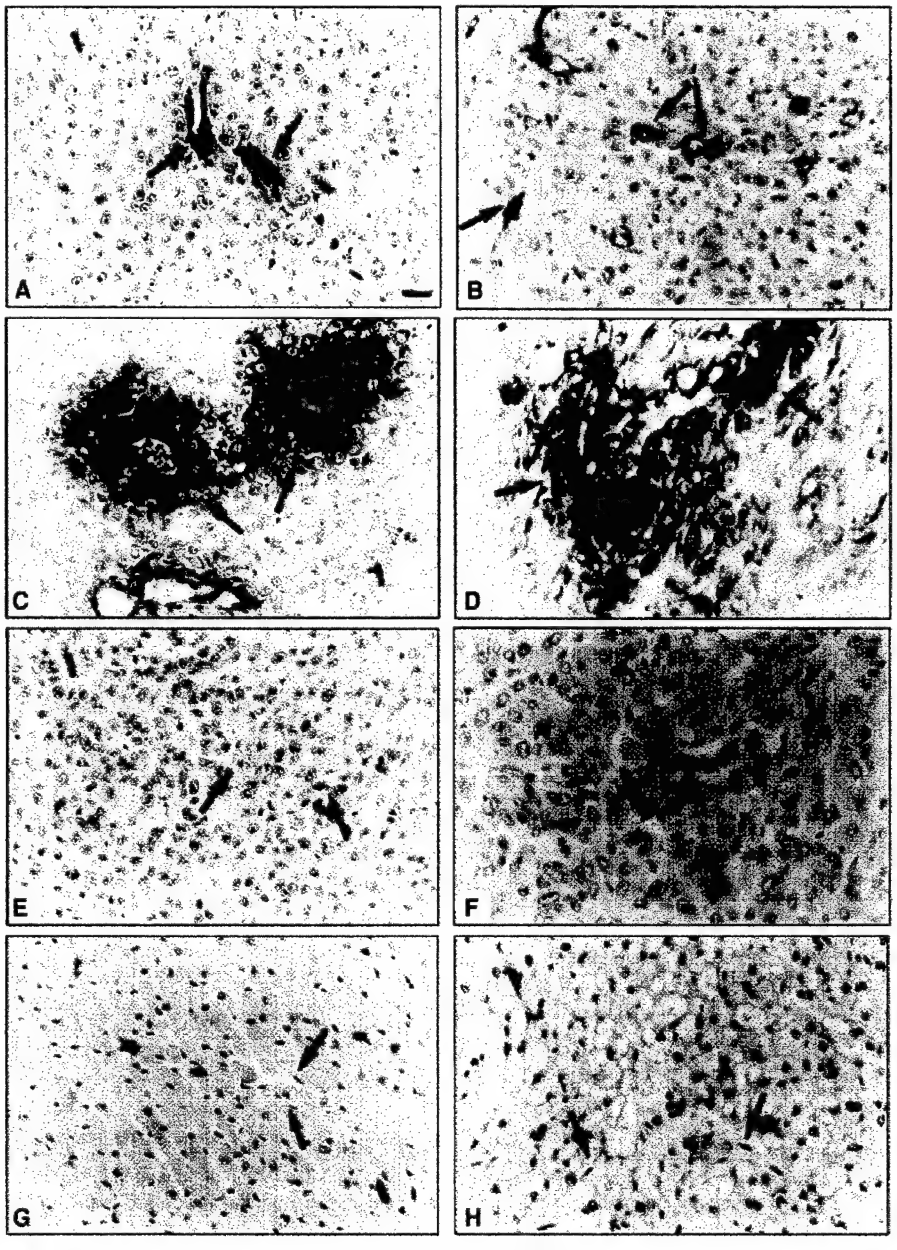

Fig. 2. Immunohistochemical staining of phage after intravenous injection into tumor-bearing mice. Phage displaying the peptide CNGRCVSGCAGRC (**A** to **D**, **G**, and **H**) or control phage with no insert (**E** and **F**) were injected intravenously into mice bearing MDA-MB-435–derived breast carcinoma (A, C, and E) and SLK-derived Kaposi's sarcoma (B, D, and F) xenografts. Phage was allowed to circulate for 4 min (A, B, E, and F) or for 24 hours (C, D, G, and H). Tumors and control organs were removed, fixed in Bouin solution, and embedded in paraffin for preparation of tissue sections. An antibody to M-13 phage (Pharmacia) was used for the staining. Heart (G) and mammary gland (H) are shown as control organs (*16*). Arrows point to blood vessels. Scale bar in (A), 5 μm.

ation and tumor necrosis, whereas these signs were not observed in any of the control groups. At necropsy, the mice treated with the dox-RGD-4C conjugate had significantly smaller tumors (t test, $P = 0.02$), less spreading to regional lymph nodes ($P < 0.0001$), and fewer pulmonary metastases ($P < 0.0001$) than did the mice treated with free dox (Fig. 3, B to D). Similar results were obtained in five independent experiments. Histopathological analysis revealed pronounced destruction of the tumor architecture and widespread cell death in the tumors of mice treated with the dox-RGD-4C conjugate; tumors treated with free dox at this dose were only minimally affected. In contrast, the dox-RGD-4C conjugate was less toxic to the liver and heart than was free dox (Fig. 3E). In some experiments, dox together with unconjugated soluble peptide was used as a control; the drug-peptide combination was no more effective than free dox (*12*).

To assess toxicity, we used 200 μg of dox-equivalent in mice with large (~5 cm^3), size-matched tumors (*13*, *21*). Mice treated with the dox-RGD-4C conjugate survived more than a week, whereas all of the dox-treated mice died within 48 hours of drug administration (Fig. 3F). Accumulation of dox-RGD-4C within the large tumors thus appeared to have sequestered the conjugated drug, thereby reducing its toxicity to other tissues.

Less extensive data with the CNGRC peptide conjugate indicated an efficacy similar to that of the RGD-4C conjugate. In all experiments, tumors treated with the dox-CNGRC conjugate were one-fourth to one-fifth as large as tumors treated in the control groups (Fig. 4A). A marked reduction in metastasis and a prolongation of long-term survival were also seen (Log-Rank test, $P = 0.0064$; Wilcoxon test, $P = 0.0343$) (Fig. 4B). Two of the six dox-CNGRC–treated animals were still alive more than 11 weeks after the last of the control mice died. The dox-CNGRC conjugate was also less toxic than the free drug (Fig. 4C). CNGRC peptide alone failed to reproduce the effect of the conjugate, even in doses up to 150 μg/week. Unconjugated CNGRC-dox mixture

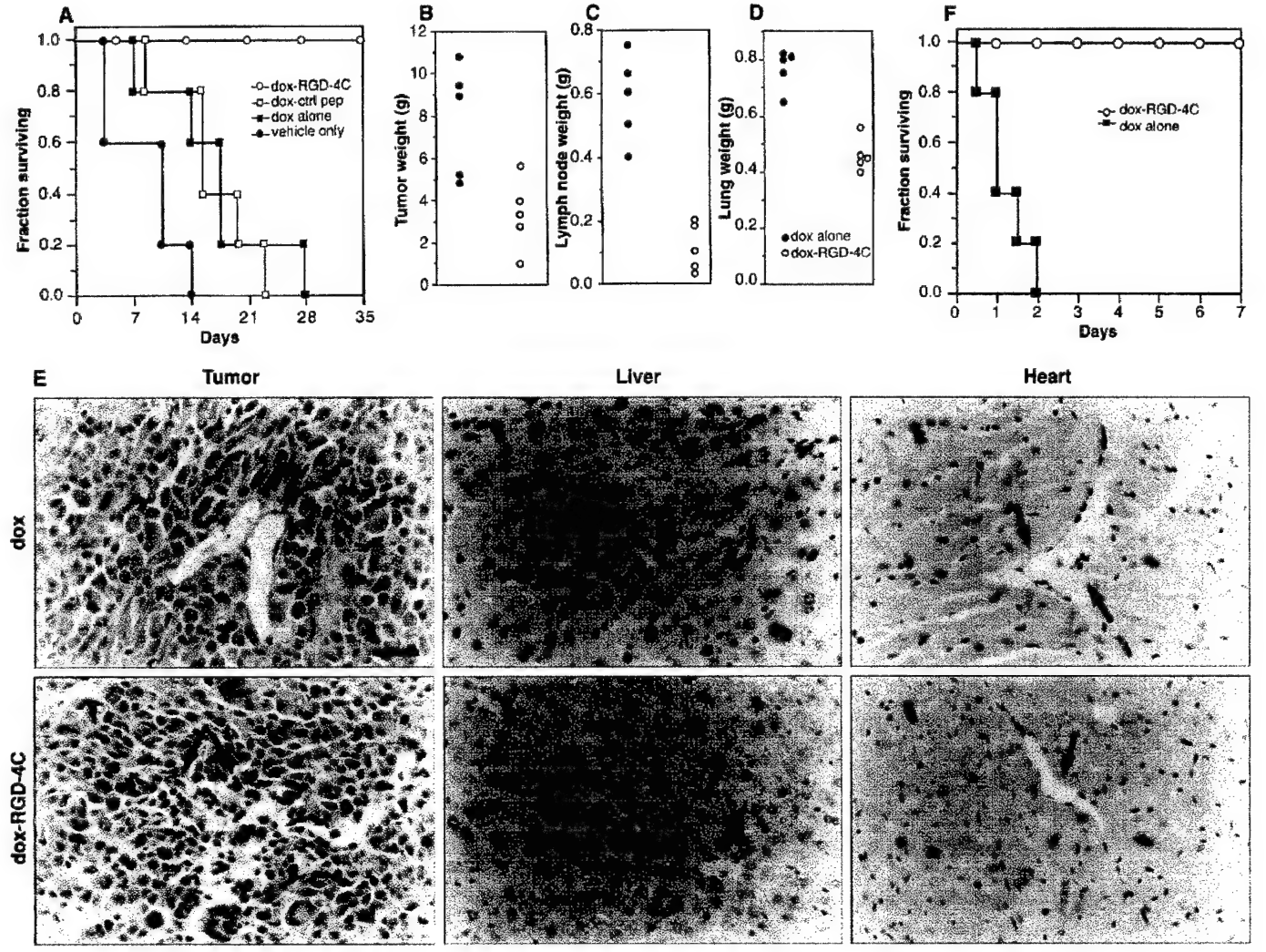

Fig. 3. Treatment of mice bearing MDA-MB-435–derived breast carcinomas with dox-RGD-4C peptide conjugate. Mice with size-matched tumors (~1 cm^3) were randomized into four treatment groups (five animals per group): vehicle only, free dox, dox-control peptide (GACVFSIAHECGA; dox-ctrl pep), and dox-RGD-4C conjugate. (**A**) Mice were treated with 5 μg/week of dox-equivalent. A Kaplan-Meier survival curve is shown. (**B** to **D**) Mice were treated with 30 μg of dox-equivalent every 21 days. The animals were killed, and tumors (B), axillary lymph nodes (C), and lungs (D) were weighed after three treatments. (**E**) Histopathological analysis (hematoxylin and eosin stain) of MDA-MB-435 tumors, liver, and heart treated with dox or dox-RGD-4C conjugate. Vascular damage was observed in the tumors treated with dox-RGD-4C conjugate (arrows, lower left panel), but not in the tumors treated with free dox (arrows, upper left panel). Signs of toxicity were seen in the liver and heart of mice treated with dox (arrows, upper middle and upper right panels), whereas the blood vessels were relatively undamaged in the mice treated with the dox-RGD-4C conjugate. The changes were scored blindly by a pathologist; representative micrographs are shown. Scale bar, 7.5 μm. (**F**) Mice bearing large (~5 cm^3) MDA-MB-435 breast carcinomas (four animals per group) were randomized to receive a single dose of free dox or dox-RGD-4C conjugate at 200 μg of dox-equivalent per mouse. A Kaplan-Meier survival curve is shown.

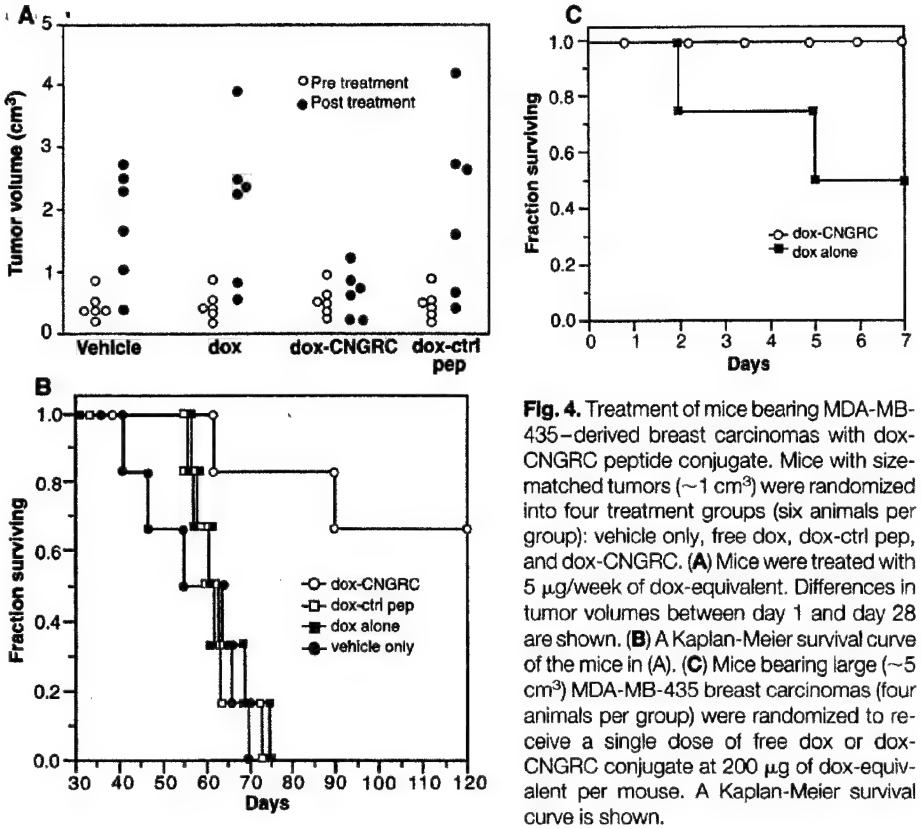

Fig. 4. Treatment of mice bearing MDA-MB-435–derived breast carcinomas with dox-CNGRC peptide conjugate. Mice with size-matched tumors (~1 cm^3) were randomized into four treatment groups (six animals per group): vehicle only, free dox, dox-ctrl pep, and dox-CNGRC. (**A**) Mice were treated with 5 μg/week of dox-equivalent. Differences in tumor volumes between day 1 and day 28 are shown. (**B**) A Kaplan-Meier survival curve of the mice in (A). (**C**) Mice bearing large (~5 cm^3) MDA-MB-435 breast carcinomas (four animals per group) were randomized to receive a single dose of free dox or dox-CNGRC conjugate at 200 μg of dox-equivalent per mouse. A Kaplan-Meier survival curve is shown.

was no different from dox alone. The dox-CNGRC conjugates were also effective against xenografts derived from another human breast carcinoma cell line, MDA-MB-231 (*12*).

We expect the NGR and RGD-4C motifs to target human vasculature as well, because (i) the NGR phage binds to blood vessels of human tumors and less so than to vessels in normal tissue (*22*), and (ii) the RGD-4C peptide binds to human α_v integrins (*9*, *10*), which are known to be selectively expressed in human tumor blood vessels (*23*). Thus, these peptides are potentially suitable for tumor targeting in patients. The RGD-4C peptide is likely to carry dox into the tumor vasculature and also to the tumor cells themselves, because the MDA-MB-435 breast carcinoma expresses α_v integrins (*10*). Because many human tumors express the α_v integrins (*23*), our animal model is a reasonable mimic of the situation in at least a subgroup of cancer patients. The targeting of drugs into tumors is a new use of the selective expression of α_v integrins and other receptors in tumor vasculature. The effectiveness of the CNGRC conjugate may be derived entirely from vascular targeting because the NGR peptides do not bind to the MDA-MD-435 cells (*12*).

The tumor vasculature is a particularly suitable target for cancer therapy because it is composed of nonmalignant endothelial cells that are genetically stable and therefore unlikely to mutate into drug-resistant variants (*24*). In addition, these cells are more accessible to drugs and have an intrinsic amplification mechanism; it has been estimated that elimination of a single endothelial cell can inhibit the growth of 100 tumor cells (*24*). New targeting strategies, including the ones described here, have the potential to markedly improve cancer treatment.

REFERENCES AND NOTES

1. J. Folkman, *Nature Med.* **1**, 27 (1995); W. Risau and I. Flamme, *Annu. Rev. Cell Biol.* **11**, 73 (1995); D. Hanahan and J. Folkman, *Cell* **86**, 353 (1996); J. Folkman, *Nature Biotechnol.* **15**, 510 (1997).
2. P. C. Brooks, R. A. F. Clark, D. A. Cheresh, *Science* **264**, 569 (1994); P. C. Brooks *et al.*, *Cell* **79**, 1157 (1994); M. Friedlander *et al.*, *Science* **270**, 1500 (1995); H. P. Hammes, M. Brownlee, A. Jonczyk, A. Sutter, K. T. Preissner, *Nature Med.* **2**, 529 (1996).
3. G. Martini-Baron and D. Marme, *Curr. Opin. Biotechnol.* **6**, 675 (1995); D. Hanahan, *Science* **277**, 48 (1997); W. Risau, *Nature* **386**, 671 (1997).
4. R. Pasqualini and E. Ruoslahti, *Nature* **380**, 364 (1996).
5. D. Rajotte *et al.*, in preparation.
6. Phage libraries were screened in mice carrying human MDA-MB-435 breast carcinoma xenografts as in (*4*, *10*). The structure of the libraries, the sequences recovered, and their prevalence (percent of insert sequenced) were as follows: $CX_3CX_3CX_3C$ library: CNGRCVSGCAGRC (26%), CGRECPRLCQSSC (15%), CGEACGGQCALPC (6%); CX_7C library: CDCRGDCFC (80%), CTCVSTLSC (5%), CFRDFLATC (5%), CSHLTRNRC (5%), CDAMLSARC (5%); CX_5C library: CGSLVRC (35%), CGLSDSC (12%), CYTADPC (8%), CDDSWKC (8%), CPRGSRC (4%).
7. E. Ruoslahti, *Annu. Rev. Cell Dev. Biol.* **12**, 697 (1996).
8. Abbreviations for the amino acid residues are as follows: A, Ala; C, Cys; D, Asp; E, Glu; F, Phe; G, Gly; H, His; I, Ile; K, Lys; L, Leu; M, Met; N, Asn; P, Pro; Q, Gln; R, Arg; S, Ser; T, Thr; V, Val; W, Trp; and Y, Tyr.
9. E. Koivunen, B. Wang, E. Ruoslahti, *Biotechnology* **13**, 265 (1995).
10. R. Pasqualini, E. Koivunen, E. Ruoslahti, *Nature Biotechnol.* **15**, 542 (1997).
11. E. Koivunen, D. Gay, E. Ruoslahti, *J. Biol. Chem.* **268**, 20205 (1993); E. Koivunen, B. Wang, E. Ruoslahti, *J. Cell Biol.* **124**, 373 (1994); J. M. Healy *et al.*, *Biochemistry* **34**, 3948 (1995).
12. W. Arap, R. Pasqualini, E. Ruoslahti, unpublished data.
13. Tumor-bearing mice (*10*) were anesthetized with Avertin intraperitoneally and phage or drugs were administered into the tail vein. All animal experimentation was reviewed and approved by the institute's Animal Research Committee.
14. R. K. Jain, *Cancer Metastasis Rev.* **9**, 253 (1996); C. H. Blood and B. R. Zetter, *Biochim. Biophys. Acta* **1032**, 89 (1990); H. F. Dvorak, J. A. Nagy, A. M. Dvorak, *Cancer Cells* **3**, 77 (1991); T. R. Shockley *et al.*, *Ann. N.Y. Acad. Sci.* **618**, 367 (1991).
15. M. S. Bretscher, *EMBO J.* **8**, 1341 (1989); S. L. Hart *et al.*, *J. Biol. Chem.* **269**, 12468 (1994).
16. A complete immunostaining panel of control organs is available online at www.burnham-inst.org/papers/arapetal.
17. M. R. Getter, M. E. Trigg, C. R. Merril, *Nature* **246**, 221 (1973).
18. The peptides RGD-4C (*9*, *10*), CNGRC, CGSLVRC, and GACVFSIAHECGA were synthesized, cyclized at high dilution, and purified by high-performance liquid chromatography (HPLC). The peptides were conjugated to dox (Aldrich) with 1-ethyl-3-(3-dimethyl-aminopropyl) carbodiimide hydrochloride (EDC; Sigma) and *N*-hydroxysuccinimide (NHS; Sigma) [S. Bauminger and M. Wilcheck, *Methods Enzymol.* **70**, 151 (1980)]. The conjugates were freed of reactants by gel filtration on a Sephadex G25 and contained <5% free drug, as assessed by HPLC and nuclear magnetic resonance (NMR). The carbodiimide conjugation method precluded a determination of the stoichiometry of the conjugates by mass spectrometry. Preliminary experiments (*12*) with a compound prepared by a different chemistry [A. Nagy *et al.*, *Proc. Natl. Acad. Sci. U.S.A.* **93**, 7269 (1996)] were homogeneous by HPLC, had a peptide-dox ratio of 1, and had an antitumor activity similar to that of the carbodiimide conjugates.
19. R. Steiner, in *Angiogenesis: Key Principles—Science, Technology and Medicine*, R. Steiner, P. B. Weisz, R. Langer, Eds. (Birkhauser, Basel, Switzerland, 1992), pp. 449–454.
20. D. P. Berger, B. R. Winterhalter, H. H. Fiebig, in *The Nude Mouse in Oncology Research*, E. Boven and B. Winograd, Eds. (CRC Press, Boca Raton, FL, 1991), pp. 165–184.
21. The concentration of dox was adjusted by measuring the absorbance of the drug and conjugates at 490 nm. A calibration curve for dox was used to calculate the dox-equivalent concentrations. Experiments with MDA-MB-435 cells and activated endothelial cells in vitro showed that the conjugation process did not affect the cytotoxicity of dox after conjugation.
22. M. Sakamoto, R. Pasqualini, E. Ruoslahti, unpublished data.
23. R. Max *et al.*, *Int. J. Cancer* **71**, 320 (1997); *ibid.* **72**, 706 (1997).
24. J. Denekamp, *Br. J. Radiol.* **66**, 181 (1993), F. J. Burrows and P. E. Thorpe, *Pharmacol. Ther.* **64**, 155 (1994); J. Folkman, in *Cancer: Principles and Practice of Oncology*, V. T. DeVita, S. Hellman, S. A. Rosenberg, Eds. (Lippincott, Philadelphia, 1997), pp. 3075–3085.

25. We thank E. Beutler, W. Fenical, and T. Friedmann for comments on the manuscript; N. Assa-Munt for NMR analysis; R. Kain, S. Krajewski, and M. Sakamoto for histological analysis; W. P. Tong for HPLC analysis; G. Alton and J. Etchinson for mass spectrometry analysis; E. Koivunen for a phage library; and S. Levinton-Kriss for the SLK cell line. Supported by grants CA74238-01, CA62042, and Cancer Center support grant CA30199 from the National Cancer Institute, and by the Susan G. Komen Breast Cancer Foundation.

9 September 1997; accepted 19 November 1997

Chemotherapy targeted to tumor vasculature

Wadih Arap, MD, PhD, Renata Pasqualini, PhD, and Erkki Ruoslahti, MD, PhD

Vasculature-targeted chemotherapy—the destruction of tumor blood vessels with cytotoxic agents—makes use of biochemical differences between angiogenic and resting blood vessels. This approach may minimize or eliminate some of the problems associated with conventional solid-tumor targeting, such as poor tissue penetration and drug resistance. Experiments with antiangiogenic and thrombotic factors have shown that eliminating tumor blood supply has dramatic antitumor effects in mice. Targeting chemotherapeutic agents to the tumor vasculature combines the blood vessel destruction with the usual antitumor activities of the drug, resulting in increased efficacy and reduced toxicity in experiments with tumor-bearing mice. Human clinical trials, which are soon to follow, will determine the final value of this approach.

Cancer Research Center, The Burnham Institute, 10901 North Torrey Pines Road, La Jolla, CA 92037, USA.

Current Opinion in Oncology 10:560–565

Abbreviation

VEGF vascular endothelial growth factor

ISSN 1040–8746

Systemic treatment of disseminated malignant tumors relies on cytotoxic chemotherapy. The currently used chemotherapeutic agents, however are the drugs with the narrowest therapeutic indices in all medicine. Thus, the dose of anticancer agents is restricted by their nonselective toxic effects on normal tissues. Selective delivery of cytotoxic drugs into malignant tumors may overcome these limitations. Even highly toxic agents could be rendered safer and more effective if it were possible to direct them only into the tumor, because high drug concentrations within the tumor could be obtained while sparing the normal tissues. Although achieving these goals has been a long-standing goal of cancer biology and medical oncology, there are only a few situations in which targeted drug delivery is possible. Monoclonal antibodies against tumor antigens have provided the existing targeting opportunities [1,2]. However, this approach has met with limited success; only a few tumor antigens are known and their expression on the cells within an individual tumor is not necessarily uniform. Moreover, antibodies against tumor antigens penetrate poorly into solid tumors [3–5]. Finally, because tumor cells are genetically unstable and mutations advantageous for growth accumulate readily, antibody-targeted treatments may be thwarted by clonal selection for cells that have lost the tumor antigen [6]. The targeting of therapies to the vasculature of tumors [7–9] overcomes some of the problems of conventional tumor targeting. We review some of the recent developments in this field.

Rationale for targeting of tumor vasculature

It is now widely recognized that the growth and metastasis of malignant tumors depends on angiogenesis; a tumor cannot grow beyond the size of about 1 mm in diameter without acquiring new blood vessels to nurture it [10]. The vasculature within tumors is distinct [10–12], presumably because tumor vessels growing actively match the growth of the tumor.

The activated cells in the tumor neovasculature express molecules characteristic of angiogenic vessels [11–13]. These angiogenic markers offer targets for guided chemotherapy. Figure 1 shows the principle of targeting chemotherapy to tumor blood vessels. Vascular targeting has several advantages over targeting tumor cells themselves (Table 1). The endothelial lining of tumor vasculature is readily accessible to a circulating probe. In contrast, a tumor-targeting probe has to diffuse over long distances, penetrate among closely packed tumor cells and dense tumor stroma, and overcome the high interstitial pressure typical of solid tumors [3–5]. Because tumor cells depend

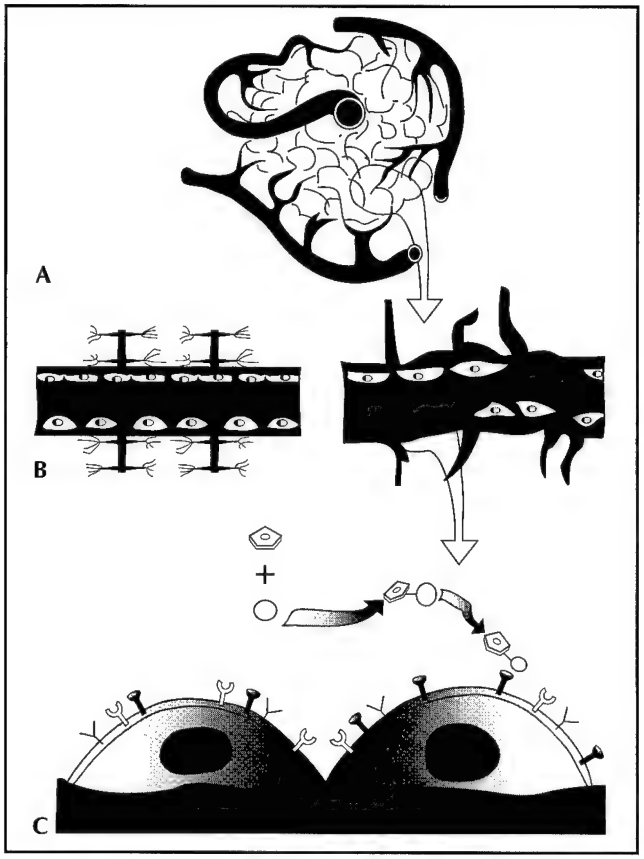

Fig. 1. The principle of chemotherapy targeted to tumor vasculature. **A,** Tumors are dependent on the formation of new blood vessels for growth. **B,** Normal vasculature (*left*) is morphologically different from tumor vasculature (*right*), which contains angiogenic markers. **C,** Drugs can be targeted to the angiogenic receptors in tumor blood vessels.

on their blood supply for survival, an antitumor therapy directed against the vasculature does not have to destroy every endothelial cell; partial denuding of the endothelium is likely to lead to the formation of an occlusive thrombus that will stop flow to the part of the tumor served by the vessel [8]. Moreover, targeting tumor vasculature, unlike conventional tumor targeting, possesses an intrinsic amplification mechanism; it has been estimated that 100 tumor cells should die for each destroyed endothelial cell in tumor blood vessels [7,8,10]. Finally, because tumor endothelial cells are diploid and nonmalignant, they are unlikely to lose a cell-surface target receptor or acquire drug resistance through mutation and clonal evolution [14]. It has been long recognized by oncologists that although tumors commonly develop resistance to chemotherapy, normal tissues do not. Thus, toxicity to normal tissues, such as chemotherapy-induced myelosuppression, continues to occur even after tumor cells have become drug resistant and progress in the face of continued treatment. Endothelial cells, being nonmalignant cells, are expected to behave in a manner analogous to bone marrow cells. Recent studies provide support for this prediction. Thus far, long-term antiangiogenic therapy has not resulted in drug resistance in either experimental animals [15••] or in clinical trials [10].

Effects of occluding tumor vasculature in experimental models

In one system, endothelial cells within transplanted mouse neuroblastoma cells were induced to express major histocompatibility complex class II antigens and the major histocompatibility complex antigens were then used to target a truncated tissue factor into the tumors [16••]. The truncated tissue factor lacked a membrane attachment region and was unable to trigger blood clotting at normal endothelium, but did so when bound through an antibody to the major histocompatibility class II–expressing endothelial cells in the tumors. Selective thrombosis in the tumor vasculature resulted in complete tumor regression. A vascular shutdown with similar results has also been accomplished by destroying the tumor endothelial cells with a ricin A–chain immunotoxin [17]. Although no naturally occurring endothelial targets exist for the probes used in these experiments, the results show that occluding tumor vasculature can have a dramatic antitumor effect. Application of such strategies will require specific markers in the blood vessels of human tumors.

Table 1

Comparison between conventional tumor targeting and vascular tumor targeting

Feature	Conventional tumor targeting	Vascular tumor targeting
Pharmacokinetic system	Multiple compartments	Single-compartment
Primary target cell type	Malignant tumor cells	Non-malignant activated tumor vascular cells
Target cell accessibility	Poor	Good
Receptor	Tumor antigen	Angiogenic marker
Receptor expression	Uneven and heterogeneous	Possibly uniform and homogeneous
Homing moiety	Monoclonal antibodies	Monoclonal antibodies, peptides
Therapeutic moiety	Cytotoxic drugs	Cytotoxic drugs, angiogenesis inhibitors
Target cell genome	Genetically unstable cells	Genetically stable, diploid cells
Acquired cytotoxic drug resistance	Yes	Not yet reported
Posttargeting amplification loop	Absent	Present
Complete elimination of target cell	Required	Not required
Potential clinical applicability	Limited by antigen heterogeneity	Broad, as angiogenic markers may be shared

Molecular targets in angiogenic tumor vasculature

Vascular targets are not necessarily limited to endothelial cells; pericytes, smooth muscle cells, macrophages [13], and perhaps even cells derived from circulating endothelial cell precursors [18•] are also important elements in tumor blood vessels.

Among the many molecules that are selectively expressed in angiogenic vasculature, integrins show particular promise in tumor targeting. Saiki *et al.* [19] were the first to report that peptides containing the integrin recognition sequence arg-gly-asp (RGD) [20] can inhibit tumor angiogenesis. More recent studies have shown that the αvβ3 and αvβ5 integrins are upregulated in angiogenic tumor endothelial cells [21], and that the inhibition of αv integrins by antibodies [22], cyclic RGD peptides [22,23], and RGD peptidomimetics [24•] can block neovascularization. To what extent the αv integrins are restricted to sites of angiogenesis remains to be analyzed in detail; αvβ5 integrin expression has been reported in the thymic vasculature [25]. The β1 integrins α1β1 and α2β1 may also be important in angiogenesis [26], but their expression levels have not thus far been reported to be upregulated in tumors.

Endothelial-specific receptor tyrosine kinases and their ligands are also of interest for vascular targeting. One such family is the vascular endothelial growth factor (VEGF) receptors [27], which play a critical role in angiogenesis [28–30] and are expressed at elevated levels in tumor blood vessels [31]. The receptors FLT-1 (VEGF receptor-1) and KDR/FLK-1 (VEGF-2) are expressed in endothelial cells of blood vessels [27], whereas the expression of FLT-4 (VEGF receptor-3) [32••] is restricted to lymphatic endothelium [33]. The Tie family—another class of tyrosine kinase receptors expressed almost exclusively in endothelial cells—and their ligands also have an essential role in vascular development [28,29]. The enhanced expression of the Tie receptors (Tie-1 and Tie-2/Tek) in the blood vessels of a variety of cancers provides novel markers for tumor vasculature [30,34].

Other promising marker candidates of the tumor vasculature include CD34, collagen type VIII, endosialin, endoglin, aminopeptidase A, high molecular weight melanoma-associated molecule, osteosarcoma-related protein, and angiomodulin (for original references and additional markers, see Burrows and Thorpe [8], Fox and Harris [11], and Molema *et al.* [12]).

Vascular targeting through known receptors and nonspecific tumor endothelium targeting

Oncofetal fibronectin is an alternatively spliced form of fibronectin present in angiogenic but not in mature blood vessels. A human antibody that recognizes this protein has been shown to accumulate in the vasculature of F9-cell murine teratocarcinomas [35•]. Unlike antibodies produced in rodents, which are immunogenic in patients, the antifibronectin antibodies used by Neri *et al.* [35•] were isolated from a phage library that expresses human antibodies that are not likely to be immunogenic in patients. It remains to be seen whether these special antifibronectin antibodies could deliver drugs into tumors.

The VEGF receptor has been used in drug targeting. A VEGF–diphtheria toxin conjugate inhibited the growth of tumor xenografts in nude mice significantly more than the diphtheria toxin alone [36].

Radioimmunotherapy using ^{213}Bi or ^{131}I targeted to lung vasculature with a monoclonal antibody against thrombomodulin has been reported [37]. The therapeutic effects of ^{213}Bi, which is an α-particle emitter, were superior to those of the β-particle emitter ^{131}I. Because thrombomodulin is selectively expressed in the pulmonary blood vessels, the antibody homed to the lungs, resulting in destruction of small tumor colonies along with collateral damage to the normal lung vasculature. Targeting the radioisotope to the tumor vasculature rather than to the regional vasculature of the organ harboring the tumor should improve this treatment.

In yet another approach, cationic liposomes were used to target angiogenic vasculature in mouse pancreatic islet cell tumors. Confocal microscopy demonstrated a 15- to 33-fold more uptake of the liposomes by angiogenic than normal endothelial cells [38]. Other types of liposomes (neutral, anionic, or sterically stabilized neutral liposomes) had no such targeting ability. Thus, appropriately designed liposomes can, at least in some cases, serve as selective targeting vehicles.

Vascular tumor targeting with *in vivo* phage display

We have devised a novel strategy to identify peptides that home to tumor vasculature. This method—*in vivo* selection of peptides from phage display peptide libraries—allows detection of circulating homing peptides without any preconceived notions about the nature of their target receptors. Once a receptor is identified as a target of a homing peptide, it can be isolated and cloned using biochemical methods.

Using the *in vivo* phage selection, we identified peptides that selectively target normal organs. The organs we targeted in this manner include the brain, kidney, lung, skin, pancreas, retina, intestine, uterus, prostate, and the adrenal gland [39,40]. These results indicate that many, perhaps all, organs modify the endothelium of their vasculature in ways that allow differential targeting with peptide probes.

We also assembled a panel of peptide motifs that home to tumor vasculature (Fig. 2). These include the sequences CDCRGDCFC (termed *RGD-4C*), NGR, and GSL [41••]. The RGD-4C peptide had been previously identified as a selective binder of αv integrins [20,42] and shown to home to tumor vasculature, as well as to cells in some human tumors [43•]. The tumor homing is possible because, as discussed previously, the αvβ3 and αvβ5 integrins are absent or expressed only at low levels in normal endothelial cells but are induced in angiogenic vasculature and in many human tumors. An RGD peptide that binds selectively to α5β1 integrin shows no tumor homing [43•].

A receptor for the RGD-4C peptide, the αvβ3 integrin, plays an important role in angiogenesis [21] because inhibiting its function with antibodies or RGD peptides blocks angiogenesis [19,22,23]. We also identified candidate receptors for the NGR and GSL peptides and are studying the function of these receptors in angiogenesis (unpublished data).

We have used the peptides that home to tumor vasculature to show that the cytotoxic drug doxorubicin coupled to targeting peptides yields compounds that are more effective and less toxic than doxorubicin alone [41••]. An example of peptide-guided chemotherapy based on this principle is shown in Figure 3. The RGD-4C peptide has also been inserted into a surface protein of an adenovirus. The resulting adenoviral vector showed promise in gene therapy targeting [44].

We have also shown that our tumor-targeting peptides bind to blood vessels in human tumors, but not in normal tissues (Sakamoto *et al.*, Unpublished data). These data—along with the fact that the candidate receptors identified in mouse tumor vasculature have human homologues—indicate that our homing peptides would also home to tumors in human patients.

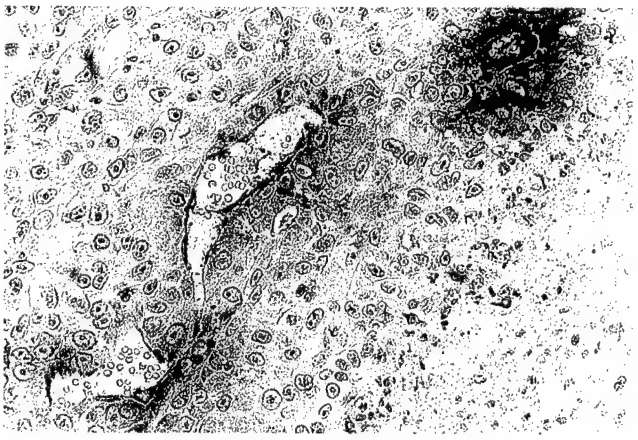

Fig. 2. Tumor-homing peptide carried by a phage homes to the blood vessels. A mouse bearing an MDA-MB-435 breast carcinoma xenograft was injected intravenously with the peptide–phage; the tumor was recovered after 24 hours and stained with antiphage antibodies. The phage is present in blood vessels.

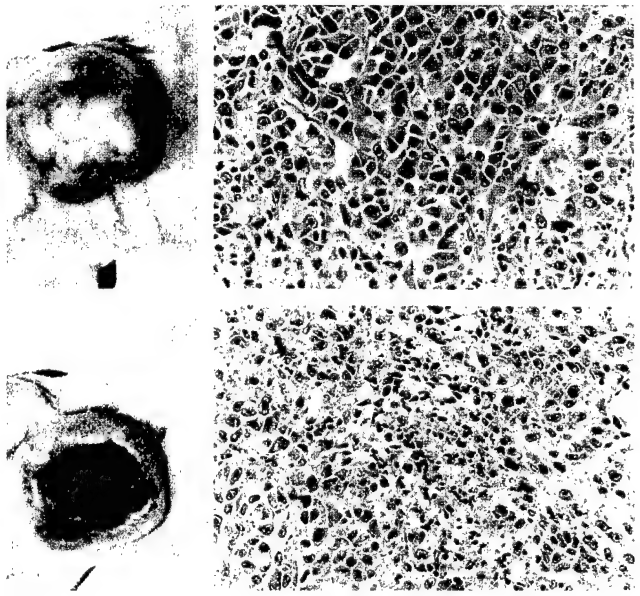

Fig. 3. Chemotherapy targeted to tumor vasculature. MDA-MB-435 breast carcinoma xenografts in nude mice treated with doxorubicin (dox) (*upper panels*) or doxorubicin-RGD-4C (dox-RGD-4C) (*lower panels*). The mice received three treatments of 30 μg of doxorubicin-equivalent every 3 weeks. The tumor in the mouse treated with the targeted drug shows macroscopic and microscopic signs of necrosis.

Antiangiogenic and vascular targeting agents

It has been long recognized that chemotherapeutic agents can damage the endothelium of normal and tumor blood vessels [45]. Doxorubicin, paclitaxel [46], and a few other cytotoxic chemotherapeutics have been found to inhibit angiogenesis in addition to being selectively toxic to tumor cells [10]. Our doxorubicin experiments [41••] also suggest that a conventional cytotoxic chemotherapeutic drug can be adapted to become a vascular targeting agent.

Antivascular agents that act preferentially on angiogenic tumor vessels have been developed in the past few years; these include tubulin-binding agents such as combretastatin A-4 [47] and drugs related to flavone acetic acid [48]. In addition, several angiogenesis inhibitors such as TNP-470, thalidomide, carboxyaminotriazole, linomide, pentosan polysulfate, tecogalan, 2-methoxy-estradiol, interleukin-12, and metalloproteinase inhibitors are in preclinical and clinical trials (for additional agents and references, see Gasparini [49], Pluda [50], and Twardowski and Gradishar [51]). Elucidating the mechanisms of action of these drugs is likely to advance the understanding of angiogenesis. Some of the antiangiogenesis drugs may be particularly suitable for targeting into tumor vasculature for an enhanced effect and lower toxicity. Moreover, the new targeting possibilities may make it useful to re-examine compounds that have been discarded from clinical application because of excessive toxicity.

Relatively nontoxic protein inhibitors of angiogenesis have also been discovered recently. These compounds tend to be endogenous fragments of abundant blood or tissue proteins. The two leading representatives are angiostatin (a 38-kD fragment of plasminogen) [52] and endostatin (a 20-kD fragment of collagen XVIII) [53•], but antiangiogenic fragments have also been obtained from fragments of fibronectin, prolactin, thrombospondin, SPARC (*S*ecreted *P*rotein, *A*cidic and *R*ich in *C*ysteines), platelet factor 4 (see Folkman [54] for original references), and matrix metalloprotease-2 [55•]. Finally, the hypoxic environment of solid tumors may render a combination of antiangiogenic therapy and hypoxia-selective cytotoxins such as tiperazine [56] particularly effective.

The targeting of chemotherapeutic agents into tumor vasculature would appear to offer the advantage over antiangiogenic therapy that antiangiogenic effects are combined with direct cytotoxic antitumor effects. The relative merits of the two approaches ultimately will have to be determined in clinical trials, however.

Acknowledgments

This work was supported by the National Institutes of Health grants CA 28896, CA 74238, and Cancer Center Support Grant CA 30199. Wadih Arap is the recipient of a CapCURE award.

References and recommended reading

References of particular interest, published within the annual period of review, have been highlighted as:

- • Of special interest
- •• Of outstanding interest

1. Hellström I, Trail P, Siegall C, Firestone R, Hellström KE: Immunoconjugates and immunotoxins for therapy of solid tumors. Cancer Chemother Pharmacol 1996, 38:35–36.
2. Pastan I: Targeted therapy of cancer with recombinant immunotoxins. Biochim Biophys Acta 1997, 1333:1–6.
3. Dvorak HF, Nagy JA, Dvorak AM: Structure of solid tumors and their vasculature: implications for therapy with monoclonal antibodies. Cancer Cells 1991, 3:77–85.
4. Shockley TR, Lin K, Nagy JA, Tompkins RG, Dvorak HF, Yarmush ML: Penetration of tumor tissue by antibodies and other immunoproteins. Ann N Y Acad Sci 1991, 618:367–382.
5. Jain RK: Delivery of molecular and cellular medicine to solid tumors. Microcirculation 1997, 4:3–23.
6. Nowell PC: The clonal evolution of tumor cell populations. Science 1976, 194:23–28.
7. Denekamp J: Review article: angiogenesis, neovascular proliferation and vascular pathophysiology as targets for cancer therapy. Br J Radiol 1993, 66:181–196.
8. Burrows FJ, Thorpe PE: Vascular targeting: a new approach to the therapy of solid tumors. Pharmacol Ther 1994, 64:155–174.
9. Baillie CT, Winslet MC, Bradley NJ: Tumour vasculature: a potential therapeutic target. Br J Cancer 1995, 72:257–267.
10. Folkman J: Antiangiogenic therapy. In Cancer: Principles and Practice of Oncology, edn5. Edited by DeVita VT, Hellman S, Rosenberg SA. Philadelphia: Lippincott-Raven; 1997:3075–3085.
11. Fox SB, Harris AL: Markers of tumor angiogenesis: clinical applications in prognosis and anti-angiogenic therapy. Invest New Drugs 1997, 15:15–28.
12. Molema G, de Leij LF, Meijer DK: Tumor vascular endothelium: barrier or target in tumor directed drug delivery and immunotherapy. Pharm Res 1997, 14:2–10.
13. Zetter B: Tumor angiogenesis and metastasis. Ann Rev Med 1998, 49:407–424.
14. Kerbel RS: Inhibition of tumor angiogenesis as a strategy to circumvent acquired resistance to anti-cancer therapeutic agents. Bioessays 1991, 13:31–36.
15. •• Boehm T, Folkman J, Browder T, O'Reilly MS: Antiangiogenic therapy of experimental cancer does not induce acquired drug resistance. Nature 1997, 390:404–407.

Validates the hypothesis that antiangiogenic therapies circumvent the problem of resistance to chemotherapy. See also O'Reilly *et al.* (Cell 1997, 88:277–285).

16. •• Huang X, Molema G, King S, Watkins L, Edgington TS, Thorpe PE: Tumor infarction in mice by antibody-directed targeting of tissue factor to tumor vasculature. Science 1997, 275:547–550.

An elegant proof of principle showing that a thrombosis in tumor vasculature has marked antitumor effects.

17. Burrows FJ, Thorpe PE: Eradication of large solid tumors in mice with an immunotoxin directed against tumor vasculature. Proc Natl Acad Sci U S A 1993, 90:8996–9000.
18. • Asahara T, Murohara T, Sullivan A, Silver M, van der Zee R, Li T, et al.: Isolation of putative progenitor endothelial cells for angiogenesis. Science 1997, 275:964–967.

Circulating endothelial precursor cells preferentially localize in sites of angiogenesis, opening up new targeting possibilities.

19. Saiki I, Murata J, Makabe T, Nishi N, Tokura S, Azuma I: Inhibition of tumor angiogenesis by a synthetic cell-adhesive polypeptide containing the Arg-Gly-Asp (RGD) sequence of fibronectin, poly(RGD). Jpn J Cancer Res 1990, 81:668–675.
20. Ruoslahti E: RGD and other sequence recognition sequences for integrins. Ann Rev Cell Dev Biol 1996, 12:697–715.
21. Brooks PC, Clark RA, Cheresh DA: Requirement of vascular integrin $\alpha v\beta 3$ for angiogenesis. Science 1994, 264:569–571.
22. Brooks PC, Montgomery AM, Rosenfeld M, Reisfeld RA, Hu T, Klier G, Cheresh DA: Integrin $\alpha v\beta 3$ antagonists promote tumor regression by inducing apoptosis of angiogenic blood vessels. Cell 1994, 79:1157–1164.
23. Hammes HP, Brownlee M, Jonczyk A, Sutter A, Preissner KT: Subcutaneous injection of a cyclic peptide antagonist of vitronectin receptor-type integrins inhibits retinal neovascularization. Nature Med 1996, 2:529–533.
24. • Carron CP, Meyer DM, Pegg JA, Engleman VW, Nickols MA, Settle SL, et al.: A peptidomimetic antagonist of the integrin $\alpha v\beta 3$ inhibits Leydig cell tumor growth and the development of hypercalcemia of malignancy. Cancer Res 1998, 58:1930–1935.

A potent RGD mimetic shows promise in (antiangiogenic) tumor therapy.

25. Pasqualini R, Bodorova J, Ye S, Hemler ME: Monoclonal antibodies for study of the structure, function and distribution of $\beta 5$ containing integrins J. Cell Science 1993, 105:101–111.
26. Senger DR, Claffey KP, Benes JE, Perruzzi CA, Sergiou AP, Detmar M: Angiogenesis promoted by vascular endothelial growth factor: regulation through $\alpha 1\beta 1$ and $\alpha 2\beta 1$ integrins. Proc Natl Acad Sci U S A 1997, 94:13612–1367.
27. Ferrara N, Davis-Smyth T: The biology of vascular endothelial growth factor. Endocr Rev 1997, 18:4–25.
28. Hanahan D: Signaling vascular morphogenesis and maintenance. Science 1997, 277:48–50.
29. Risau W: Mechanisms of angiogenesis. Nature 1997, 386:671–674.
30. Korpelainen EI, Alitalo K: Signaling angiogenesis and lymphangiogenesis. Curr Opin Cell Biol 1998, 10:159–164.
31. Brekken RA, Huang X, King SW, Thorpe PE: Vascular endothelial growth factor as a marker of tumor endothelium. Cancer Res 1998, 58:1952–1959.
32. • Jeltsch M, Kaipainen A, Joukov V, Meng XJ, Lakso M, Rauvala H, et al.: Hyperplasia of lymphatic vessels in VEGF-C transgenic mice. Science 1997, 276:1423–1425.

A major advance in the understanding of lymphangiogenesis controlled by VEGF-C and its VEGF receptor-3.

33. Jussila L, Valtola R, Partanen TA, Salven P, Heikkila P, Matikainen MT, et al.: Lymphatic endothelium and Kaposi's sarcoma spindle cells detected by antibodies against the vascular endothelial growth factor receptor-3. Cancer Res 1998, 58:1599–1604.

34. Peters KG, Coogan A, Berry D, Marks J, Iglehart JD, Kontos CD, et al.: Expression of Tie/Tek in breast tumour vasculature provides a new marker for evaluation of tumour angiogenesis. Br J Cancer 1998, 77:51–56.

35. • Neri D, Carnemolla B, Nissim A, Leprini A, Querze G, Balza E, et al.: Targeting by affinity-matured recombinant antibody fragments of an angiogenesis associated fibronectin isoform. Nature Biotechnol 1997, 15:1271–1275.

This paper presents a tumor-imaging application with a human antibody selected from a phage library.

36. Olson TA, Mohanraj D, Roy S, Ramakrishnan S: Targeting the tumor vasculature: inhibition of tumor growth by a vascular endothelial growth factor-toxin conjugate. Int J Cancer 1997, 73:865–870.

37. Kennel SJ, Mirzadeh S: Vascular targeted radioimmunotherapy with ^{213}Bi: an alpha-particle emitter. Nuclear Med Biol 1998, 25:241–246.

38. Thurston G, McLean JW, Rizen M, Baluk P, Haskell A, Murphy TJ, et al.: Cationic liposomes target angiogenic endothelial cells in tumors and chronic inflammation in mice. J Clin Invest 1998, 101:1401–1413.

39. Pasqualini R, Ruoslahti E: Organ targeting in vivo using phage display peptide libraries. Nature 1996, 380:364–366.

40. Rajotte D, Arap W, Hagedorn M, Koivunen E, Pasqualini R, Ruoslahti E: Molecular heterogeneity of the vascular endothelium revealed by in vivo phage display. J Clin Invest 1998, 102:430–437.

41. •• Arap W, Pasqualini R, Ruoslahti E: Cancer treatment by targeted drug delivery to tumor vasculature in a mouse model. Science 1998, 279:377–380.

Doxorubicin-homing peptide conjugates targeted to tumor vasculature dramatically improved survival of tumor-bearing mice while lowering the toxicity of the treatment.

42. Koivunen E, Wang B, Ruoslahti E: Phage libraries displaying cyclic peptides with different ring sizes: ligand specificities of the RGD-directed integrins. Biotechnology 1995, 13:265–270.

43. • Pasqualini R, Koivunen E, Ruoslahti E: av Integrins as receptors for tumor targeting by circulating ligands. Nature Biotechnol, 1997 15:542–546.

This paper shows that the tumor neovasculature can be specifically targeted by *in vivo* phage display through an integrin expressed in tumor blood vessels.

44. Wickham TJ, Tzeng E, Shears LL, Roelvink PW, Li Y, Lee GM, et al.: Increased in vitro and in vivo gene transfer by adenovirus vectors containing chimeric fiber proteins. J Virol 1997, 71:8221–8229.

45. Lazo JS: Endothelial injury caused by antineoplastic agents. Biochem Pharmacol 1986, 35:1919–1923.

46. Belotti D, Vergani V, Drudis T, Borsotti P, Pitelli MR, Viale G, et al.: The microtubule-affecting drug paclitaxel has antiangiogenic activity. Clin Cancer Res 1996, 1843–1849.

47. Dark GG, Hill SA, Prise VE, Tozer GM, Pettit GR, Chaplin DJ: Combretastatin A-4, an agent that displays potent and selective toxicity toward tumor vasculature. Cancer Res 1997, 57:1829–1834.

48. Hill S, Williams KB, Denekamp J: Vascular collapse after flavone acetic acid: a possible mechanism of its anti-tumour action. Eur J Cancer Clin Oncol 1990, 25:1419–1424.

49. Gasparini G: Antiangiogenic drugs as novel anticancer therapeutic strategy: which are the more promising agents? What are the clinical developments and indications? Crit Rev Oncol Hematol 1997, 26:147–162.

50. Pluda JM: Tumor-associated angiogenesis: mechanisms, clinical implications, and therapeutic strategies. Sem Oncol 1997, 24:203–218.

51. Twardowski P, Gradishar WJ: Clinical trials of antiangiogenic agents. Curr Opin Oncol 1997, 9:584–589.

52. O'Reilly MS, Holmgren L, Shing Y, Chen C, Rosenthal RA, Moses M, et al.: Angiostatin: a novel angiogenesis inhibitor that mediates the suppression of metastases by a Lewis lung carcinoma. Cell 1994, 79:315–328.

53. • O'Reilly MS, Boehm T, Shing Y, Fukai N, Vasios G, Lane WS, et al.: Endostatin: an endogenous inhibitor of angiogenesis and tumor growth. Cell 1997, 88:277–285.

O'Reilly *et al.* report the isolation, characterization, and cloning of endostatin, a novel antiangiogenic agent. See also Boehm *et al.* (Nature 1997, 390:404–407).

54. Folkman J: Angiogenesis and angiogenesis inhibition: an overview. EXS 1997, 79:1–8.

55. • Brooks PC, Silletti S, von Schalscha TL, Friedlander M, Cheresh DA: Disruption of angiogenesis by PEX, a noncatalytic metalloproteinase fragment with integrin binding activity. Cell 1998, 92:391–400.

This article describes a new antiangiogenic protein fragment.

56. Brown JM, Giaccia AJ: The unique physiology of solid tumors: opportunities (and problems) for cancer therapy. Cancer Res 1998, 58:1408–1416.

[CANCER RESEARCH 59, 2869–2874, June 15, 1999]

NG2 Proteoglycan-binding Peptides Target Tumor Neovasculature[1]

Michael A. Burg,[2] Renata Pasqualini, Wadih Arap, Erkki Ruoslahti, and William B. Stallcup[3]

Cancer Research Center, The Burnham Institute, La Jolla, California 92037

ABSTRACT

NG2 is the rat homologue of the human melanoma proteoglycan, also known as the high molecular weight melanoma-associated antigen. This developmentally regulated membrane-spanning chondroitin sulfate proteoglycan is expressed primarily by glial, muscle, and cartilage progenitor cells. Upon maturation, these cell types down-regulate NG2 expression. In adult animals, the expression of NG2 is restricted to tumor cells and angiogenic tumor vasculature, making this proteoglycan a potential target for directing therapeutic agents to relevant sites of action. To this end, we have identified specific NG2-binding peptides by screening a phage-displayed random peptide library on purified NG2. Several rounds of biopanning on NG2 resulted in the specific enrichment of two phage-displayed decapeptides, TAASGVRSMH and LTLRWVGLMS. The binding of these phages to NG2 was inhibitable both by soluble NG2 and by glutathione *S*-transferase (GST) fusion proteins containing the cognate peptide sequences. In addition, direct binding between GST-TAASGVRSMH and GST-LTLRWVGLMS fusion proteins and NG2 was demonstrated in solid-phase binding assays. Interestingly, these NG2-binding fusion proteins cross-inhibited each other's binding to NG2, suggesting that the two sequences bind to the same or overlapping sites on the proteoglycan. Upon injection into tumor-bearing mice, NG2-binding phages specifically homed to tumor vasculature in wild-type mice but did not localize to the tumor vasculature in NG2 knockout mice. The *in vivo* targeting capability of these sequences suggests that they can be used for tumor targeting.

INTRODUCTION

Current anticancer strategies have been directed at the identification and characterization of molecules that are preferentially expressed by either tumor cells or cells of the angiogenic blood vessels associated with the tumor. Once identified, these molecules serve as potential targets for directing chemotherapeutic or immunotherapeutic agents to tumor cells and/or their associated vasculature (1–7).

The rat proteoglycan NG2 (8) and its homologue, HMP[4] (9), are possible targets for anticancer therapy. NG2/HMP is widely expressed by several different tumors, including glioblastomas, chondrosarcomas, melanomas, and some leukemias (10–13). Numerous reports have shown that NG2/HMP expression increases the proliferative capacity of melanoma cells (14–17). Moreover, antibodies against NG2/HMP inhibit melanoma cell growth both *in vitro* (15) and *in vivo* (14–16). Recently, we have shown that transfection of NG2 into NG2-negative B16F1 and B16F10 mouse melanoma cell lines increases both the proliferative capacity of these cells *in vitro* and tumor size *in vivo* (17). NG2 expression also increased lung colonization for both B16F1 and B16F10 cells in experimental metastasis studies. Although the specific mechanism by which NG2 enhances the proliferative and metastatic properties of these cells is unclear, association of NG2 with known extracellular matrix ligands such as type VI collagen (18–21) or cellular ligands such as CD44 and $\alpha_4\beta_1$ integrin (17, 22) and its ability to enhance cellular responses to at least one growth factor, platelet-derived growth factor-AA (23, 24), appear to be important in these processes.

NG2/HMP is also widely expressed by angiogenic blood vessels. This is true not only for the expanding vasculature of normally developing tissues (23) but also for the neovasculature found in tumor stroma and in granulation tissue of healing wounds (12, 25, 26). In contrast, NG2/HMP is not detectable in normal quiescent vasculature. Immunohistochemical studies have suggested that NG2/HMP expression in neovasculature is limited to the neovascular pericytes (25, 26). However, NG2/HMP expression by endothelial cells in developing brain capillaries has also been reported (12, 23). Pericytes are intimately associated with endothelial cells in developing vasculature (27) and are thought to affect angiogenesis by regulating endothelial cell proliferation, directing microvessel outgrowth, and stabilizing capillary walls (27–30).

Because of the selective expression of NG2/HMP in tumor cells and tumor vasculature, several groups have chosen this molecule as a target for immunotherapy of cancer. An anti-NG2/HMP mAb-doxorubicin conjugate was shown to suppress malignant melanoma growth in a nude mouse model (31). Additionally, anti-NG2/HMP mAb-toxin and ^{131}I-radiolabeled conjugates have been shown to have some therapeutic value for patients with malignant melanoma (32, 33). However, these trials have not been as successful as one might have hoped. In general, antibody-based therapies are often found to have limitations, mostly due to poor tissue penetration and unwanted immune responses (3, 6, 34–37). The alternative approach of using small peptides capable of targeting cells within tumor vasculature or stroma may alleviate many of the problems associated with antibody-based targeting strategies (2, 7, 37).

Phage display of random peptide libraries has proven to be successful in the isolation of peptides capable of binding to integrins (38–40), growth factor receptors (41), and other tumor cell-associated proteins (42–44). Moreover, *in vivo* phage targeting has allowed us to identify several peptides that home to vasculature of specific organs as well as to tumor neovasculature (45–47). Here, we have used phage display to isolate peptides that bind to the NG2 proteoglycan and home to NG2-expressing tumor neovasculature.

MATERIALS AND METHODS

Materials. B16F10 mouse melanoma cells were obtained from the Division of Cancer Treatment Tumor Bank, National Cancer Institute-Frederick Cancer Research Facility (Frederick, MD). Rat antimouse CD31 antibodies were obtained from PharMingen (La Jolla, CA). Rabbit antibodies against NG2 have been described previously (23, 24).

Fuse5 vector and K91 bacterial strain were a gift from G. Smith (University of Missouri-Columbia, Ref. 48). Construction of the random linear decapeptide phage library has been described (39). The library titer was $\sim 10^{13}$ TU/ml.

Isolation of NG2-binding Phages. A recombinant fragment of rat NG2 consisting of the NH_2-terminal two-thirds of the extracellular domain (NG2ECΔ3) was purified from transfected human embryonic kidney 293 cells as described (21). Recombinant NG2Δ3 diluted in PBS (2 μg of NG2 per well) was coated onto microtiter wells overnight at 4°C. Wells were blocked with

Received 12/22/98; accepted 4/16/99.

The costs of publication of this article were defrayed in part by the payment of page charges. This article must therefore be hereby marked *advertisement* in accordance with 18 U.S.C. Section 1734 solely to indicate this fact.

[1] This work was supported by NIH Grants R01CA74238 (to E. R.), R01NS21990, and R01NS32767 (to W. B. S.) and by Cancer Center Support Grant CA30199 from the National Cancer Institute. M. A. B. is supported by NIH Fellowship F32CA72220 and W. A. is the recipient of a CaPCURE award.

[2] Present address: Selective Genetics, Inc., 11035 Roselle Street, San Diego, CA 92121.

[3] To whom requests for reprints should be addressed, at Cancer Research Center, The Burnham Institute, 10901 North Torrey Pines Road, La Jolla, CA 92037. Phone: (619) 455-6480 ext. 3220; Fax: (619) 646-3197; E-mail: stallcup@burnham-inst.org.

[4] The abbreviations used are: HMP, human melanoma proteoglycan; mAb, monoclonal antibody; TU, transducing unit(s); GST, glutathione *S*-transferase.

2% PBS-BSA for 1 h at room temperature. For biopanning, phages (1×10^{11} TU) from a linear decapeptide phage library diluted in 2% BSA were added to proteoglycan-coated wells and incubated for 2 h at room temperature. Wells were washed with PBS containing 0.1% Tween 20 to remove unbound phages. Bound phages were recovered by direct infection of wells with exponentially growing K91kan bacteria, followed by phage amplification overnight at 37°C. Amplified phages were then subjected to four subsequent rounds of selection on NG2-coated wells. Phage binding was quantified by counting colonies from aliquots of phage-infected bacteria removed from NG2-coated wells. Phages were sequenced from randomly selected clones as described (39).

Binding of individual phage clones or an aliquot of unselected phage library control to NG2Δ3 or BSA-coated control wells was performed as described above using 1×10^9 input phages per well. For competition studies, phage incubations were performed in the presence of increasing concentrations of soluble NG2Δ3 or GST fusion proteins. Soluble GST alone was used as a control in these competition experiments.

Solid-phase Binding Assays. GST fusion proteins containing the decapeptide inserts were constructed as described previously (47) and dissolved in PBS. Briefly, peptide inserts were PCR-amplified from the phages using specific M13 primers. PCR products were then digested with *Bam*HI and *Eco*RI and inserted into the pGEX2TK vector. Fusion proteins were produced and purified according to manufacturer's instructions (Pharmacia, Buckinghamshire, England).

Solid-phase assays were performed as described previously (19). Briefly, GST fusion proteins or GST alone (2 μg/well) were coated onto microtiter

Table 1 *Selection of NG2-binding phage from a linear decapeptide phage library*[a]

III	IV	V
TAASGVRSMH	TAASGVRSMH (16)	TAASGVRSMH (8)
LTLRWVGLMS	LTLRWVGLMS (10)	LTLRWVGLMS (7)
GGGTRAGMKY (2)		
WGKIEDPLRA		
AGQTLTASGD		
DLLAVSWLRA		
SAERGVVAMS		
AIHSELMWVS		
FWTERAGWAY		
MVWSKGPLFL		
AGTRMSWEVL		
VSRSSRWGSI		
DAHVLVPRTP		
AQGIVLQLAL		
LSPLLSPATA		

[a] An aliquot (2×10^{11} TU) of a random linear decapeptide phage library was biopanned on immobilized NG2Δ3 as described in "Materials and Methods." Five successive rounds of biopanning were performed. Shown are the peptide sequences from the inserts displayed from the last three rounds of selection. Numbers in parentheses are the numbers of clones displaying the same sequence.

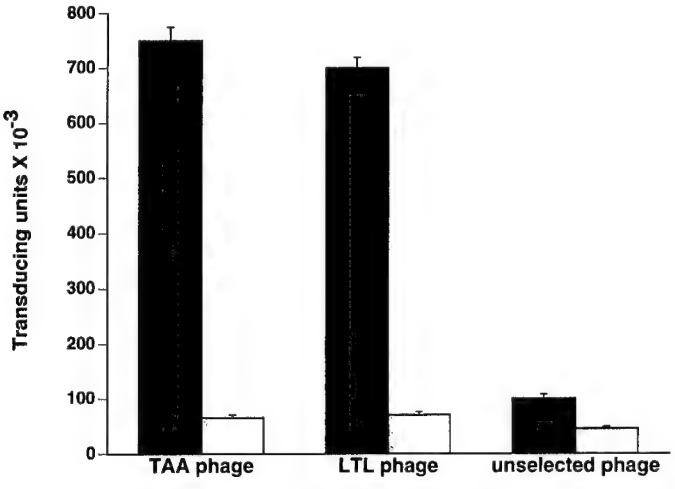

Fig. 1. Phage attachment assay. Purified TAASGVRSMH (TAA) and LTLRWVGLMS (LTL) phages or an unselected library mix (unamplified decapeptide library) were incubated in NG2Δ3-coated (■) or BSA-coated (□) microtiter wells and bound phages were quantified as described in "Materials and Methods." Results are representative of three independent experiments. *Columns*, means from triplicate platings; *bars*, SE. All differences are statistically highly significant, as assessed by the Student's *t* test ($P < 0.01$).

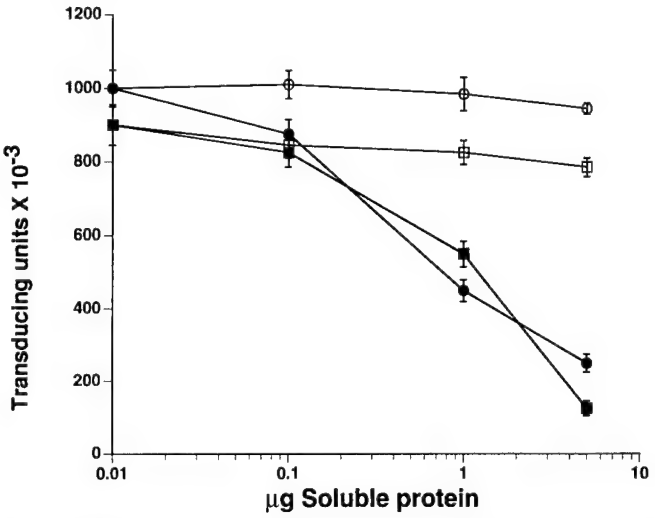

Fig. 2. Inhibition of phage binding by soluble NG2. Purified TAASGVRSMH phage (○ and ●) and LTLRWVGLMS phage (□ and ■) were incubated in NG2Δ3-coated wells in the presence of the indicated concentrations of soluble NG2Δ3 (● and ■) or soluble GST (○ and □). Bound phages were quantified as described above. Results are representative of three independent experiments. *Data points*, means from triplicate platings of duplicate wells; *bars*, SE.

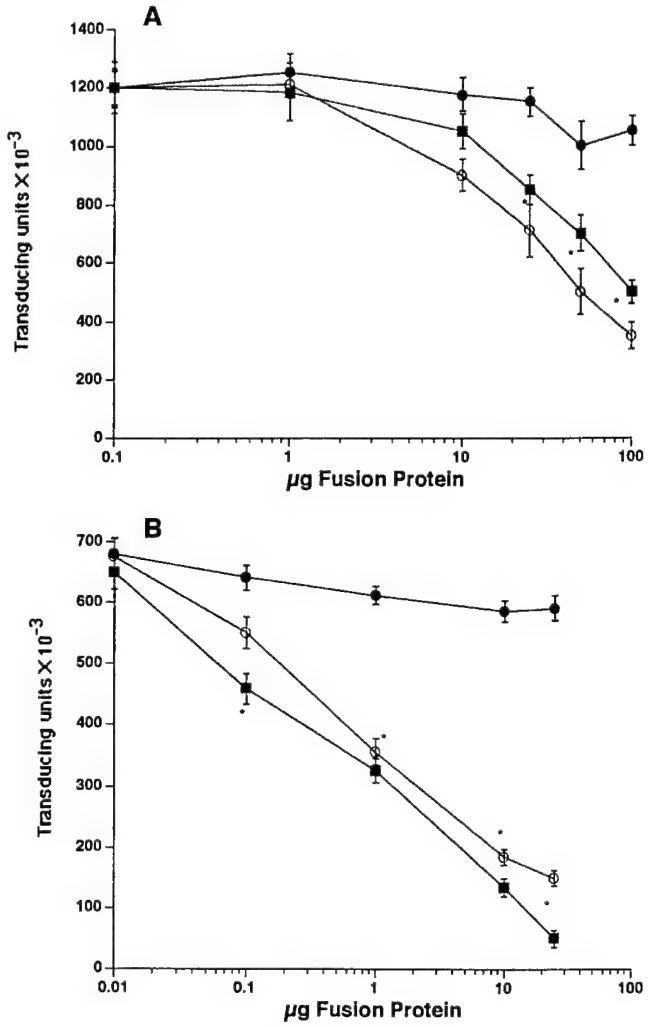

Fig. 3. Inhibition of phage binding by cognate sequences. Purified phages were incubated in NG2Δ3-coated wells in the presence of the indicated concentrations of GST-TAASGVRSMH fusion protein (○), GST-LTLRWVGLMS fusion protein (■), or GST alone (●), and phage binding was quantified. Results are representative of three independent experiments. *Data points*, means from triplicate platings of duplicate wells; *bars*, SE. *, considered highly significant by the Student's *t* test ($P < 0.01$). *A*, binding of TAASGVRSMH phage. *B*, binding of LTLRWVGLMS phage.

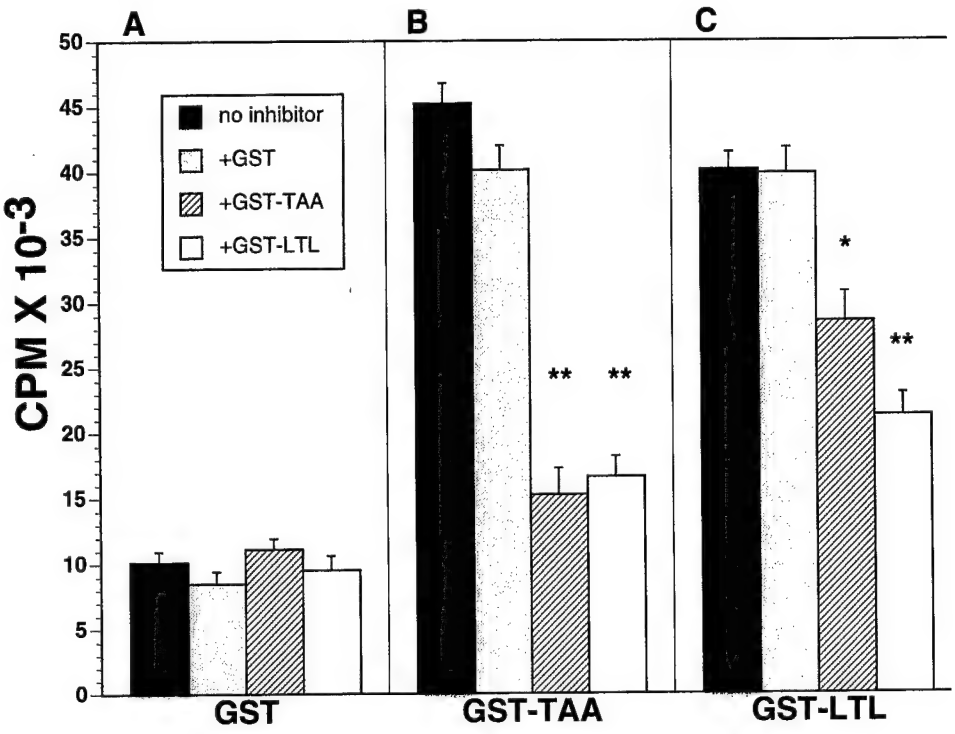

Fig. 4. Binding of NG2 to immobilized fusion proteins. Purified NG2Δ3 was incubated in GST or GST fusion protein-coated wells in the absence of inhibitor (■) or after preincubation with 50 μg of soluble GST (▨), GST-TAASGVRSMH (▨), or GST-LTLRWVGLMS (□). Binding of NG2Δ3 was determined as described in "Materials and Methods." Results are representative of three independent experiments. *Columns*, means from triplicate wells; *bars*, SE. *, considered significant by Student's *t* test ($P < 0.05$); **, considered highly significant by Student's *t* test ($P < 0.01$). *A*, binding to GST-coated wells (*GST*). *B*, binding to GST-TAASGVRSMH-coated wells (*GST-TAA*). *C*, binding to GST-LTLRWVGLMS-coated wells (*GST-LTL*).

wells overnight at 4°C. Wells were blocked with 2% BSA-PBS and incubated with soluble NG2Δ3 (1 μg/well) for 2 h at room temperature. After washing, wells were incubated with an anti-NG2 polyclonal antibody followed by washing and incubation with an ^{125}I-labeled goat antirabbit IgG. After a final washing, bound radioactivity was determined using a gamma counter. For competition studies, soluble NG2Δ3 was preincubated for 15 min with increasing concentrations of soluble GST fusion proteins prior to incubation on GST fusion protein-coated wells. Preincubation with GST alone served as a control in these competition experiments.

***In Vivo* Phage Targeting.** *In vivo* phage targeting was performed on 4–6-week-old NG2 knockout mice and control F_1 wild-type mice. Generation and characterization of these mice has been previously described (49). For tumor generation, B16F10 mouse melanoma cells were harvested from subconfluent cultures using nonenzymatic cell dissociation buffer (Life Technologies, Inc., Gaithersburg, MD). Cells (1×10^6 cells in 0.2 ml of DMEM) were injected s.c. into the mouse right flank. Tumors were monitored between 10 and 20 days postinjection, and animals bearing tumors of ~1–2 cm in diameter were selected for phage targeting.

Tumor targeting using phages was performed as described previously (46). Briefly, phages (1×10^9–1×10^{10}) were injected i.v. (lateral tail vein) into anesthetized (0.017 ml per g of Avertin) mice and allowed to circulate for 5 min. Mice were then perfused through the heart with 5 ml of DMEM. Tumors and brains were removed and weighed. Tissues were homogenized in DMEM containing protease inhibitors (45), and phages were rescued and quantified from these tissues as described (45, 46).

Immunohistochemistry. For immunohistochemistry, B16F10 tumors were grown in NG2 knockout and F_1 control mice as described above. Tumors were removed and fresh-frozen, and 25-μm sections were cut on a cryostat. Tumor vascularization was visualized using a mixture of a rat antimouse CD31 mAb (Pharmacia) and anti-NG2 polyclonal antibodies. Secondary staining was performed with FITC-conjugated antirabbit immunoglobulin and rhodamine isothiocyanate-conjugated antirat immunoglobulin antibodies (Biosource International, Camarillo, CA). Confocal images were obtained using a Zeiss LSM 410 laser scanning confocal microscope (Carl Zeiss, Thornwood, NY).

RESULTS

Isolation of NG2-binding Phages. To identify peptide motifs capable of interacting with NG2, we coated recombinant NG2 fragments consisting of the NH_2-terminal two-thirds of the extracellular domain of the proteoglycan (NG2Δ3) onto microtiter wells and used them to select phage clones from a random decapeptide phage display library. Bound phages were isolated and used for successive rounds of panning on the proteoglycan. Random clones were sequenced from rounds II–V. Sequence analysis from the final three rounds of panning (Table 1) indicates the specific enrichment of two decapeptide sequences, TAASGVRSMH and LTLRWVGLMS. These sequences first appeared in round II and III and became the exclusive motifs bound to NG2 in the subsequent rounds of selection.

Binding Characteristics of the TAASGVRSMH and LTLRWVGLMS Phages. Phages displaying TAASGVRSMH or LTLRWVGLMS were tested individually for their ability to bind to NG2Δ3-coated wells. The results showed that both phages specifically bind to the proteoglycan. An equivalent number of control phages from the unselected decapeptide phage library (Fig. 1) or phages containing no peptide inserts (data not shown) showed negligible binding to NG2. Moreover, binding of the TAASGVRSMH and LTLRWVGLMS phages to BSA was minimal compared to their binding to the proteoglycan.

To confirm the specificity of these interactions, we incubated both species of NG2-binding phages with increasing concentrations of soluble recombinant NG2Δ3 prior to incubation with NG2Δ3-coated wells. The results show a dose-dependent inhibition of binding of both phage populations to the NG2-coated substratum (Fig. 2). As a control, preincubation of the two phage species with GST did not inhibit binding to NG2Δ3. In addition, the low level of binding of unselected phages to NG2Δ3 (as illustrated in Fig. 1) was not affected by incubation with either soluble NG2Δ3 or GST, confirming the nonspecific nature of this binding (data not shown).

Inhibition of Phage Binding with Cognate Sequences. GST fusion proteins containing the two NG2-binding motifs were constructed and tested for their ability to inhibit binding of phages to NG2Δ3-coated wells. When TAASGVRSMH phages were allowed to bind to NG2Δ3 coated wells in the presence of increasing concentra-

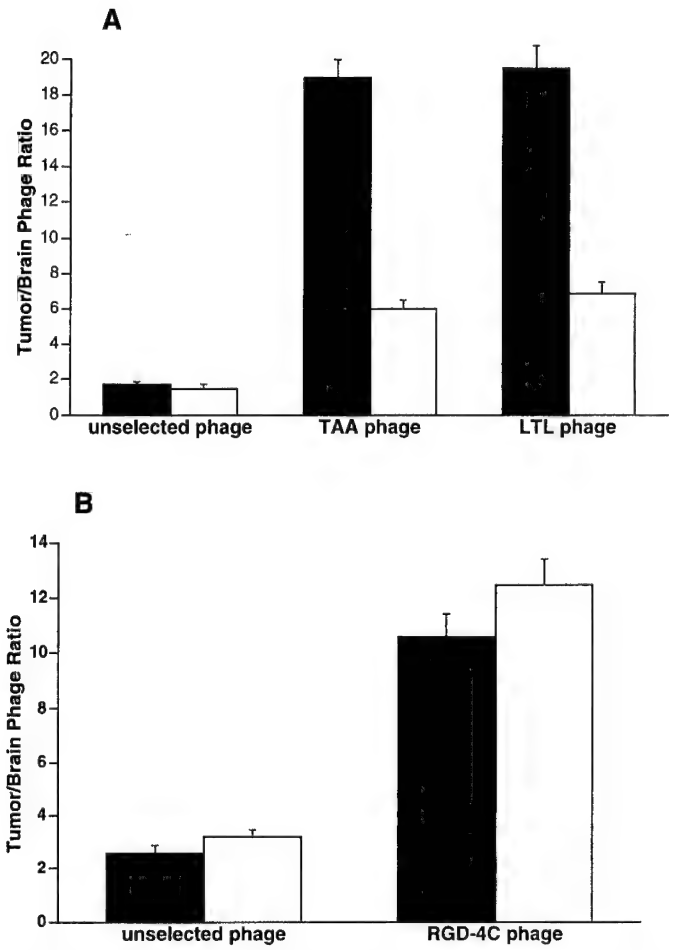

Fig. 5. Homing of phages to tumor vasculature. Tumor (B16F10)-bearing NG2-null (□) or F_1 wild-type (■) mice were injected i.v. via the tail vein with 10^{10} TU of purified RGD-4C, TAASGVRSMH, LTLRWVGLMS, or unselected library mix (unamplified decapeptide library) phages. Five min after injection, mice were perfused, and phages were recovered from tumors and from brain as described in "Materials and Methods." Phage yields were quantified as the number of TU recovered per g of tissue. As a measure of specific homing to tumors, results in the figure are expressed as a ratio of tumor homing phages to brain homing phages. Results are representative of three independent experiments. *Columns*, means from triplicate platings; *bars*, SE. All differences in *A* are considered highly significant by Student's *t* test ($P < 0.01$). *A*, homing of NG2-binding phages. *B*, homing of RGD-4C phages.

tions of the cognate fusion protein, a dose-dependent decrease in binding was observed (Fig. 3*A*). Interestingly, the binding of these phages to NG2Δ3 was also inhibited by increasing concentrations of GST-LTLRWVGLMS. In contrast, incubation of the phages with a control GST protein without a peptide insert did not significantly inhibit binding.

A similar result was obtained when the binding of LTLRWVGLMS phage was tested in the presence of increasing concentrations of GST fusion proteins. Both fusion proteins inhibited the binding of this phage species to NG2Δ3, whereas the control GST protein had no significant effect on the binding (Fig. 3*B*).

Solid-phase Binding of GST Fusion Proteins to NG2. The ability of soluble NG2Δ3 to bind to GST, GST-TAASGVRSMH, and GST- LTLRWVGLMS was tested by using a solid-phase assay. The results indicate that the soluble proteoglycan binds much more effectively to the immobilized fusion proteins than to GST alone (Fig. 4). In addition, preincubation of NG2Δ3 with increasing concentrations of GST-TAASGVRSMH resulted in a dose-dependent decrease in binding of the proteoglycan to wells coated with this same fusion protein (Fig. 4*B*). Preincubation of NG2Δ3 with increasing concentrations of GST-LTLRWVGLMS also inhibited binding of the proteoglycan to wells coated with GST-TAASGVRSMH. These results reinforce the notion that the two peptides bind to similar sites on NG2. Both of the soluble fusion proteins also inhibited the binding of NG2Δ3 to wells coated with GST-LTLRWVGLMS (Fig. 4*C*). In both cases, preincubation of the proteoglycan with soluble GST failed to give significant inhibition of binding to the GST fusion proteins (Fig. 4, *B* and *C*). In addition, the level of nonspecific binding of NG2Δ3 to GST alone was not further reduced by preincubation with GST or GST fusion proteins (Fig. 4*A*).

Tumor Targeting *in Vivo* Using NG2-binding Phages. We were interested in determining whether NG2-binding phages were capable of targeting NG2 within tumor vasculature. We compared the ability of NG2-binding phages to home to the vasculature of B16 melanoma xenografts growing in either wild-type or NG2-null mice. When an equivalent number of NG2-binding phages were injected i.v. into the two lines of tumor-bearing mice, both TAASGVRSMH and LTLRWVGLMS phages were found to home specifically to tumors of NG2-expressing wild-type mice. In contrast, there was much less homing to tumors established in NG2 null mice (Fig. 5*A*). In addition, control phages did not show selective accumulation to the tumors established in either wild-type or NG2 knockout mice. In a separate experiment, tumor targeting phage previously shown to bind to α_v integrins (46) exhibited equivalent abilities to target tumors in wild-type and NG2-null mice (Fig. 5*B*). This result indicates that the homing of NG2-binding phages to tumors in wild-type mice is mediated by NG2 expression and is not due to other differences between tumor vasculature of wild-type and NG2-null mice.

Immunohistochemical examination of the tumor vasculature in wild-type mice showed NG2 expression was limited to vascular pericytes, which were abluminally associated with CD31-positive endothelial cells (Fig. 6, *A–C*). NG2-knockout mice exhibited no NG2 immunoreactivity but showed normal CD31-positive endothelial cell staining (Fig. 6, *D–F*). No other major difference between vasculature of B16 tumors grown in wild-type and NG2 knockout mice was observed.

DISCUSSION

Here, we have described the use of phage display to identify two novel peptide ligands for the NG2 proteoglycan. These decapeptides compete with one another for binding to NG2, suggesting that they recognize the same or overlapping sites on the proteoglycan. The two sequences are clearly different but may act as mimotopes of each other on the basis of small areas of similarity (VR *versus* LR, SM *versus* MS, and ASG *versus* LTL). Database searches revealed no significant similarities between the two decapeptide sequences and known ligands for the proteoglycan (17, 19, 21). They, therefore, represent either novel ligands or mimotopes of sequences present in previously characterized ligands.

Both of the NG2-binding sequences are able to direct the homing of peptide-bearing phages to the NG2-positive neovasculature of melanoma xenografts in mice. Significantly, this tumor homing is greatly reduced in NG2-null mice, illustrating the importance of NG2 as the target molecule. In wild-type mice, we were able to localize NG2 expression to pericytes in the angiogenic vasculature of the xenografts. This agrees with earlier reports of NG2 localization in tumor vasculature (25, 26). Because the phages are relatively large particles and not likely to be able to penetrate an intact endothelial layer in the short time we used for the homing, our results show that pericytes in tumor vessels are accessible to circulating probes. The reason for this may be that tumor vessels are "leaky" (50–52). The localization and accessibility of NG2 on pericytes suggest the potential use of NG2-homing sequences for targeting delivery of therapeutic agents to

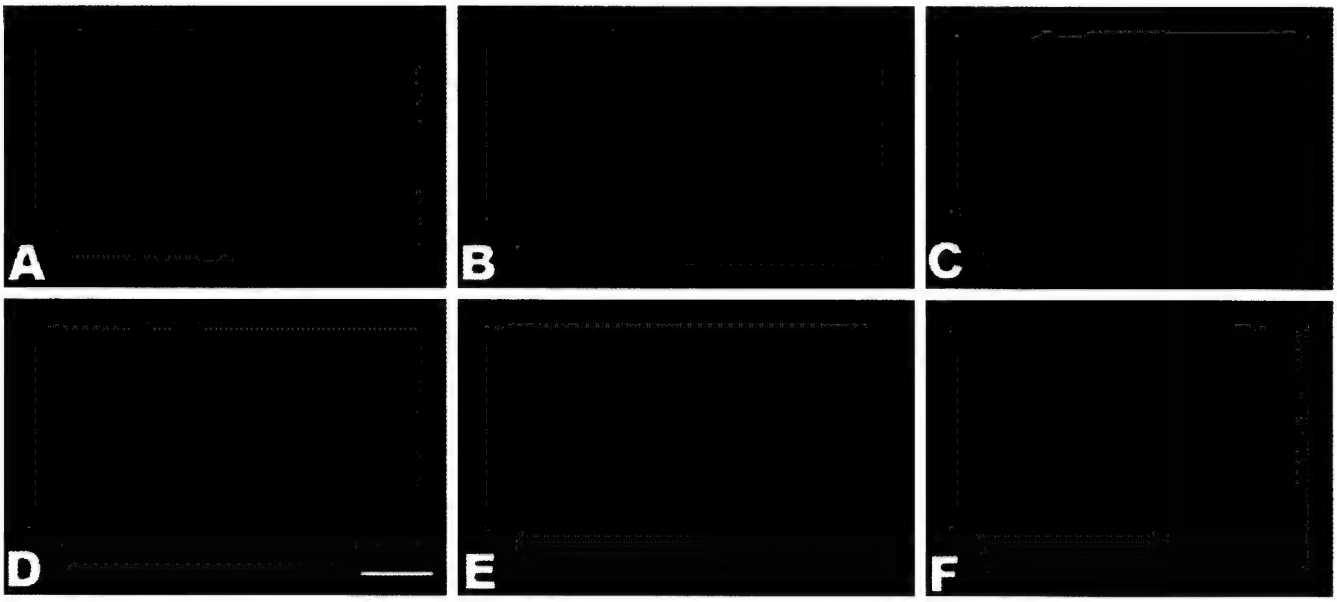

Fig. 6. Immunohistochemical analysis of tumor vasculature in NG2-knockout and wild-type mice. Cryostat sections prepared from B16F10 tumors isolated from NG2-knockout (*D–F*) or F_1 wild-type (*A–C*) mice were double labeled with a polyclonal antiserum directed against NG2 (*A* and *D*) and a rat mAb against CD31 (*B* and *E*). Sections were then stained with fluorescein-conjugated goat antirabbit and rhodamine-conjugated goat antirat secondary antibodies, and confocal images through a single section were obtained. Superimposition of confocal images reveals NG2 expression on pericytic cells abluminally apposed to CD31-positive endothelial cells in wild-type mice (*C*). No NG2 expression was observed in the tumor vasculature of the NG2 knockout mouse (*D* and *F*). Note that the B16 cells themselves are NG2 and CD31 negative and do not contribute to the staining pattern. *Scale bar* (*D*), 10 μm.

tumors. Several reports have suggested that pericytes play an important role in controlling endothelial cell proliferation and stabilization during angiogenesis (27–30). Thus, anticancer strategies based on the targeting of pericytes in angiogenic vasculature may complement approaches based on endothelial cell targeting. Because NG2 is also expressed by the tumor cells themselves in many types of tumors (10–13), the NG2-binding peptides could deliver therapeutics to the tumor cells themselves in addition to targeting tumor vasculature. The small peptides may prove superior to antibodies in terms of penetration into tumors. Future studies will evaluate the relative merits of peptides and antibodies as targeting vectors for NG2.

Specific targeting of tumor vasculature or combined targeting of vasculature and tumor cells offers several advantages over therapies that are strictly tumor-directed. Probes that target tumor cells themselves are limited by both the heterogeneous expression of tumor antigens within the tumor, as well as by the high rate of tumor cell mutation (1, 2, 6, 53). In contrast, cells that comprise tumor vasculature are nonmalignant, relatively homogenous cell populations. The development of resistance to chemotherapy resulting from the high rate of tumor cell mutations is also circumvented by targeting normal cells of the tumor vasculature (54–56).

Finally, the NG2-binding peptides may allow us to identify additional physiological ligands for NG2. Such insights may help elucidate the role of NG2 during development and in pathological conditions. NG2 expression has been found to affect cellular responses to platelet-derived growth factor-AA and cellular interactions with extracellular matrix components (18, 20, 23, 24). In addition, the expression of NG2 increases the malignant potential of tumor cells (17). These findings suggest that NG2 may play a functional role in angiogenesis and tumor development. The peptides we have isolated in this work may prove to be useful probes for analyzing these functions.

REFERENCES

1. Folkman, J. Angiogenesis in cancer, vascular, rheumatoid and other disease. Nat. Med., *1:* 27–31, 1995.
2. Folkman, J. Antiangiogenic therapy. *In:* V. T. DeVita, S. Hellman, and S. A. Rosenberg (eds.), Cancer: Principles and Practice of Oncology, Ed. 5, pp. 3075–3085. Philadelphia: Lippincott-Raven, 1997.
3. Baillie, C. T., Winslet, M. C., and Bradley, N. J. Tumour vasculature: a potential therapeutic target. Br. J. Cancer, *72:* 257–267, 1995.
4. Rak, J. W., St. Croix, B. D., and Kerbel, R. S. Consequences of angiogenesis for tumor progression, metastasis and cancer. Anticancer Drugs, *6:* 3–18, 1995.
5. Derbyshire, E. J., and Thorpe, P. E. Targeting the tumour endothelium using specific antibodies. *In:* R. Bicknell, C. E. Lewis, and N. Ferrara (eds.), Tumor Angiogenesis, pp. 343–356, 1998.
6. Burrows, F. J., and Thorpe, P. E. Eradication of large solid tumors in mice with an immunotoxin directed against tumor vasculature. Proc. Natl. Acad. Sci. USA, *90:* 8996–9000, 1993.
7. Arap, W., Pasqualini, R., and Ruoslahti, E. Chemotherapy targeted to tumor vasculature. Curr. Opin. Oncol., *10:* 560–565, 1998.
8. Nishiyama, A., Dahlin, K. J., Prince, J. T., Johnstone, S. R., and Stallcup, W. B. The primary structure of NG2, a novel membrane-spanning proteoglycan. J. Cell Biol., *114:* 359–371, 1991.
9. Pluschke, G., Vanek, M., Evans, A., Dittmar, T., Schmid, P., Itin, P., Filardo, E., and Reisfeld, R. Molecular cloning of a human melanoma-associated chondroitin sulfate proteoglycan. Proc. Natl. Acad. Sci. USA, *93:* 9710–9715, 1996.
10. Behm, F. G., Smith, F. O., Raimondi, S. C., Pui, C-H., and Bernstein, I. D. Human homologue of the rat chondroitin sulfate proteoglycan, NG2, detected by monoclonal antibody 7.1, identifies childhood acute lymphoblastic leukemias with t(4;11)(q21; q23) or t(11;19)(q23;13) and MLL gene rearragements. Blood, *87:* 1134–1139, 1996.
11. Real, F. X., Houghton, A. N., Albino, Cordon-Cardo, C., Melamed, M. R., Oettgen, H. F., and Old, L. J. Surface antigens of melanomas and melanocytes defined by mouse monoclonal antibodies: specificity, analysis, and comparison of antigen expression in cultured cells and tissues. Cancer Res., *45:* 4401–4411, 1985.
12. Schrappe, M., Klier, F. G., Spiro, R. C., Waltz, T. A., Reisfeld, R. A., and Gladson, C. L. Correlation of chondroitin sulfate proteoglycan expression on proliferating brain capillary endothelial cells with the malignant phenotype of astroglial cells. Cancer Res., *51:* 4986–4993, 1991.
13. Leger, O., Johnson-Leger, C., Jackson, E., Coles, B., and Dean. C. The chondroitin sulfate proteoglycan NG2 is a tumor specific antigen on the chemically induced rat chondrosarcoma HSN. Int. J. Cancer, *58:* 700–705, 1994.
14. Bumol, T. F., Wang, Q. C., Reisfeld, R. A., and Kaplan, N. O. Monoclonal antibody and an antibody-toxin conjugate to a cell surface proteoglycan of melanoma cells suppress *in vivo* tumor growth. Proc. Natl. Acad. Sci. USA, *80:* 529–533, 1983.
15. Harper, J. R., and Reisfeld, R. A. Inhibition of anchorage-independent growth of human melanoma cells by a monoclonal antibody to a chondroitin sulfate proteoglycan. J. Natl. Cancer Inst. (Bethesda), *71:* 259–263, 1983.
16. Harper, J. R., and Reisfeld, R. A. Cell-associated proteoglycans in human malignant melanoma. *In:* T. Wight and R. Mecham (eds.), Biology of Proteoglycans, pp. 345–366. New York: Academic Press, 1987.
17. Burg, M. A., Grako, K. A., and Stallcup, W. B. Expression of the NG2 proteoglycan enhances the growth and metastatic properties of melanoma cells. J. Cell. Physiol., *177:* 299–312, 1998.

18. Nishiyama, A., and Stallcup, W. B. Expression of NG2 proteoglycan causes retention of type VI collagen on the cell surface. Mol. Biol. Cell, *4:* 1097–1108, 1993.
19. Burg, M. A., Tillet, E., Timpl, R., and Stallcup, W. B. Binding of the NG2 proteoglycan to type VI collagen and other extracellular matrix molecules. J. Biol. Chem., *271:* 26110–26116, 1996.
20. Burg, M. A., Nishiyama, A., and Stallcup, W. B. A central segment of the NG2 proteoglycan is critical for the ability of glioma cells to bind and migrate toward type VI collagen. Exp. Cell Res., *235:* 254–264, 1997.
21. Tillet, E., Ruggiero, F., Nishiyama, A., and Stallcup, W. B. The membrane-spanning proteoglycan NG2 binds to collagen V and VI through the central non-helical portion of the ectodomain. J. Biol. Chem., *272:* 10769–10776, 1997.
22. Iida, J., Meijne, A., Spiro, R., Roos, E., Furcht, L., and McCarthy, J. Spreading and focal contact formation of human melanoma cells in response to the stimulation of both NG2 and $\alpha_4\beta_1$ integrin. Cancer Res., *55:* 2177–2185, 1995.
23. Grako, K., and Stallcup, W. B. Participation of the NG2 proteoglycan in rat aortic smooth muscle cell responses to platelet-derived growth factor. Exp. Cell Res., *221:* 231–240, 1995.
24. Nishiyama, A., Lin, X-H., Giese, N., Heldin, C-H., and Stallcup, W. B. Interaction between NG2 proteoglycan and PDGF α receptor is required for optimal response to PDGF. J. Neurosci. Res., *43:* 315–330, 1996.
25. Schlingemann, R. O., Rietveld, F. J. R., de Waal, R. M. W., Ferrone, S., and Ruiter, D. J. Expression of the high molecular weight melanoma-associated antigen by pericytes during angiogenesis in tumors and in healing wounds. Am. J. Pathol., *136:* 1393–1405, 1990.
26. Schlingemann, R. O., Rietveld, F. J., Kwaspen, F., van de Kerkhof, P. C., de Waal, R. M., and Ruiter, D. J. Differential expression of markers for endothelial cells, pericytes, and basal lamina in the microvasculature of tumors and granulation tissue. Am. J. Pathol., *138:* 1335–1347, 1991.
27. Sims, D. E. The pericyte: a review. Tissue Cell, *18:* 153–174, 1986.
28. Hirschi, K. K., and D'Amore, P. A. Control of angiogenesis by the pericyte: molecular mechanisms and significance. *In:* I. D. Goldberg and E. M. Rosen (eds.), Regulation of Angiogenesis, pp. 419–428. Basel, Switzerland: Birkhauser Verlag, 1997.
29. Lindahl, P., and Betsholtz, C. Not all myofibroblasts are alike: revisiting the role of PDGF-A and PDGF-B using PDGF-targeted mice. Curr. Opin. Nephrol. Hypertens., *7:* 21–26, 1998.
30. Lindahl, P., Johansson, B. R., Leveen, P., and Betsholtz, C. Pericyte loss and microaneurysm formation in PDGF-B-deficient mice. Science (Washington DC), *277:* 242–245, 1997.
31. Yang, H. M., and Reisfeld, R. A. Doxorubicin conjugated with a monoclonal antibody directed to a human melanoma-associated proteoglycan suppresses the growth of established tumor xenografts in nude mice. Proc. Natl. Acad. Sci. USA, *85:* 1189–1193, 1988.
32. Spitler, L. E., del Rio, M., Khentigan, A., Wedel, N. I., Brophy, N. A., Miller, L. L., Harkonen, W. S., Rosendorf, L. L., Lee, H. M., Mischak, R. P., Kawahata, R. T., Stoudemire, J. B., Fradkin, L. B., Bautista, E. E., and Scannon, P. J. Therapy of patients with malignant melanoma using a monoclonal anti-melanoma antibody-ricin immunotoxin. Cancer Res., *47:* 1717–1723, 1987.
33. Bigner, D. D., Brown, M., Coleman, R. E., Friedman, A. H., Friedman, H. S., McLendon, R. E, Bigner, S. H., Zhao, X-G., Wikstrand, C. J., Pegram, C. N., Kerby, T., and Zalutsky, M. R. Phase I studies of treatment of malignant gliomas and neoplastic meningitis with ^{131}I-radiolabeled monoclonal antibodies anti-tenascin 81C6 and anti-chondroitin sulfate proteoglycan Mel-14F(ab')$_2$: a preliminary report. J. Neuro-Oncol., *24:* 109–122, 1995.
34. Shockley, T. R., Lin, K., Nagy, J. A., Tompkins, R. G., Dvorak, H. F., and Yarmush, M. L. Penetration of tumor tissue by antibodies and other immunoproteins. Ann. N. Y. Acad. Sci., *618:* 367–382, 1991.
35. Dvorak, H. F., Nagy, J. A., and Dvorak, A. M. Structure of solid tumors and their vasculature: implications for therapy with monoclonal antibodies. Cancer Cells, *3:* 77–85, 1991.
36. Molema, G., de Leij, L. F., and Meijer, D. K. Tumor vascular endothelium: barrier or target in tumor directed drug delivery and immunotherapy. Pharm. Res., *14:* 2–10, 1997.
37. Jain, R. K. Delivery of molecular and cellular medicine to solid tumors. Microcirculation, *4:* 3–23, 1997.
38. Koivunen, E., Wang, B., and Ruoslahti, E. Phage libraries displaying cyclic peptides with different ring sizes: ligand specificities of the RGD-directed integrins. BioTechnology, *13:* 265–270, 1995.
39. Koivunen, E., Restel, B., Rajotte, D., Lahdenranta, J., Hagedorn, M., Arap, W., and Pasqualini, R. Integrin-binding peptides from phage display peptide libraries. Integrin protocols. Methods Mol. Biol., in press, 1999.
40. Murayama, O., Nishida, H., and Sekiguchi, K. Novel peptide ligands for integrin $\alpha_6\beta_1$ selected from a phage display library. J. Biochem., *120:* 445–451, 1996.
41. Yanofsky, S. D., Baldwin, D. N., Butler, J. H., Holden, F. R., Jacobs, J. W., Balasubramanian, P., Chinn, J. P., Cwirla, S. E., Peters-Bhatt, E., Whitehorn, E. A., Tate, E. H., Adeson, A., Bowlin, T. L., Dower, W. J., and Barret, R. W. High affinity type I interleukin 1 receptor antagonists discovered by screening recombinant peptide libraries. Proc. Natl. Acad. Sci. USA, *93:* 7381–7386, 1996.
42. Popkov, M., Lussier, I., Medvedkine, V., Esteve, P-E., Alakhov, V., and Mandeville, R. Multidrug-resistance drug-binding peptides generated by using a phage display library. Eur. J. Biochem., *251:* 155–163, 1998.
43. Pennington, M. E., Lam, K. S., and Cress, A. E. The use of a combinatorial library method to isolate human tumor cell adhesion peptides. Mol. Divers., *2:* 19–28, 1996.
44. Goodson, R. J., Doyle, D. V., Kaufman, S. E., and Rosenberg, S. High-affinity urokinase receptor antagonists identified with bacteriophage peptide display. Proc. Natl. Acad. Sci. USA, *91:* 7129–7133, 1994.
45. Pasqualini, R., and Ruoslahti, E. Organ targeting *in vivo* using phage display peptide libraries. Nature (Lond.), *380:* 364–366, 1996.
46. Pasqualini, R., Koivunen, E., and Ruoslahti, E. αv integrins as receptors for tumor targeting by circulating ligands. Nat. Biotechnol., *15:* 542–546, 1997.
47. Rajotte, D., Arap, W., Hagedorn, M., Koivunen, E., Pasqualini, R., and Ruoslahti, E. Molecular heterogeneity of the vascular endothelium revealed by *in vivo* phage display. J. Clin. Invest., *102:* 430–437, 1998.
48. Smith, G. P., and Scott, J. K. Libraries of peptides and proteins displayed in filamentous phage. Methods Enzymol., *21:* 228–257, 1993.
49. Grako, K. A., Ochiya, T. A., Barritt, D., Nishiyama, A., and Stallcup, W. B. PDGF α-receptor is unresponsive to PDGF-AA in aortic smooth muscle cells from the NG2 knockout mouse. J. Cell Sci., *112:* 905–915, 1999.
50. Blood, C. H., and Zetter, B. R. Tumor interactions with the vasculature: angiogenesis and tumor metastasis. Biochim. Biophys. Acta, *1032:* 89–118, 1990.
51. Nagy, J. A., Brown, L. F., Senger, D. R., Lanir, N., Van de Water, L., Dvorak, A. M., and Dvorak, H. F. Pathogenesis of tumor stroma generation: a critical role for leaky blood vessels and fibrin deposition. Biochim. Biophys. Acta, *948:* 305–326, 1989.
52. Dvorak, H. F., Nagy, J. A., Dvorak, J. T., and Dvorak, A. M. Identification and characterization of the blood vessels of solid tumors that are leaky to circulating macromolecules. Am. J. Pathol., *133:* 95–109, 1989.
53. Nowell, P. C. The clonal evolution of tumor cell populations. Science (Washington DC), *194:* 23–28, 1976.
54. Kerbel, R. S. Inhibition of tumor angiogenesis as a strategy to circumvent acquired resistance to anti-cancer therapeutic agents. BioEssays, *13:* 31–36, 1991.
55. Kerbel, R. S. A cancer therapy resistant to resistance. Nature (Lond.), *390:* 335–336, 1997.
56. Boehm, T., Folkman, J., Browder, T., and O'Reilly, M. S. Antiangiogenic therapy of experimental cancer does not induce acquired drug resistance. Nature (Lond.), *390:* 404–407, 1997.

Anti-cancer activity of targeted pro-apoptotic peptides

H. Michael Ellerby, Wadih Arap, Lisa M. Ellerby, Renate Kain, Rebecca Andrusiak, Gabriel Del Rio, Stanislaw Krajewski, Christian R. Lombardo, Rammohan Rao, Erkki Ruoslahti, Dale E. Bredesen & Renata Pasqualini

Program on Aging and Cancer and Program on Cell Adhesion, The Burnham Institute, 10901 North Torrey Pines Rd., La Jolla, California 92037, USA
H.M.E., L.M.E., G.D.R., R.R. & D.E.B. present address: The Buck Center for Research in Aging, 8001 Redwood Blvd, Novato, California 94945, USA
R.K. present address: Clinical Institute for Clinical Pathology, Dept. Ultrastructural Pathology and Cell Biology, University of Vienna/AKH Wien, Währinger Gürtel 18-20, A-1090 Wien, Austria
W.A. & R.P. present address: The University of Texas M.D. Anderson Cancer Center, 1515 Holcombe Boulevard, Houston, Texas 77030, USA
Correspondence should be addressed to E.R., D.B. or R.P.; emails: ruoslahti, dbredesen or pasqualini@burnham-inst.org

We have designed short peptides composed of two functional domains, one a tumor blood vessel 'homing' motif and the other a programmed cell death-inducing sequence, and synthesized them by simple peptide chemistry. The 'homing' domain was designed to guide the peptide to targeted cells and allow its internalization. The pro-apoptotic domain was designed to be non-toxic outside cells, but toxic when internalized into targeted cells by the disruption of mitochondrial membranes. Although our prototypes contain only 21 and 26 residues, they were selectively toxic to angiogenic endothelial cells and showed anti-cancer activity in mice. This approach may yield new therapeutic agents.

Tumor cell survival, growth and metastasis require persistent new blood vessel growth[1–3] (angiogenesis). Consequently, a strategy has emerged to treat cancer by inhibiting angiogenesis[4]. Peptides have been described that selectively target angiogenic endothelial cells[5–8]. Conjugates made from these peptides and the anti-cancer drug doxorubicin induce tumor regression in mice with a better efficacy and a lower toxicity than doxorubicin alone[8]. There is also a functional class of cell death-inducing receptors, or 'dependence receptors', which have embedded pro-apoptotic amino-acid sequences[9,10]. These peptide domains are required for apoptosis induction by these receptors. The peptide fragments are thought to be released into the cytosol as cleavage products of caspase proteolysis, where they induce or potentiate apoptosis through unknown mechanisms[9,10]. However, such peptides, and structurally similar pro-apoptotic antibiotic peptides, although they remain relatively non-toxic outside of eukaryotic cells, induce mitochondrial swelling and mitochondria dependent cell-free apoptosis[10,11].

There are more than 100 naturally occurring antibiotic peptides, and their *de novo* design has received much attention[12–14]. Many of these peptides are linear, cationic and α-helix-forming. Some are also amphipathic, with hydrophobic residues distributed on one side of the helical axis and cationic residues on the other[15]. Because their cationic amino acids are attracted to the head groups of anionic phospholipids, these peptides preferentially disrupt negatively charged membranes. Once electrostatically bound, their amphipathic helices distort the lipid matrix (with or without pore formation), resulting in the loss of membrane barrier function[15,16]. Both prokaryotic cytoplasmic membranes and eukaryotic mitochondrial membranes (both the inner and the outer) maintain large transmembrane potentials, and have a high content of anionic phospholipids, reflecting the common ancestry of bacteria and mitochondria[15–19]. In contrast, eukaryotic plasma membranes (outer leaflet) generally have low membrane potentials, and are almost exclusively composed of zwitterionic phospholipids[16,18,20]. Many antibacterial peptides, therefore, preferentially disrupt prokaryotic membranes and eukaryotic mitochondrial membranes rather than eukaryotic plasma membranes.

If such nontoxic peptides were coupled to tumor targeting peptides that allow receptor-mediated internalization, the chimeric peptide would have the means to enter the cytosol of targeted cells, where it would be toxic by inducing mitochondrial-dependent apoptosis[10,11]. Thus, we designed targeted pro-apoptotic peptides composed of two functional domains. The targeting domain was designed to guide the 'homing' pro-apoptotic peptides to targeted cells and allow their internalization[8,21,22]. The pro-apoptotic domain was designed to be non-toxic outside of cells, but toxic when internalized into targeted cells by the disruption of mitochondrial membranes.

Design of the pro-apoptotic peptide

A computer-generated model and the sequence of one of our prototypes are shown in Fig. 1. For the targeting domain, we used either the cyclic (disulfide bond between cysteines) CNGRC peptide (Fig. 1) or the double-cyclic ACDCRGDCFC peptide (called RGD-4C), both of which have 'tumor-homing' properties[5,8] and for which there is evidence of internalization[8,21,22]. We synthesized this domain from all-L amino acids because of the presumed chiral nature of the receptor interaction. For the pro-apoptotic domain, we selected the synthetic 14-amino-acid peptide KLAKLAKKLAKLAK (Fig. 1), called $(KLAKLAK)_2$, because it killed bacteria at concentrations 1% of those required to kill eukaryotic cells[13]. We used the all-D enan-

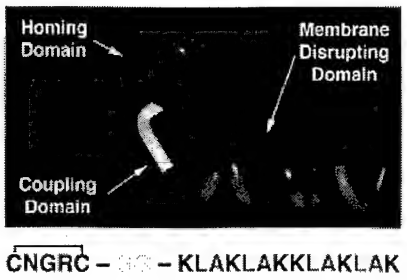

Fig. 1 Computer-generated model and amino-acid sequence of CNGRC-GG$_D$(KLAKLAK)$_2$. This peptide is composed of a 'homing' domain (blue) and a membrane-disrupting (pro-apoptotic) domain (red hydrophilic and green hydrophobic residues), joined by a coupling domain (yellow).

tiomer $_D$(KLAKLAK)$_2$ to avoid degradation by proteases[12,23]. This strategy was possible because such peptides disrupt membranes by chiral-independent mechanisms[23,24]. We coupled the targeting (CNGRC or RGD-4C) and pro-apoptotic $_D$(KLAKLAK)$_2$ domains with a glycinylglycine bridge (Fig. 1) to impart peptide flexibility and minimize potential steric interactions that would prevent binding and/or membrane disruption.

D(KLAKLAK)2 disrupts mitochondrial membranes

We evaluated the ability of $_D$(KLAKLAK)$_2$ to disrupt mitochondrial membranes preferentially rather than eukaryotic plasma membranes by mitochondrial swelling assays, in a mitochondria-dependent cell-free system of apoptosis, and by cytotoxicity assays[10]. There was morphological evidence of damage to mitochondrial membranes by electron microscopy. The peptide $_D$(KLAKLAK)$_2$ induced considerable mitochondrial swelling at a concentration of 10 μM (Fig. 2*a*). Mild swelling was evident even at 3 μM (data not shown), 1% the concentration required to kill eukaryotic cells (approximately 300 μM), as determined by the lethal concentration required to kill 50% of a cell monolayer (LC_{50}; Table 1). These results demonstrate that $_D$(KLAKLAK)$_2$ preferentially disrupts mitochondrial membranes rather than eukaryotic plasma membranes. Moreover, the peptide activated mitochondria-dependent cell-free apoptosis in a system composed of mitochondria suspended in cytosolic extract[10], as measured by characteristic caspase-3-processing from an inactive zymogen to active protease[25] (Fig. 2*b*). A non-α-helix-forming peptide, DLSLARLATARLAI (negative control), did not induce mitochondrial swelling (Fig. 2*a*), was inactive in the cell-free system (Fig. 2*b*) and was not lethal to eukaryotic cells[10]. We also analyzed morphologic alterations in isolated mitochondria by electron microscopy. The peptide $_D$(KLAKLAK)$_2$ induced abnormal mitochondrial morphology, whereas the control peptide DLSLARLATARLAI did not (Fig. 2*c*).

Targeted pro-apoptotic peptides induce apoptosis

We evaluated the efficacy and specificity of CNGRC-GG-$_D$(KLAKLAK)$_2$ in KS1767 cells, derived from Kaposi sarcoma[26,27] (Fig. 3*a–d*), and MDA-MB-435 human breast carcinoma cells[5,8] (Table 1). We used KS1767 cells because they bind the CNGRC targeting peptide just as endothelial cells do. This may relate to the endothelial origin of the KS1767 cells[27]. We used MDA-MB-435 cells as negative control cells because they do not bind the CNGRC targeting peptide[8]. Although CNGRC-GG-$_D$(KLAKLAK)$_2$ was considerably toxic to KS1617 cells, an equimolar mixture of uncoupled CNGRC and $_D$(KLAKLAK)$_2$ (negative control), or $_D$(KLAKLAK)$_2$ alone, was much less toxic, indicative of a targeting effect (Table 1). In contrast, CNGRC-GG-$_D$(KLAKLAK)$_2$ was not very toxic to MDA-MB-435 cells, which do not bind the CNGRC peptide (Table 1). The other targeted peptide (RGD-4C)-GG-$_D$(KLAKLAK)$_2$, showed toxic effects similar to those of CNGRC-GG-$_D$(KLAKLAK)$_2$ on KS1617 cells, whereas an equimolar mixture of uncoupled RGD-4C and $_D$(KLAKLAK)$_2$, used as a negative control, was not very toxic (Table 1; Fig. 3*c–d*).

Although evidence for internalization of CNGRC and RGD-4C into the cytosol of cells has been published[5,8,21,22], we directly demonstrated internalization using biotin-labeled peptides. CNGRC–biotin, but not untargeted CARAC–biotin, was internalized into the cytosol of cells (Fig. 3*e–f*). We also obtained direct evidence for internalization from experiments based on cell fractionation and mass spectrometry. CNGRC-GG-$_D$(KLAKLAK)$_2$, but not CARAC-GG-$_D$(KLAKLAK)$_2$, was indeed internalized and could be detected in mitochondrial as well as cytosolic fractions (data not shown).

Next, we evaluated the efficacy and specificity of CNGRC-GG-$_D$(KLAKLAK)$_2$ in a tissue culture model of angiogenesis[28]. During angiogenesis, capillary endothelial cells proliferate and migrate[1,2]. Cord formation is a type of migration that can be studied *in vitro* by a change in endothelial cell morphology from the usual 'cobblestones' to chains or cords of cells[27]. We tested the effect of CNGRC-GG-$_D$(KLAKLAK)$_2$ on normal human dermal microvessel endothelial cells (DMECs) in the angiogenic conditions of proliferation and cord formation and in the angiostatic condition of a monolayer maintained at 100% confluency.

The treatment of DMECs with 60 μM CNGRC-GG-$_D$(KLAKLAK)$_2$ led to a decrease in the percent viability over time compared with that of untreated controls, in the conditions of proliferation (Fig. 4*a*) or cord formation (Fig. 4*b*). In contrast, treatment with the untargeted peptide $_D$(KLAKLAK)$_2$ as a negative control led to a negligible loss in viability. Furthermore, the LC_{50} for proliferating or migrating DMECs treated with CNGRC-GG-$_D$(KLAKLAK)$_2$ was 10% of the LC_{50} for angiostatic DMECs maintained in a monolayer at 100% confluency (Table 1). This result indicates that CNGRC-GG-$_D$(KLAKLAK)$_2$ kills cells in angiogenic but not angiostatic conditions. The LC_{50} for the untargeted control $_D$(KLAKLAK)$_2$ in angiogenic con-

Table 1 LC_{50} (μM) for eukaryotic cells treated with targeted pro-apoptotic peptides

	DMEC			KS1767	MDA-MB-435
	Angiostatic	Angiogenic			
		Proliferation	Cord Form	Proliferation	Proliferation
$_d$(KLAKLAK)$_2$	492	346	368	387	333
CNGRC-GG-$_D$(KLAKLAK)$_2$	481	51[a]	34[a]	42[a]	415
(RGD-4C)-GG-$_D$(KLAKLAK)$_2$	–	–	–	10[a]	–

Results are means of three independent experiments. [a]$P<0.03$, t-test.

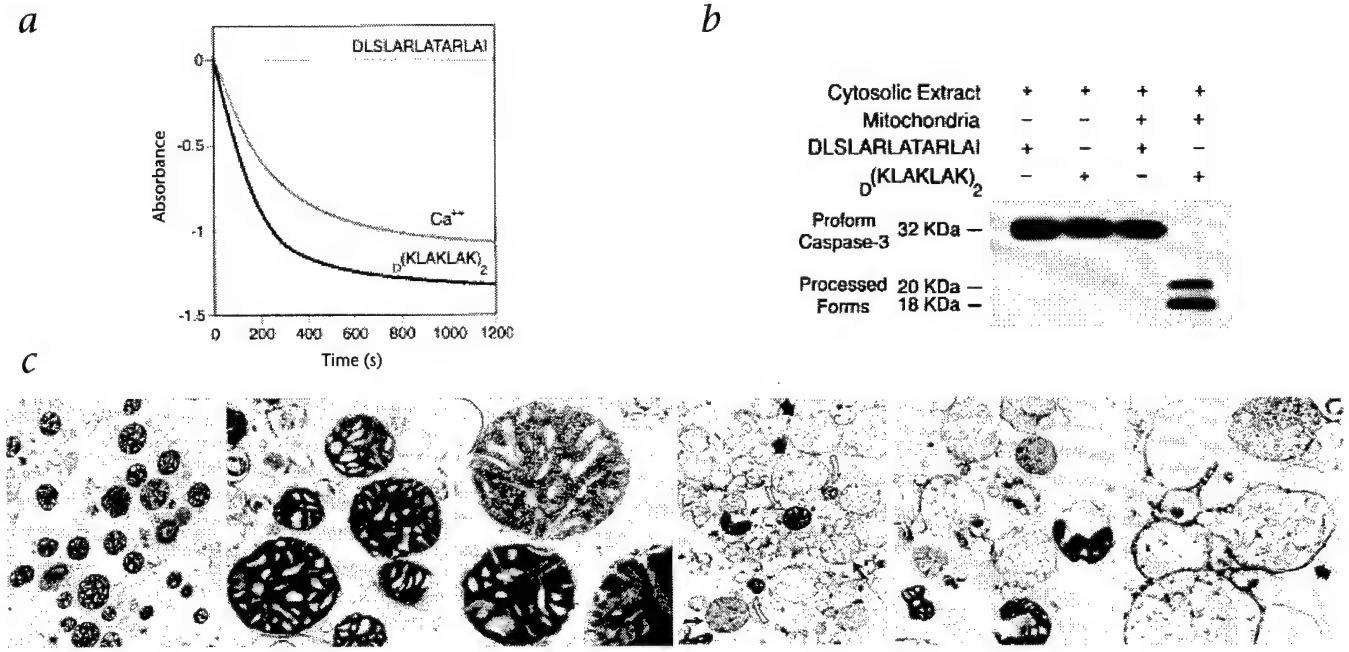

Fig. 2 $_D$(KLAKLAK)$_2$ disrupts mitochondrial membranes. ***a***, $_D$(KLAKLAK)$_2$ or Ca^{2+} (positive control) induced mitochondrial swelling, whereas the non-α-helix-former DLSLARLATARLAI (negative control) did not, as shown by mitochondrial swelling curves (optical absorbance spectrum). ***b***, $_D$(KLAKLAK)$_2$ activates cell-free apoptosis in a system composed of normal mitochondria and cytosolic extract, but DLSLARLATARLAI does not. An immunoblot of caspase-3 cleavage from proform (32-kDa) to processed forms (18- and 20-kDa) demonstrates a mitochondria-dependent cell-free apoptosis (left margin, sizes). Results were reproduced in two independent experiments. ***c***, Morphologic alterations in isolated mitochondria analyzed by electron microscopy. Mitochondria incubated for 15 min with 3 μM DLSLARLATARLAI show normal morphology (left panels). In contrast, mitochondria incubated for 15 min with 3 μM $_D$(KLAKLAK)$_2$ show extensive morphological changes. The damage to mitochondria progressed from the stage of focal matrix resolution (short black arrow), through homogenization and dilution of condensed matrix content with sporadic remnants of cristae (long black arrows), to extremely swollen vesicle-like structures (thick black arrows; bottom right, higher magnification); few mitochondria had normal morphology (open arrows). Ultrathin sections are shown. Original magnification, ×4,000–×40,000.

ditions was similar to the LC_{50} for CNGRC-GG-$_D$(KLAKLAK)$_2$ under angiostatic conditions. An equimolar mixture of uncoupled $_D$(KLAKLAK)$_2$ and CNGRC, a non-targeted form CARAC-GG-$_D$(KLAKLAK)$_2$, and a 'scrambled' form, CGRNC-GG-$_D$(KLAKLAK)$_2$, all gave results similar to those of $_D$(KLAKLAK)$_2$.

We also studied the mitochondrial morphology of DMECs in the condition of proliferation, after treatment with 60 μM CGRNC-GG-$_D$(KLAKLAK)$_2$ or untargeted $_D$(KLAKLAK)$_2$. The mitochondria in intact DMECs treated for 24 hours with the equimolar mixture CNGRC and $_D$(KLAKLAK)$_2$ remained morphologically normal (Fig. 4*d*), whereas those treated with CGRNC-GG-$_D$(KLAKLAK)$_2$ showed altered mitochondrial morphology, evident in approximately 80% of cells (Fig. 4*e*), before the cells rounded-up. Ultimately, the DMECs treated with CNGRC-GG-$_D$(KLAKLAK)$_2$ showed the classic morphological indicators of apoptosis, including nuclear condensation and fragmentation, as seen at 72 hours (Fig. 4 *f* and *g*)(ref. 10). Apoptotic cell death (Fig. 4*g*) was confirmed with an assay for

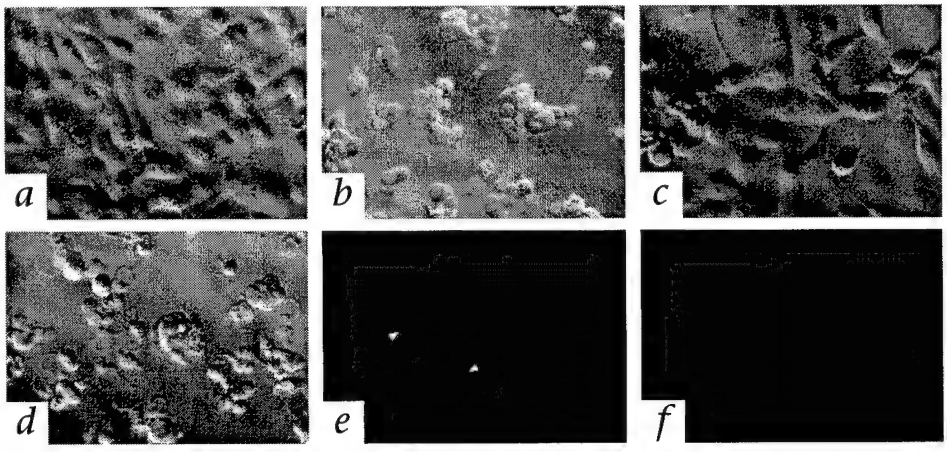

Fig. 3 CNGRC-GG-$_D$(KLAKLAK)$_2$ and (RGD-4C)-GG-$_D$(KLAKLAK)$_2$ induce apoptosis. ***a***, KS1767 cells treated with 100 μM of non-targeted CARAC-GG-$_D$(KLAKLAK)$_2$ (negative control) remain unaffected after 48 h. ***b***, KS1767 cells treated with 100 μM of CNGRC-GG-$_D$(KLAKLAK)$_2$ undergo apoptosis, as shown at 48 h. Condensed nuclei and plasma membrane blebbing are evident. ***c***, KS1767 cells treated with 10 μM of an equimolar mixture of (RGD-4C) and $_D$(KLAKLAK)$_2$ (negative control) remain unaffected after 48 h. ***d***, KS1767 cells treated with 10 μM of (RGD-4C)-GG-$_D$(KLAKLAK)$_2$ undergo apoptosis, as shown at 48 h. Condensed nuclei and plasma membrane blebbing are evident. Scale bar represents 250 μm. ***e*** and ***f***, KS1767 cells treated with 100 μM of CNGRC-biotin (*e*) or CARAC-biotin (*f*) for 24 h and subsequently treated with streptavidin FITC demonstrate internalization of CNGRC-biotin, but not CARAC-biotin, into the cytosol.

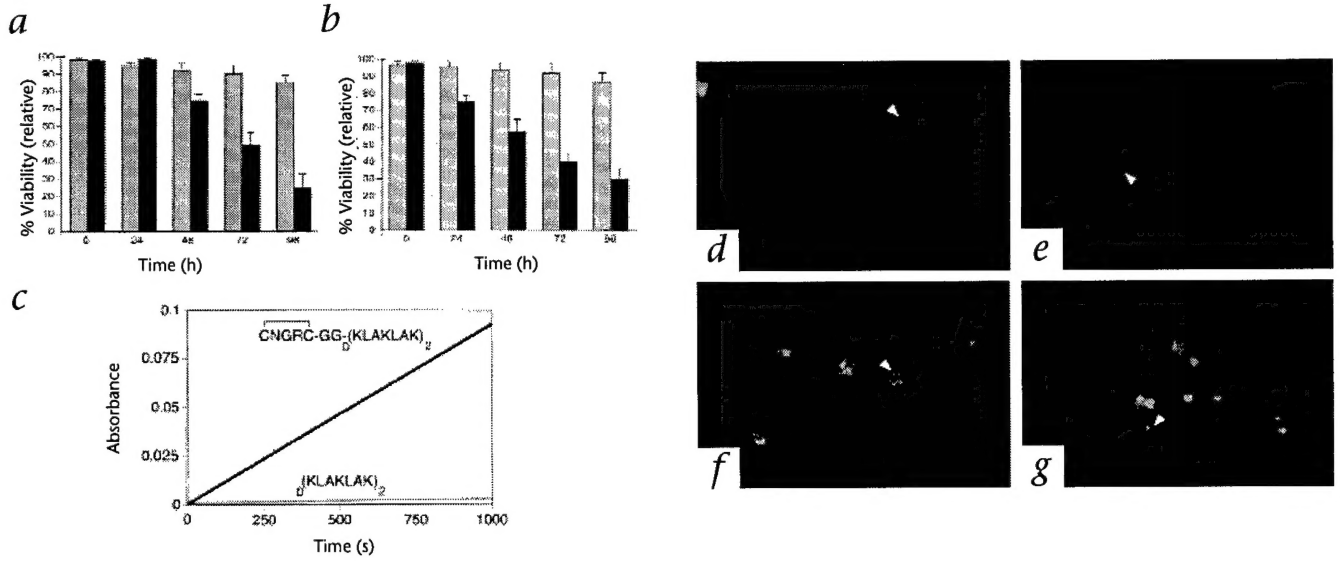

Fig. 4 CNGRC-GG-$_D$(KLAKLAK)$_2$ induces apoptosis and mitochondrial swelling in DMECs. ***a***, Proliferating DMECs treated with CNGRC-GG-$_D$(KLAKLAK)$_2$ (filled bars) lose viability (apoptosis) over time ($P < 0.02$), but those treated with the control peptide $_D$(KLAKLAK)$_2$ (gray bars) do not ($P < 0.05$). ***b***, Cord-forming DMECs lose viability (apoptosis) over time (filled bars), but those treated with $_D$(KLAKLAK)$_2$ (gray bars) do not ($P < 0.05$). ***c***, Apoptotic cell death was confirmed with an assay for caspase 3 activity, as shown by the hydrolysis of DEVD-pNA with time. Results were reproduced in three independent experiments. ***d***, Proliferating DMECs show normal nuclear (blue) and mitochondrial (red) morphology after 24 h of treatment with a mixture of 100 μM $_D$(KLAKLAK)$_2$ and CNGRC. ***e–g***, Proliferating DMECs treated with 100 μM CNGRC-GG-$_D$(KLAKLAK)$_2$. After 24 h (*e*), cells show normal nuclear (blue) but abnormal mitochondrial (red) morphology. Mitochondrial swelling and dysfunction is shown by a decrease in fluorescence intensity and a change in morphology from an extended lace-like network to a condensed clumping of spherical structures. Classic morphological indicators of mid- to late apoptosis (for example, condensed and fragmented nuclei) are evident at 48 h (*f*) and 72 h (*g*) (arrow).

caspase 3 activity[10]. We also tested a caspase inhibitor for its effect on cell death induced by CNGRC-GG-$_D$(KLAKLAK)$_2$. We used Kaposi sarcoma cells, as these cells bind CNGRC. The inhibitor zVAD.fmk, at a concentration (25 μM) that inhibits caspases but not non-caspase proteases, inhibited the cell death induced by CNGRC-GG-$_D$(KLAKLAK)$_2$ (data not shown). This result is compatible with the earlier demonstration that the CNGRC-GG-$_D$(KLAKLAK)$_2$ peptide is pro-apoptotic. Although the relatively early mitochondrial swelling is consistent with the putative mechanism of action, that is, a direct activation of the apoptotic machinery, we cannot rule out the possibility that the peptides actually kill by inducing some irreversible damage to cells which then activates the apoptotic program.

In addition to the fluorescence studies shown above, we studied cultured cells by electron microscopy to confirm that CNGRC-GG-$_D$(KLAKLAK)$_2$ induces abnormal mitochondrial morphology in intact cells (Fig. 5). Kaposi sarcoma-derived KS1767 cells treated with the control peptide CARAC-GG-$_D$(KLAKLAK)$_2$ for 72 hours showed no overall changes, with no or very minor changes in the mitochondria (Figs. 5*a–c*). In contrast, the mitochondria in KS1767 cells incubated for 12 hours

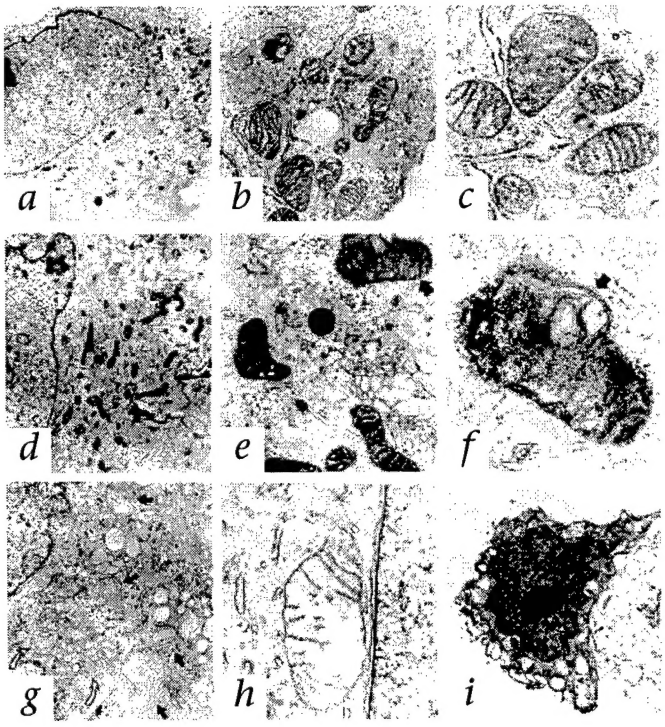

Fig. 5 Electron microscopic studies of cultured cells. *a–c*, KS1767 cells treated with 100 μM CARAC-GG-$_D$(KLAKLAK)$_2$ for 72 h show the representative ultrastructural details of normal cells, with no or negligible changes seen in the mitochondria. Original magnifications: ***a***, ×4,000; ***b***, ×25,000; ***c***, ×45,000. ***d–f***, In contrast, the mitochondria in KS1767 cells incubated for 12 h with 100 μM CNGRC-GG-$_D$(KLAKLAK)$_2$ begin to show a condensed appearance and vacuolization despite a relatively normal cell morphology (black arrows). Original magnifications: *d*, ×12,000; *e*, ×20,000; *f*, ×45,000). *g* and *h*, Progressive damage to KS1767 cells is evident after 24 h, when many mitochondria show typical large matrix compartments and prominent cristae, ultrastructural features of low level of oxidative phosphorylation. Original magnifications: ***g***, ×12,000; ***h***, ×40,000. Some of the swollen mitochondria (*g*, black arrows) are similar in appearance to those in isolated mitochondria treated with 100 μM $_D$(KLAKLAK)$_2$ (Fig. 2*c*, bottom right). ***I***, In some cells, this process progressed to a final stage, with extensive vacuolization and the pyknotic, condensed nuclei typical of apoptosis. Original magnification, ×8,000.

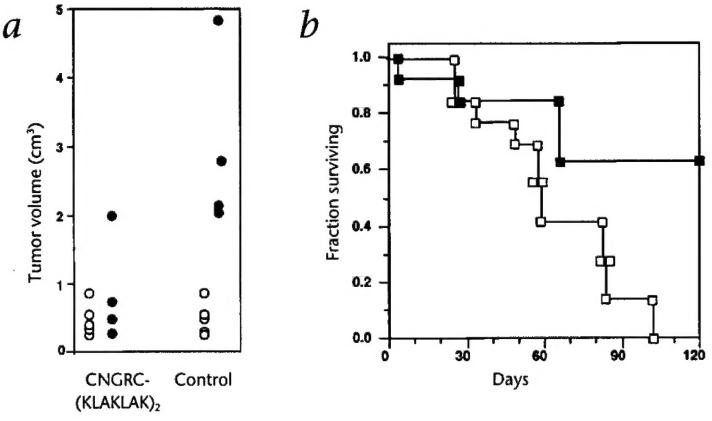

Fig. 6 Treatment of nude mice bearing MDA-MB-435-derived human breast carcinoma xenografts with CNGRC-GG-$_D$(KLAKLAK)$_2$. ***a***, Tumors treated with CNGRC-GG-$_D$(KLAKLAK)$_2$ are smaller than control tumors treated with CARAC-GG-$_D$(KLAKLAK)$_2$, as shown by differences in tumor volumes between day 1 (○) and day 50 (●). P = 0.027, t-test. One mouse in the control group died before the end of the experiment. ***b***, Mice treated with CNGRC-GG-$_D$(KLAKLAK)$_2$ (■) survived longer than control mice treated with an equimolar mixture of $_D$(KLAKLAK)$_2$ and CNGRC (□), as shown by a Kaplan-Meier survival plot (n = 13 animals/group). $P < 0.05$, log-rank test.

with CNGRC-GG-$_D$(KLAKLAK)$_2$ showed abnormal condensation and vacuolization despite a relatively preserved cell morphology (Fig. 5*d–f*, black arrows). Progressive cellular damage could be seen after 24 hours, when many mitochondria showed ultrastructural features of low-level oxidative phosphorylation (Fig. 5*g* and *h*); in later stages, some of the damaged mitochondria (Fig. 5g, black arrows) showed profound changes, as seen in the isolated mitochondria treated with $_D$(KLAKLAK)$_2$ (Fig. 2*c*, right lower panel). In some cells, this process progressed to a late apoptotic stage. Typical vacuolization and condensed nuclei became evident (Fig. 5*i*). These results show that the mitochondria underwent changes in morphology and function that were well-represented by a progression from a state of normal morphology and normal oxidative phosphorylation (Fig. 5*a*) to a state of condensed morphology and a high rate of oxidative phosphorylation (Fig. 5*d*) to a final edemic state (Fig. 5*g*) associated with a low energy level.

Treatment of nude mice bearing human tumor xenografts with CNGRC-GG-$_D$(KLAKLAK)$_2$ and (RGD-4C)-GG-$_D$(KLAKLAK)$_2$

Given our results in culture, we proceeded to test both targeted pro-apoptotic peptides *in vivo*, using nude mice with human MDA-MD-435 breast carcinoma xenografts. Tumor volume in the groups treated with CNGRC-GG-$_D$(KLAKLAK)$_2$ was on average 10% that of control groups (Fig. 6*a*); survival was also longer in these groups than in control groups (Fig. 6*b*). The control was a non-targeted 'mimic' CARAC-GG-$_D$(KLAKLAK)$_2$ peptide; the CARAC sequence has a charge, size and general structure similar to that of CNGRC. Some of the mice treated with CNGRC-GG-$_D$(KLAKLAK)$_2$ outlived control mice by several months, indicating that both primary tumor growth and metastasis were inhibited by CNGRC-GG-$_D$(KLAKLAK)$_2$. Treatment in nude mice bearing MDA-MD-435 breast carcinoma xenografts with (RGD-4C)-GG-$_D$(KLAKLAK)$_2$ also resulted in a significantly reduced tumor and metastatic burden (Fig. 7). Experimental parameters included tumor volumes before and after treatment (Fig. 7*a*), wet weights of the tumors (Fig. 7*b*, right) and weight of lung metastases (Fig. 7*b*, left). The control group was treated with an equimolar mixture of RGD-4C and $_D$(KLAKLAK)$_2$. Histopathological and TUNEL analysis showed cell death in the treated tumors and evidence of apoptosis and necrosis (data not shown).

To assess toxicity in mice without tumors, we have administered CNGRC-GG-$_D$(KLAKLAK)$_2$ or (RGD-4C)-GG-$_D$(KLAKLAK)$_2$ to both immunocompetent (balb/c) and to immunodeficient (balb/c nude) mice at a dose of 250 μg/mouse per week for eight doses. No apparent toxicities have been found in 3 months. Moreover, in these conditions, the peptides are not immunogenic, as determined by ELISA of blood obtained from the immunocompetent mice (data not shown).

We have also evaluated the stability of the CNGRC-GG-$_D$(KLAKLAK)$_2$ and (RGD-4C)-GG-$_D$(KLAKLAK)$_2$ peptides *ex vivo* and in mice. We analyzed the two targeted peptides using mass spectrometry. In the first set of experiments, the targeted peptides were pre-mixed with whole blood and incubated at 37 °C.

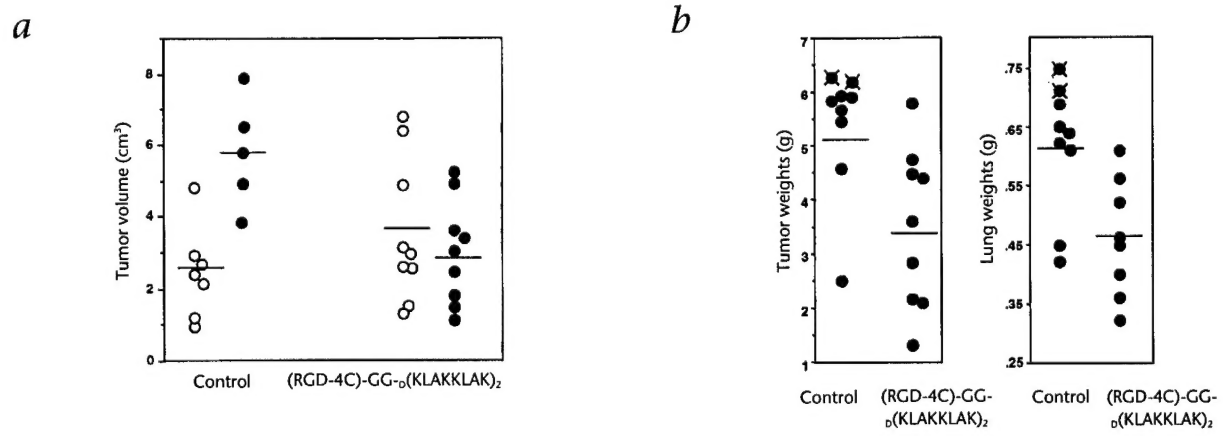

Fig. 7 Treatment of nude mice bearing MDA-MB-435-derived human breast carcinoma xenografts with (RGD-4C)-GG-$_D$(KLAKLAK)$_2$. ***a***, Tumors treated with (RGD-4C)-GG-$_D$(KLAKLAK)$_2$ are smaller than control tumors treated with an equimolar mixture of RGD-4C peptide and $_D$(KLAKLAK)$_2$. Tumor volumes were assessed on day 1 (○) and day 90 (●). P = 0.027, t-test. ***b***, Tumor weights (right) and lung metastatic burden (left) are also decreased in mice treated with (RGD-4C)-GG-$_D$(KLAKLAK)$_2$; these were measured when the experiment ended, on day 110 (n = 9 animals/group). $P < 0.05$, t-test.

The peptides were intact up to 1 hour in these conditions. In the second set of experiments, mice were injected intravenously with the two targeted peptides and blood samples were analyzed; the peptides were present at 10 minutes after administration (data not shown). We chose these short circulation times to coincide with the experimental conditions established for 'homing' of targeted peptides *in vivo*[5,7,8].

Targeted pro-apoptotic peptides represent a potential new class of anti-cancer agents; their activity may be optimized for maximum therapeutic effect by adjusting properties such as residue placement, domain length, peptide hydrophobicity and hydrophobic moment[29]. Beyond this, future targeted pro-apoptotic peptides might be designed to disrupt membranes using a completely different type of pro-apoptotic domain such as β-strand/sheet-forming peptides[30]. Our results provide a glimpse at a new cancer therapy combining two levels of specificity: 'homing' to targeted cells and selective apoptosis of such cells after entry.

Methods

Reagents. Human recombinant vascular endothelial growth factor (VEGF; PharMingen, San Diego, California), antibody against caspase-3 (Santa Cruz Biotechnology, Santa Cruz, California), streptavidin FITC (Sigma) and N-acetyl-Asp-Glu-Val-Asp-pNA (DEVD-pNA; BioMol, Plymouth Meeting, Pennsylvania) were obtained commercially. Peptides were synthesized to our specifications at greater than 90% purity by HPLC (DLSLARLATARLAI, Coast (San Diego, California); all other peptides, AnaSpec (San Jose, California).

The computer-generated model was made with Insight II (Molecular Simulations, San Diego, California) running on an O_2 work station (Silicon Graphics, Mountain View, California)

Cell culture. Dermal microvessel endothelial cells (DMECs) were grown in CADMEC Growth Media™ (media and cells from Cell Applications, San Diego, California). DMECs were then cultured in three experimental conditions: proliferation (30% confluency in a growth media supplemented with 500 ng/ml VEGF); no proliferation (100% confluency in media formulated to maintain a monolayer); and cord formation (60% confluency (required for induction) in media formulated to induce cord formation). KS1767 and MDA-MB-435 cells were cultured as described[5,8,27,28].

Internalization assay. KS1767 cells grown on coverslips were treated with 100 μM biotin-labeled CNGRC or biotin-labeled CARAC (negative control) for 24 h. Streptavidin FITC was added to the coverslips, and cells were then viewed on an inverted microscope (Nikon TE 300) using a FITC filter.

Mitochondrial swelling assays. Rat liver mitochondria were prepared as described[10]. The concentrations used were 10 μM $_D$(KLAKLAK)$_2$, 10 μM DLSLARLATARLAI (negative control), or 200 μM Ca^{2+} (positive control). The peptides were added to mitochondria in a cuvette, and swelling was quantified by measuring the optical absorbance at 540 nm.

Cell-free apoptosis assays. Cell-free systems were reconstituted as described[10]. For the mitochondria-dependent reactions, rat liver mitochondria were suspended in normal (non-apoptotic) cytosolic extracts of DMECs. The peptides were added at a concentration of 100 μM. After incubation for 2 h at 30 °C or 37 °C, mitochondria were removed by centrifugation, and the supernatant was analyzed by SDS–PAGE and immunoblotting (12% gels, BioRad, Richmond, California). Proteins were transferred to PVDF membranes (BioRad, Richmond, California) and incubated with antibody against caspase-3, followed by ECL detection (Amersham).

Caspase activity of cell lysates. The caspase activity of DMEC lysates was measured as described[10]. Aliquots of cell lysates (1 μl lysate; 8–15 mg/ml) were added to 100 μM DEVD-pNA (100 μl; 100 mM HEPES, 10% sucrose, 0.1% CHAPS and 1 mM DTT, pH 7.0). Hydrolysis of DEVD-pNA was monitored by spectrophotometry (400 nm) at 25 °C.

Morphological quantification of cellular apoptosis. Percent viability and LC_{50} (Table 1) were determined by apoptotic morphology[10]. For the percent viability assay, DMECs were incubated with 60 μM active peptide or control peptide. Cell culture medium was aspirated at various times from adherent cells, and the cells were gently washed once with PBS at 37 °C. Then, a 20-fold dilution of the dye mixture (100 μg/ml acridine orange and 100 μg/ml ethidium bromide) in PBS was gently pipetted on the cells, which were viewed on an inverted microscope (Nikon TE 300). The cell death seen was apoptotic cell death and was confirmed by a caspase activation assay. Not all cells progressed through the stages of apoptosis at the same time. At the initial stages, a fraction of the cells were undergoing early apoptosis. At later stages, this initial fraction had progressed to late apoptosis and even to the necrotic-like stage associated with very late apoptosis (for example, loss of membrane integrity in apoptotic bodies). However, these cells were joined by a new fraction undergoing early apoptosis. Thus, cells with nuclei showing margination and condensation of the chromatin and/or nuclear fragmentation (early/mid-apoptosis; acridine orange-positive) or with compromised plasma membranes (late apoptosis; ethidium bromide-positive) were considered not viable. At least 500 cells per time point were assessed in each experiment. Percent viability was calculated relative to untreated controls. LC_{50} for monolayer, proliferation (60% confluency), and cord formation were assessed at 72 h.

Mitochondrial morphology. DMECs after 24 and 72 h of treatment with peptide were incubated for 30 min at 37 °C with a mitochondrial stain (100 nM MitoTracker Red™ CM-H_2XRos; the nonfluorescent, reduced form of the compound) and a nuclear stain (500 nm DAPI; Molecular Probes, Eugene, Oregon). Mitochondria were then visualized under fluorescence microscopy (100x objective) under an inverted microscope using a triple wavelength filter set (Nikon).

Electron microscopy. Rat liver mitochondria were prepared as described[10]. The mitochondria were incubated either with a control peptide (DLSLARLATARLAI) or with 3 μM $_D$(KLAKLAK)$_2$. The effects of the treatment were assessed at different times (Fig. 2*c*). Kaposi sarcoma cells were collected from 24-well Biocoat Cell culture inserts for electron microscopy (Becton Dickinson, Franklin Lakes, New Jersey). Cell monolayers at 80% confluency were exposed to either 100 μM CARAC-GG-$_D$(KLAKLAK)$_2$ (control) or CNGRC-GG-$_D$(KLAKLAK)$_2$ (targeted) (Fig. 5). All specimens were fixed with 3% glutaraldehyde in 0.1 M potassium phosphate buffer, pH 7.4 for 30 to 45 min at the room temperature, followed by postfixation with aqueous 1% osmium tetroxide and 2% uranyl acetate. After dehydration using a graded series of ethanol rinses, tissues were embedded in resin. Ultrathin sections after additional counterstainings were viewed and photographed on an electron microscope (Hitachi H-600).

Human tumor xenografts. MDA-MB-435-derived tumor xenografts were established in female nude mice 2 months old (Jackson Labs, Bar Harbor, Maine) as described[33]. The mice were anesthetized with Avertin as described[31]. The peptides were administered at a dose of 250 μg/week per mouse, given slowly through the tail vein in a volume of 200 μl. Three-dimensional measurements of tumors were made by caliper on anesthetized mice, and were used to calculate tumor volume[5,8]. Then, tumors and lungs were surgically removed and the wet weights recorded. Animal experimentation was reviewed and approved by the Institute's Animal Research Committee.

Acknowledgments

We thank W.K. Cavenee and G. Salvesen for comments and critical reading of the manuscript. This work was supported by grants CA74238, CA28896 (to ER) NS33376 and Cancer Center support grant CA30199 (to R.P., D.B. and E.R.) from the National Cancer Institute (USA), and DAMD17-98-1-8581 (to D.B. and R.P.) from the DOD-PCRP. H.M.E. is the recipient of a NS10050 NRSA senior fellowship grant. W.A. is the recipient of a CaP CURE award.

RECEIVED 11 MAY; ACCEPTED 30 JUNE 1999

1. Risau, W. Mechanisms of angiogenesis. *Nature* **386**, 671–674 (1997).
2. Zetter, B.R. Angiogenesis and tumor metastasis. *Annu. Rev. Med.* **49**, 407–424

(1998).
3. Bicknell, R. in *Tumour Angiogenesis.* (eds. Bicknell, R., Lewis, C.E. & Ferrara, N.) 19–28 (Oxford University Press, Oxford 1997).
4. Folkman, J. in *Cancer: Principles and Practice of Oncology.* (eds. DeVita, V.T., Hellman, S. & Rosenberg, S.A.) 3075–3087 (Lippincott-Raven, New York, 1997).
5. Pasqualini, R., Koivunen, E. & Ruoslahti, E. αv integrins as receptors for tumor targeting by circulating ligands. *Nature Biotechnol.* **15,** 542–546 (1997).
6. Arap, W., Pasqualini, R. & Ruoslahti, E. Chemotherapy targeted to tumor vasculature. *Curr. Opin. Oncol.* **10,** 560–565 (1998).
7. Pasqualini, R., Arap, W., Rajotte, D. & Ruoslahti, E. in *Phage Display of Proteins and Peptides* (eds. Barbas, C., Burton, D., Silverman, G. & Scott, J.) (Cold Spring Harbor, New York, in the press).
8. Arap, W., Pasqualini, R. & Ruoslahti, E. Cancer treatment by targeted drug delivery to tumor vasculature in a mouse model. *Science* **279,** 377–380 (1998).
9. Bredesen D.E. *et al.* P75(NTR) and the concept of cellular dependence – seeing how the other half die. *Cell Death Differ.* **5,** 365–371 (1998).
10. Ellerby, H.M. *et al.* Establishment of a cell-free system of neuronal apoptosis: comparison of premitochondrial, mitochondrial, and postmitochondrial phases. *J. Neurosci.* **17,** 6165–6178 (1997).
11. Mehlen, P. *et al.* The DCC gene product induces apoptosis by a mechanism requiring receptor proteolysis. *Nature* **395,** 801–804 (1998).
12. Bessalle, R., Kapitkovsky, A., Gorea, A., Shalit, I. & Fridkin, M. All-D-magainin: chirality, antimicrobial activity and proteolytic resistance. *FEBS Lett.* **274,** 151–155 (1990).
13. Javadpour, M.M. *et al. De novo* antimicrobial peptides with low mammalian cell toxicity. *J. Med. Chem.* **39,** 3107–3113 (1996).
14. Blondelle, S.E. & Houghten, R.A. Design of model amphipathic peptides having potent antimicrobial activities. *Biochemistry* **31,** 12688–12694 (1992).
15. Epand, R.M. in *The Amphipathic Helix* (CRC, Boca Raton, Florida, 1993).
16. de Kroon, A., Dolis, D., Mayer, A., Lill, R. & de Kruijff, B. Phospholipid composition of highly purified mitochondrial outer membranes of rat liver and Neurospora crassa. Is cardiolipin present in the mitochondrial outer membrane? *Biochim. Biophys. Acta* **1325,** 108–116 (1997).
17. Matsuzaki, K., Murase, O., Fujii, N. & Miyajima, K. Translocation of a channel-forming antimicrobial peptide, magainin 2, across lipid bilayers by forming a pore. *Biochemistry* **34,** 6521–6526 (1995).
18. Hovius, R., Thijssen, J., van der Linden, P., Nicolay, K. & de Kruijff, B. Phospholipid asymmetry of the outer membrane of rat liver mitochondria: Evidence for the presence of cardiolipin on the outside of the outer membrane. *FEBS Lett.* **330,** 71–76 (1993).
19. Baltcheffsky, H., & Baltcheffsky, M. in *Mitochondria and Microsomes* (eds. Lee, C.P., Schatz, G., Dallner, G.) 519–540 (Addison-Wesley, Reading, Massachusetts, 1981).
20. Daum, G. Lipids of Mitochondria. *Biochim. Biophys. Acta* **882,** 1–42 (1985).
21. Hart, S.L. *et al.* Cell binding and internalization by filamentous phage displaying a cyclic Arg-Gly-Asp-containing peptide. *J. Biol. Chem.* **269,** 12468–12474 (1994).
22. Bretscher, M.S. Endocytosis and recycling of the fibronectin receptor in CHO cells. *EMBO J.* **8,** 1341–1348 (1989).
23. Dathe, M. *et al.* Hydrophobicity, hydrophobic moment, and angle subtended by charged residues modulate antibacterial and haemolytic activity of amphipathic helical peptides. *FEBS Lett.* **403,** 208–212 (1997).
24. Alvarez-Bravo, J., Kurata, S. & Natori, S. Novel synthetic antimicrobial peptides effective against methicillin-resistant *Staphylococcus aureus. Biochem. J.* **302,** 535–538 (1994).
25. Alnemri, E.S. *et al.* ICE/CED-3 protease nomenclature. *Cell* **87,** 171 (1996).
26. Hernier, B.G. *et al.* Characterization of a human Kaposi's sarcoma cell line that induces angiogenic tumors in animals. *AIDS* **8,** 575–581 (1994).
27. Samaniego, F. *et al.* Vascular endothelial growth factor and basic fibroblast growth factor present in Kaposi's sarcoma (KS) are induced by inflammatory cytokines and synergize to promote vascular permeability and KS lesion development. *Amer. J. Path.* **152,** 1433–1443 (1998).
28. Goto, F., Goto, K., Weindel, K. & Folkman, J. Synergistic effects of vascular endothelial growth factor and basic fibroblast growth factor on the proliferation and cord formation of bovine capillary endothelial cells within collagen gels. *Lab. Invest.* **69,** 508–517 (1993).
29. Wade, D. *et al.* All-D amino acid-containing channel-forming antibiotic peptides. *Proc. Natl Acad. Sci. USA* **87,** 4761–4765 (1990).
30. Mancheno, J.M., Martinez del Pozo, A., Albar, J.P., Onaderra, M. & Gavilanes, J.G. A peptide of nine amino acid residues from α-sarcin cytotoxin is a membrane-perturbing structure. *J. Peptide Res.* **51,** 142–148 (1998).
31. Pasqualini, R. & Ruoslahti, E. Organ targeting *in vivo* using phage display peptide libraries. *Nature* **380,** 36–366 (1996).